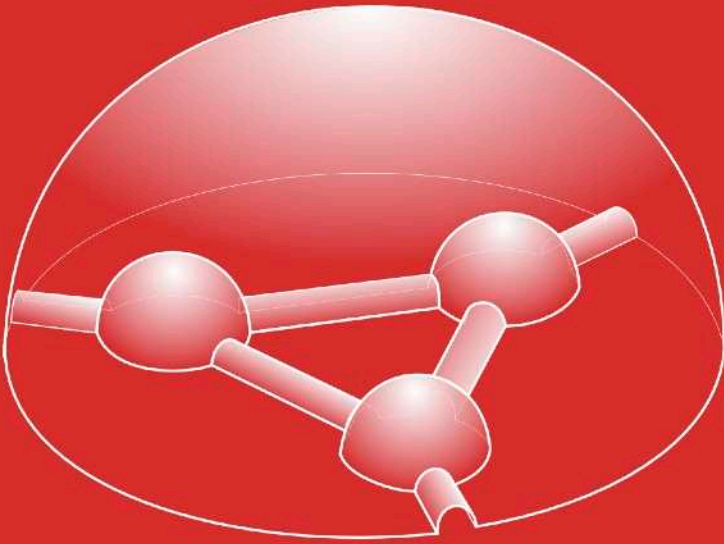


Asymptotics of quantum spin networks



Roland Ivo van der Veen

Asymptotics of quantum spin networks

ACADEMISCH PROEFSCHRIFT

ter verkrijging van de graad van doctor
aan de Universiteit van Amsterdam
op gezag van de Rector Magnificus
prof. dr. D.C. van den Boom
ten overstaan van een door het college voor promoties ingestelde
commissie, in het openbaar te verdedigen in de Agnietenkapel
op vrijdag 10 September 2010, te 10 uur

door

Roland Ivo van der Veen

geboren te Amsterdam

Promotor: prof. dr. E. M. Opdam
Copromotor: prof. dr. S. Garoufalidis

Overige leden: prof. dr. J. E. Andersen
prof. dr. R. H. Dijkgraaf
dr. R. Kashaev
prof. dr. T. H. Koornwinder
dr. H. B. Posthuma
prof. dr. N. Y. Reshetikhin
dr. J. Stokman

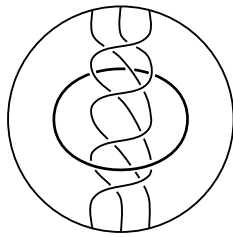
Faculteit der Natuurwetenschappen, Wiskunde en Informatica

Dit proefschrift werd mede mogelijk gemaakt door:

THOMAS STIELTJES INSTITUTE
FOR MATHEMATICS



Asymptotics of quantum spin networks



Roland Ivo van der Veen

Contents

1	Introduction	7
1.1	Background	7
1.2	Main results	10
1.3	Brief history of the conjecture	11
1.4	Approach	12
1.5	Overview of the thesis	14
1.6	Generalizations	15
2	Proof of the volume conjecture for Whitehead Chains	17
2.1	Introduction	17
2.2	Proof of the main theorem	19
2.3	Proof of the lemmas	21
3	The volume conjecture for augmented knotted trivalent graphs	27
3.1	Introduction	27
3.2	Knotted Trivalent Graphs	32
3.3	The colored Jones invariant of a KTG	36
3.4	The geometry of the complement of an augmented KTG	43
3.5	Conclusion	51
4	Asymptotics of classical spin networks	53
4.1	Introduction	53
4.2	Existence of asymptotics	56
4.3	Asymptotics of $6j$ -symbols	59
4.4	A generating function for spin network evaluations	62
4.5	Plan of the paper	63
4.6	Evaluation of spin networks	64
4.7	G -functions and existence of asymptotic expansions	68
4.8	Computation of asymptotic expansions using Borel transform	69
4.9	Asymptotics of the $6j$ -symbol	71
4.10	Computation of asymptotic expansions using the WZ method	79
4.11	Chromatic evaluation of spin networks	81
4.12	Challenges and future directions	84
5	Asymptotics of quantum spin networks at a fixed root of unity	87
5.1	Introduction	87
5.2	Evaluation of quantum spin networks	92
5.3	Proof of Theorems 5.3, 5.4, 5.5 and 5.6	99

5.4	Examples	104
5.5	Open problems	108
6	A cabling formula for the colored Jones polynomial	109
6.1	Introduction	109
6.2	Proof of the cabling formula	111
6.3	Application to the volume conjecture	118
7	Samenvatting	121
7.1	Kristallen	122
7.2	Roeren	123
7.3	Tekenen	125
7.4	Kwantumrekenen	126
7.5	Asymptotiek van kwantum-spin-netwerken	127

Chapter 1

Introduction

This thesis deals with the interface of low-dimensional topology, geometry and representation theory. These fields come together in the interpretation of the quantum invariants of knots and 3-manifolds such as the Jones polynomial. Although these invariants derived from quantum groups have revolutionized the field of low-dimensional topology, their geometric meaning is still not understood well [RT], [Wit1], [Wit2]. Great progress towards a geometrical interpretation of the quantum invariants was made in the formulation of the volume conjecture [Ka2], [MM].

In the volume conjecture the quantum invariants are connected to Thurston's geometrization program [Th2]. Recently settled by Perelman, this program implies that every 3-manifold can be decomposed into pieces, each of which admits one of eight homogeneous geometries. Of these geometries hyperbolic geometry is the most relevant to knot theory. According to the volume conjecture, the Jones polynomial are related to the hyperbolic geometry of the knot complement. More precisely, in its simplest form the volume conjecture asserts the following:

Conjecture 1.1. (Volume Conjecture) [Ka2], [MM] *Let K be a knot and denote its N -colored Jones polynomial by $J_N(K)(q)$.*

$$\lim_{N \rightarrow \infty} \frac{2\pi}{N} \log |J_N(K)(e^{\frac{2\pi i}{N}})| = \text{Vol}(\mathbb{S}^3 - K) \quad (1.1)$$

More precisely the claim is the limit on the left hand side exists and is equal to the right hand side.

1.1 Background

In this section we briefly explain some of the basic notions necessary for understanding the definition of the terms used in the description of the volume conjecture above. This section can safely be skipped by people familiar with the area.

1.1.1 Geometrization of knot complements

Recall that a knot K in \mathbb{S}^3 is called hyperbolic if its complement $\mathbb{S}^3 - K$ admits a complete metric of constant sectional curvature -1 . Alternatively we can

say that in that case the complement is homeomorphic to \mathbb{H}^3/Γ , where \mathbb{H}^3 is standard hyperbolic space and Γ is a discrete torsion free subgroup of the group of its orientation preserving isometries.

It is clear that if two hyperbolic knot complements are isometric then the complements are homeomorphic as well. What is far from obvious is that the converse should be true. One might expect non trivial parameter spaces or moduli spaces of complete hyperbolic structures on a knot complement. However by the Mostow-Prasad Rigidity theorem this is not the case. If it exists at all, the complete hyperbolic metric is unique [BP]. More precisely, two knot complements \mathbb{H}^3/Γ_1 and \mathbb{H}^3/Γ_2 are homeomorphic if and only if Γ_1 and Γ_2 are conjugate in the isometry group.

One can also phrase the property of hyperbolicity of a knot in terms of representations of its fundamental group $\rho : \pi_1(\mathbb{S}^3 - K) \rightarrow SL(2, \mathbb{C})$. The complete hyperbolic structure gives rise to a unique (up to conjugation) faithful representation. More general representations of the knot group also have a geometric role to play and indeed the geometry of the corresponding character variety seems to play a dominant role in the volume conjecture.

The main point of all this is that the hyperbolic structure on the knot complement is a topological property of the knot. One can thus use geometric information to distinguish knots and indeed this is employed by the fastest known algorithms to tell knots apart [Wee].

It may seem that being hyperbolic is a rather restrictive condition on a knot but this is not quite the case. It follows from Thurston's geometrization theorem that the only prime knots that are non-hyperbolic are torus knots or satellite knots [BP]. By a torus knot we mean a knot that can be realized as a simple closed curve on the surface of a standard torus. A satellite knot K is constructed from a non-trivial knot P inside a solid torus T and embedding it in \mathbb{S}^3 such that T becomes the solid torus neighborhood of a second nontrivial knot C . The knot P is called the pattern knot and can also be viewed as a two component link in \mathbb{S}^3 by replacing the solid torus by its meridian. C is called the companion knot. In the figure below we have drawn an example of a satellite knot (left).

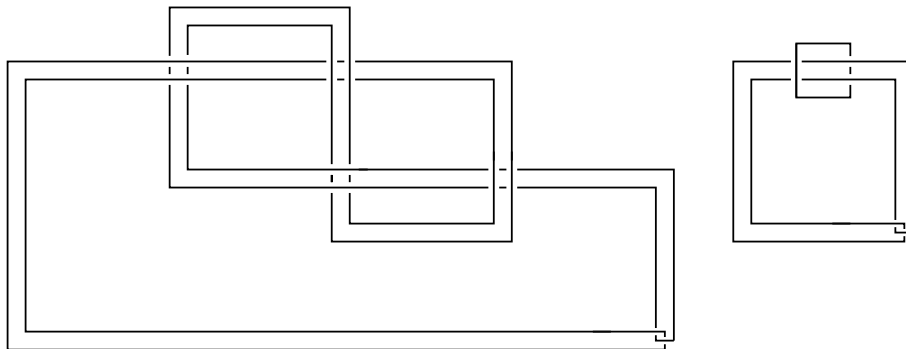


Figure 1.1: Left: a satellite knot of the figure eight knot. The companion knot is the figure eight knot and the pattern link is the Whitehead link shown on the right.

It should be clear now that for hyperbolic knots the hyperbolic volume is a topological invariant and this is what the right hand side of the volume conjecture refers to. What is not yet clear is how to define the volume in case the knot is not hyperbolic. It is standard to extend the hyperbolic volume by stating that it is additive under connected sum so we can restrict to prime knots. So suppose we have a non-hyperbolic prime knot. By Thurston's theorem such a knot is either a torus knot or a satellite knot. We now define the volume of a torus knot to be zero and the volume of a satellite knot to be the volume of its companion plus the volume of its pattern. This provides a natural extension of the volume to all knot complements that is known to agree with the Gromov norm of knot complement.

If one would be allowed only one real number to describe a knot, the extended hyperbolic volume would be a natural choice that retains a lot of information. By the above definition the family of zero volume knots is exactly those that can be obtained from the unknot by repeating the operations connected sum and cabling. By cabling we mean the satellite operation where the pattern is a torus knot. On the other hand, it is known that given any $B > 0$ there are only finitely many hyperbolic knots whose volume is less than B , see [BP]. Although the volume is not a complete invariant it does quite well at distinguishing the hyperbolic ones.

1.1.2 The colored Jones polynomial

The Jones polynomial is the simplest of the Reshetikhin Turaev invariants or quantum knot invariants that are derived from quantum groups. In this elementary account we will base our definition of the Jones polynomial on the Kauffman bracket. As is usual we will work with framed knots throughout, which can be thought of as knotted ribbons instead of strings. The Kauffman bracket of a knot diagram, notation $\langle K \rangle$, is defined by the following relations.

$$\begin{aligned} \langle \emptyset \rangle &= 1 \\ \langle \text{cross} \rangle &= A \langle \text{cup} \rangle + A^{-1} \langle \text{cap} \rangle \\ \langle \text{circle} \cup \text{D} \rangle &= (-A^2 - A^{-2}) \cdot \langle \text{D} \rangle \end{aligned}$$

It is readily shown that the Kauffman bracket is a Laurent polynomial in A which is invariant under the second and third Reidemeister moves. Therefore it is an actual invariant of (framed) knots. The Jones polynomial is a modification of the Kauffman bracket which makes it an invariant of oriented unframed links. But this distinction is irrelevant for the applications we have in mind so we will use (as is customary in the literature) the terminology Kauffman bracket and Jones polynomial interchangeably to refer to the framed version of the invariant.

The (framing dependent) colored Jones polynomial is a more elaborate version of the same construction where one now considers not only the knot but also its parallels. Given a knot K we define its (0-framed) n -th parallel K^n to be the satellite link whose pattern is n parallel unknots and whose companion knot is K . Alternatively K^n is what one gets when one ties the knot K in n parallel strands. K^0 is by definition the empty link.

The (framing dependent) unnormalized N -colored Jones polynomial is defined to be the following linear combination of Kauffman brackets of parallels of K .

$$\tilde{J}_{N+1}(K) = \sum_{j=0}^{\lfloor \frac{N}{2} \rfloor} (-1)^j \binom{N-j}{j} \langle K^{N-2j} \rangle$$

One can give a more natural definition of the N -colored Jones polynomial as the quantum invariant corresponding to the N -dimensional irreducible representation of sl_2 [KM]. Note that the Kauffman bracket itself corresponds to the standard representation and the above formula becomes nothing more than an expression of the N -dimensional representation in terms of tensor powers of the standard representation.

Finally we normalize the invariant by dividing by the value of the unknot O :

$$J_N(K) = \tilde{J}_N(K) / \tilde{J}_N(O)$$

In the formulation of the volume conjecture it is usual to change the variable from A to q by setting $q = A^4$. This then is the version of the colored Jones polynomial referred to above.

Although we work with framed knots, there is no mention of framing in the statement of the volume conjecture. The zero framing on the knot is intended, but the framing does not matter for this version of the conjecture. This is because framing change will cause the colored Jones polynomial to change only by a power of q . Since q is on the unit circle the absolute value will not change.

As indicated before one can also define an unframed version of the Jones polynomial for oriented links by correcting with the writhe. Indeed this is in many cases the more standard terminology. We warn the reader however that in this thesis by colored Jones polynomial we always refer to the colored Kauffman bracket polynomial also known as the framing dependent colored Jones polynomial as this choice seems more natural in our context.

1.2 Main results

Despite many efforts in the last decade and a half, the volume conjecture is still open. We start with a list of knots and links for which the conjecture has been settled independently of this thesis. So far the conjecture has been proven for the figure eight knot, its $(2, q)$ -cables and Borromean doubles [MI] [LT] [YY], torus knots [KT], Whitehead doubles of $(2, q)$ torus knots and twisted Whitehead links [Zh], $(2, q)$ -torus links [Hi2], and finally the Borromean rings [GL2].

The central question addressed in this thesis is to gain elementary understanding of the volume conjecture by examining the simplest non-trivial cases and to make simpler toy models for the conjecture. The toy models we have studied are the classical spin networks and the quantum spin networks at a fixed root of unity. The spin networks we study are closely related to the Jones polynomial, but instead of knots they deal with graphs. Quantum spin networks are a generalization of the Jones polynomial to embedded graphs. Everything done in this thesis can be described as studying the asymptotics of quantum spin network evaluations. At a glance here are some of the main results in the thesis.

Theorem 1.1. (Chapter 1)

The volume conjecture is true for the infinite family of all Whitehead chains.

Theorem 1.2. (Chapter 2)

For any knot K one can add additional unlinked components to get a link L for which the volume conjecture is true.

The theorem holds equally well for when K is a link a knotted trivalent graph.

Theorem 1.3. (Chapters 3,4)

For any quantum spin network (Γ, γ) and any root of unity ζ , the sequence $\langle\langle \Gamma, N\gamma \rangle\rangle(\zeta)$ allows an asymptotic expansion of Nilsson type.

Theorem 1.4. (Chapter 5)

For all links L of volume zero, $J_N(L)(e^{\frac{2\pi i}{N}}) = \mathcal{O}(N^c)$ as $N \rightarrow \infty$ for some c depending on L .

The last theorem means that for all such links the volume conjecture holds provided that we can also give a lower bound to exclude it from decaying exponentially or being zero and we can prove the limit in the left hand side of (1.1) exists.

1.3 Brief history of the conjecture

Let us now give a short overview of the history of the volume conjecture and explain how our approach fits into this picture.

The volume conjecture originated around 1995 as R. Kashaev's conjecture on the asymptotics of his link invariant [Ka1][Ka2]. Kashaev constructed a new knot invariant in a way reminiscent of the definition of the Turaev-Viro 3-manifold invariant [TV]. Starting from a special triangulation of the knot complement he assigned a modified $6j$ -symbol to every tetrahedron in such a way that the result was independent of the chosen triangulation. However Kashaev's modified $6j$ -symbols contain extra structure to deal with the knot in the three manifold and are closely related to the quantum dilogarithm function. The quantum dilogarithm derives its name from the fact that after taking the appropriate classical limit it reduces to the actual dilogarithm function. Kashaev now observed that the dilogarithm function can be used to express the hyperbolic volume of an ideal tetrahedron in terms of its cross ratio. This was one of his motivations for expecting the classical limit of his invariant would produce the hyperbolic volume of the knot complement. This approach has inspired quantum hyperbolic field theory that has given rise to many interesting new conjectures [BB].

Five years later H. Murakami and J. Murakami identified Kashaev's invariant as the N -colored Jones polynomial at the N -th root of unity and reformulated Kashaev's conjecture as we have done above. Together with Y. Yokota they amplified the above motivation for the volume conjecture as follows. Given a knot diagram one can compute the colored Jones polynomial as a trace of a composition of R -matrices and twist parameters, where each R -matrix corresponds to a crossing [MIn]. On the topological side we can also use the crossings to

subdivide the complement of the knot. For each crossing we get an ideal octahedron. Supposing the rate of growth of each R -matrix contributes the volume of the corresponding octahedron one would obtain the volume conjecture. Indeed treating the composition of R -matrices as an integral and applying the method of stationary phase, they derive equations for the parameters of the R -matrices. These equations turn out to be exactly the equations on the shape parameters of the octahedra that ensure that one gets the complete hyperbolic structure [Ch]. Although progress has been made in this direction to make this approach rigorous, there seem to be serious problems in terms of the contour of integration and the choice of diagram.

The volume conjecture can also be fruitfully approached and motivated from the point of view of physics, in particular Chern-Simons theory. Witten [Wit1] gave an interpretation of the Jones polynomial in terms of Chern-Simons theory with gauge group $SU(2)$. By complexifying the gauge group the hyperbolic volume was also interpreted in terms of Chern-Simons theory [Gu]. However, how exactly one passes to the complexification as one takes the classical limit seems as yet unclear [Wit2], [DG], [DGLZ]. Recently the volume conjecture was also interpreted in terms of topological string theory [DF].

1.4 Approach

The common thread that runs through all the chapters in the thesis is to study the colored Jones polynomial by expressing it in terms of $6j$ -symbols. The associated objects in the graphical calculus are called quantum spin networks and this is where the title comes from. Although this way of calculating the Jones polynomial is far from new [KR], [MV], [KL], [Tu], the above theorems show that this approach does have some merit for studying the volume conjecture. Below we briefly sketch the main points of this approach, our motivation for taking it and how it fits with what had already been done.

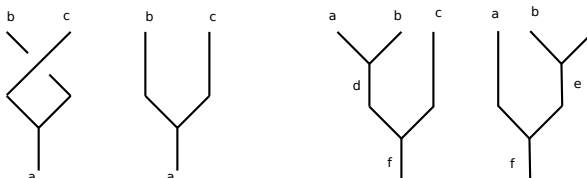


Figure 1.2: The Y shaped figure depicts a projector mapping the bottom representation a into the tensor product of the top two $b \otimes c$. The crossing depicts the R -matrix composed with the flip.

The essence of the approach is depicted graphically in the above picture. As is usual in graphical calculus, the strands are colored by representations of the quantum group. When read from bottom to top, a Y shaped figure (second from the left) depicts the canonical projection that maps the representation a on the bottom edge into the tensor product $b \otimes c$ of the representations present at the top edges. A very important point to make is that since we will always work with quantum sl_2 the tensor product of two irreducible representations decomposes in a multiplicity free way. This fact simplifies matters enormously.

The map Y can also be read as a change of basis that diagonalizes the R -matrix. Indeed by Schur's lemma it is clear that the two left most maps in the figure can only differ by a scalar. We can apply this to any knot diagram, by fusing the strands close to any crossing. After having removed the crossings in this way we are left with a labeled planar graph that represents a composition of Y maps. To evaluate such graphs (also known as spin networks) one can employ the orthogonality relations of the maps but only after making a series of base changes. These base changes connect the two natural bases of the triple tensor product, graphically depicted in the rightmost two pictures of the figure. The coefficients of these base changes are by definition the $6j$ -symbols. The conclusion is that every colored Jones polynomial can be expressed in terms of a sum of products of $6j$ -symbols and powers of q .

In the thesis we choose to shift our attention from the calculation of the colored Jones polynomial for knots to calculating it for trivalent graphs embedded in the three sphere. When such graphs are colored with representations and to be evaluated by the same Reshetikhin-Turaev functor that is used to compute the ordinary Jones polynomials the graphs are called quantum spin networks. Taking spin networks as the fundamental objects has as an advantage that all stages of the computation of the colored Jones polynomial can be treated on equal footing, knot or not. This also puts the volume conjecture within a larger context of questions about the asymptotics of quantum spin networks.

We were led to the viewpoint of quantum spin networks by an attempt to apply a variation of the strategy of Murakami, Murakami and Yokota. Instead of using the crossings as a fundamental building block for both the quantum invariant and the geometry of the knot complement we turn to the standard quantum $6j$ -symbols. Although the quantum $6j$ -symbols we are referring to differ from Kashaev's modified $6j$ -symbols, they are still known to be related to volumes of geometric tetrahedra, [Co3], [CM]. In trying to match the combinatorial triangulation to the $6j$ -symbols in the expression of the colored Jones polynomial it becomes very natural to consider graphs as more fundamental than knots.

Another advantage of viewing the volume conjecture in terms of quantum spin networks is that non-trivial toy models become available by leaving the root of unity fixed. In the case of knots and links this leads to trivial results but the study of the asymptotics of quantum spin networks at a fixed root of unity is far from settled. The simplest toy model that appears in such a way are the classical spin networks. These are quantum spin networks evaluated at $q = 1$.

By going back to classical spin networks we reconnect the volume conjecture mathematics that already existed before the Jones polynomial. Classical spin networks have been studied since the beginning of quantum mechanics under the name of addition of quantum angular momentum. And indeed their asymptotics have been studied intensively resulting in a conjecture by Ponzano and Regge [PR] relating the asymptotics of the tetrahedral spin network to the Euclidean geometric tetrahedron. This conjecture then can be interpreted as a toy version of the volume conjecture and studying it will tell us something about the original conjecture. Later on classical spin networks were used by Penrose [Pe1] in attempts to quantize gravity combinatorially and they still play an important role in three-dimensional quantum gravity [Ro].

1.5 Overview of the thesis

Let us now give a brief overview of the chapters to come in the light of the common theme asymptotics of spin networks described above.

In the second chapter we deal with a family of links obtained by composing three simple 2-2 tangles. By composing these tangles with the Y map as sketched above we find explicit formulas for the colored Jones polynomial and relate them to the geometry of the complement. One of these 2-2 tangles, the belt tangle, plays a significant role in simplifying matters even further, as does the arithmeticity of the links involved and these two aspects motivated the results in the next chapter.

The third chapter is largely a continuation and expansion of the ideas presented in chapter one. Here the belt tangle introduced in chapter one is exploited in full to augment arbitrary knots. This augmentation dramatically reduces the complexity of both the Jones polynomial of the knot and the geometry of its complement.

Furthermore we present an extension of the volume conjecture to links and quantum spin networks where all components have equal color. From the point of view of the calculation this is natural and the same proof that works in the knot case works extends to quantum spin networks. The main point of the proof is that changing the diagram step by step one can simultaneously observe how the colored Jones polynomial and the geometry of the complement change. Both are described by the same graphical formalism.

In chapter four we turn away from the full volume conjecture to focus on the toy model that deals with classical spin networks. Here we give a new semi explicit evaluation for classical spin networks in terms of a generating function. We then remark that the classical spin network evaluations can be expressed as sums of hypergeometric terms. Using Wilf-Zeilberger theory [PWZ] we thus conclude that every spin network satisfies a recursion relation when one scales the labels. Coupled with the theory of (Siegel) G -functions this allows us to prove the existence of a full asymptotic expansion of any classical spin network evaluation. We study the special case of the tetrahedral spin network in detail and settle rigorously the previously unknown cases of the Ponzano-Regge conjecture using Borel transforms.

Chapter five is largely a generalization to quantum spin networks of the main results on classical spin networks obtained in the previous chapter. However the quantum spin networks are still required to be evaluated at a fixed root of unity. In order to be able to evaluate at a root of unity at all we first prove an integrality result extending work of Costantino [Co2]. It should be noted that there also exists a different notion of evaluating at a root of unity where one works with the quantum group itself at a root of unity, [GR]. These evaluations gives rise more refined behavior and are not covered in our work. Finally we formulate a conjecture about how the leading asymptotics at any fixed root of unity is controlled by the leading asymptotics of the corresponding classical spin network.

In the final chapter we return to the original volume conjecture and examine some limitations of our approach using $6j$ -symbols. Here we study the class of knots and links whose (generalized) hyperbolic volume equals zero. In many ways such knots possess the simplest topology and there exists a full classification of them. Yet the method of calculating the colored Jones polynomial we

consider gives very unsatisfying results in this case. Most of the terms in the resulting sum of $6j$ -symbols show exponential growth, but we know the volume is zero. So if the volume conjecture is to hold all such terms should cancel to very high order. And indeed they do.

Using different approach based on Schur-Weyl duality we prove a general cabling formula for the evaluation of all zero volume links and knots. From this formula it is immediate that the invariants are growing at most polynomially when q is on the unit circle. An interesting point about the cabling formula is that it motivates considering more general asymptotics than the one we concentrate on in the volume conjecture.

It should be noted that most of the results of chapters three and four generalize naturally from spin network evaluations to holonomic and q -holonomic sequences, where q is set to a fixed root of unity. (By a (q) -holonomic sequence we mean a sequence satisfying a (q) -difference equation). In some sense spin networks merely provide natural geometric examples for studying such sequences. This theme persists in the case of the original volume conjecture in the sense that it was shown that the sequence of colored Jones polynomials is always q -holonomic [GaLe]. In the AJ-conjecture this q -recursion was related to the $SL(2, \mathbb{C})$ character variety of the knot in [Ga0]. This is a theme that plays a central role in the volume conjecture.

1.6 Generalizations

We end this introduction with a brief account of the various ways the volume conjecture has been generalized and extended so far. We have already seen the volume conjecture can be generalized to links and graphs (spin networks) to some extent but in the case of general colors problems may arise [LT], [GR].

The conjecture can also be generalized by varying the ambient 3-manifold. Specializing to the case of the empty link in a general 3-manifold this becomes of the asymptotics of quantum invariants of 3-manifolds for which there are related conjectures [Gu], [And]. One can reformulate the question in terms of links in the three-sphere by presenting the 3-manifold as surgery on an auxiliary link. Of course the surgery link has to be colored in the appropriate way, so we have to consider more general mixed asymptotics of Jones polynomials of links.

A different generalization involves changing the evaluation of q from $q = \frac{2\pi i}{N}$ to $q = \frac{c}{N}$. It is conjectured that the asymptotics one now sees is related to incomplete geometric structures on the complement or more generally to other points on the character variety [GuM], [MuE]. Indeed we have already mentioned that the complete hyperbolic structure corresponds to a very special point on the character variety. Also for c very close to 0 this has been verified to correspond to the abelian representations. This is an extension of the proof of the Melvin–Morton–Rozanski conjecture [BG], [GL2].

The last generalization we mention is to change the Lie algebra sl_2 and consider the asymptotics of quantum invariants related to other (simple) Lie algebras. Due to technical difficulties there are not many concrete indications of what geometric quantity the asymptotics should measure [HL] [DG]. To gain intuition in this case it would be fruitful to extend the toy model of classical spin networks to this case but even this seems to be a daunting problem.

Chapters one and two were published as two papers in [V1], [V2]. Chapters

three and four are joint papers with Stavros Garoufalidis that are submitted.
Chapter five appeared as a preprint [V3].

Chapter 2

Proof of the volume conjecture for Whitehead Chains

2.1 Introduction

The volume conjecture relates the colored Jones polynomials of a knot to the simplicial volume of its complement. More precisely, let us denote the normalized N -colored Jones polynomial of a knot K by $J_N(K)$ and let $\text{Vol}(K)$ be v_3 times the simplicial volume (Gromov norm) of $\mathbb{S}^3 - K$, where v_3 is the volume of the hyperbolic regular ideal tetrahedron. The volume conjecture can now be stated as follows:

Conjecture 2.1. (*Volume conjecture*) [MM]

For any knot K we have:

$$\lim_{N \rightarrow \infty} \frac{2\pi}{N} \log |J_N(K)(e^{\frac{2\pi i}{N}})| = \text{Vol}(K)$$

So far the conjecture has been proven for only the figure eight knot, torus knots, Whitehead doubles of certain torus knots and connected sums of these knots, [MI], [KT], [Zh].

It is well known that the volume conjecture is false for many splittable links so it is unclear how to extend the volume conjecture to links. On the other hand, the volume conjecture has been shown to hold for the Whitehead link [Zh] and the Borromean rings [GL2]. In this paper, we introduce the family of Whitehead chains generalizing both the Whitehead link and the Borromean rings and we settle the volume conjecture for this family.

The Whitehead chains are defined in terms of the tangles Belt, Clasp and Twist depicted in the figure 2.1 on the next page.

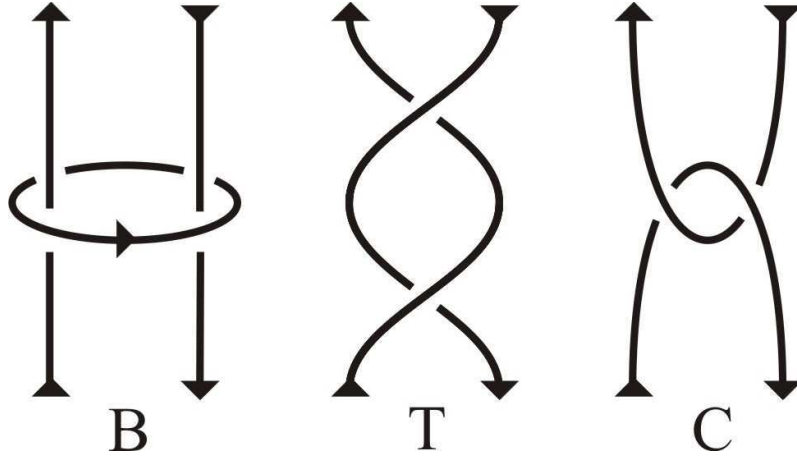


Figure 2.1: The tangles Belt, Twist and Clasp

Definition 2.1. Let a, b, c, d be integers such that $b \geq 1$ and $c, d \geq 0$. Define the Whitehead chain $W_{a,b,c,d}$ to be the closure of the composition of a tangles of type Twist (or a mirror images of type Twist when $a < 0$), b tangles of type Belt, c tangles of type Clasp and d mirror images of tangles of type Clasp.

The tangles Belt, Twist, Clasp and their mirror images commute, so the order of composition is immaterial. Therefore the Whitehead chains are well defined. In the notation of the previous definition the Whitehead link is $W_{0,1,1,0}$ and the Borromean rings are $W_{0,1,1,1}$.

Our main theorem is the following asymptotic expansion for the colored Jones polynomial of a Whitehead chain. In the statement below the notation $x_N \sim y_N$ means that the quotient x_N/y_N converges to 1 as N goes to infinity.

Main theorem. Let a, b, c, d be integers, such that $b \geq 1$ and $c, d \geq 0$.

$$J_N(W_{a,b,c,d})(e^{\frac{2\pi i}{N}}) \sim \exp\left(\frac{1}{2\pi}\{(\text{Vol}(W_{a,b,c,d}) + i\text{CS})N + D \log(N) + E\}\right)$$

- The value of CS is $\frac{-4a+c-d}{8}2\pi^2$ if $c+d=1$ and $\frac{-4a-7c+7d}{8}2\pi^2$ otherwise.
- If $b=1$ we have $D=3\pi$ and $\exp(E)$ can be expressed explicitly as an integral depending on a, c, d , see the end of the proof of lemma 4.
- If $b \geq 2$ the expansion is only valid for odd N and $J_{2M}(W_{a,b,c,d})(e^{\frac{2\pi i}{2M}}) = 0$. For odd N we find $D=2\pi b$ and $E = -2\pi(c+d) \log 2 + \frac{4a+3c-3d}{4}2\pi^2 i$.

By taking absolute values and restricting ourselves to the leading term we see that the volume conjecture holds true for $b=1$, while it is false for $b \geq 2$. In the latter case the volume conjecture is true when we restrict to odd values of N . This phenomenon might have something to do with the fact that the complement of the Whitehead chain is hyperbolic when $b=1$, while the torus decomposition contains a Seifert-fibered piece when $b \geq 2$.

According to the complexified volume conjecture proposed in [MMOTY] the value of CS is equal to $2\pi^2$ times the Chern-Simons invariant. For $a = 0$ this is indeed the case because the Chern-Simons invariant is additive with respect to belted sum and its value on the Whitehead link and its mirror image is $\pm\frac{1}{8}$, [Ou].

In [Hi1] the number D in the above asymptotic expansion is conjectured to be the number of prime factors of a knot. In [GuM] a different interpretation is given in terms of the knot complement. In the same paper it is also conjectured that the number E is determined by the Ray-Singer torsion of the complement twisted by the holonomy representation. We hope to investigate these conjectures for the Whitehead chains in a subsequent publication.

The main theorem shows that the original volume conjecture may fail even for non-splittable links, but adds credibility to the following weaker version of the volume conjecture for links:

Conjecture 2.2. *For any non-splittable link L we have:*

$$\limsup_{N \rightarrow \infty} \frac{2\pi}{N} \log |J_N(L)(e^{\frac{2\pi i}{N}})| = \text{Vol}(L)$$

2.2 Proof of the main theorem

In this section we give an overview of the proof of the main theorem, postponing the proofs of the more technical lemmas to the next section.

The first step is to obtain an expression for the colored Jones polynomials of a general Whitehead chain.

Lemma 2.1. *Let a, b, c, d be integers, with $b \geq 2$ and $c, d \geq 0$. We have the following formulas for the colored Jones polynomial:*

$$J_N(W_{a,1,c,d})(e^{\frac{2\pi i}{N}}) = \phi_N \sum_{n=0}^{N-1} (2n+1) \chi_{N,n}^{4a-c+d} \left(\sum_{k=0}^{N-1-n} S_{n,k} \right)^{c+d}$$

$J_N(W_{a,b,c,d})(e^{\frac{2\pi i}{N}}) = 0$ when N is even and for $N = 2M + 1$ we have:

$$J_N(W_{a,b,c,d})(e^{\frac{2\pi i}{N}}) = \phi_N N^b \chi_{N,M}^{4a-c+d} \left(\sum_{k=0}^M S_{M,k} \right)^{c+d}$$

Where we define $\phi_N = \exp\left(\frac{(N-1)(c-d)}{N}\pi i\right)$ if $c+d = 1$ and $\phi_N = (-1)^{(N-1)(c-d)}$ otherwise, and we define χ and S by

$$\chi_{N,n} = \exp\left(\frac{n(n+1-N)}{2N}\pi i\right), \quad S_{n,k} = \prod_{j=1}^n \frac{2 \sin^2\left(\frac{(k+j)\pi}{N}\right)}{\sin\left(\frac{j\pi}{N}\right)}$$

Proof. Recall that the unnormalized N -colored Jones invariants are intertwining operators of $V_N \otimes V_N$, where V_N corresponds to the N -dimensional irreducible representation of sl_2 . Using the decomposition $V_N \otimes V_N = \bigoplus_{n=0}^{N-1} V_{2n+1}$ one

can write the unnormalized colored Jones invariants of the tangles in figure 2.1 in the following way [Zh]:

$$\tilde{J}_N(t) = \bigoplus_{n=0}^{N-1} \text{Tangle}(n, t) \cdot \text{id}_{V_{2n+1}}$$

where the function $\text{Tangle}(n, t)$ depends on the tangle and $t = e^h$. If we define $[n] = \frac{t^{\frac{n}{2}} - t^{-\frac{n}{2}}}{t^{\frac{1}{2}} - t^{-\frac{1}{2}}}$ then the functions for the tangles in figure 2.1 are:

$$\text{T}(n, t) = t^{n(n+1)}, \quad \text{B}(n, t) = \frac{[N(2n+1)]}{[2n+1]}$$

$$\text{C}(n, t) = t^{(N^2-1)/2 + N(N-1)/2} \sum_{k=0}^{N-1-n} t^{-N(n+k)} \prod_{j=1}^n \frac{(1-t^{N-j-k})(1-t^{j+k})}{1-t^j}$$

The colored Jones polynomials of the mirror-images of these tangles are obtained by replacing t by t^{-1} . The factor $t^{(N^2-1)/2}$ in the formula for $\text{C}(n, t)$ is a correction due to framing that should be included only if both strands in the clasp belong to the same component. For Whitehead chains this means that it should be included only when $c + d = 1$.

By the multiplicativity of the colored Jones invariant with respect to composition of tangles we can now calculate the colored Jones polynomial of all Whitehead chains. The general formula for the normalized version of the colored Jones polynomial of the Whitehead chains is:

$$J_N(W_{a,b,c,d})(t) = \sum_{n=0}^{N-1} \frac{[2n+1]}{[N]} \text{T}(n, t)^a \text{B}(n, t)^b \text{C}(n, t)^c \text{C}(n, t^{-1})^d$$

The factor $\frac{[2n+1]}{[N]}$ comes from the normalization and from taking the closure of composition of the tangles.

Routine calculations now yield the above formulas. △

From now on we will use the shorthand $J_{N,a,b,c,d} = J_N(W_{a,b,c,d})(e^{\frac{2\pi i}{N}})$.

The next step in proving the main theorem is to investigate the asymptotics of the above formulas for the colored Jones polynomials as $N \rightarrow \infty$. The factors $S_{n,k}$ turn out to play a crucial role because they dominate the absolute value of the (n, k) -th term. There exists a unique maximum $\tilde{S}_N = S_{\lfloor \frac{N}{2} \rfloor, \lfloor \frac{N}{4} \rfloor}$ for the $S_{n,k}$. This term dominates all others so that most of the asymptotics of $J_{N,a,b,c,d}$ can be read off from this term only. In order to make this precise we need to compare the other values of $S_{n,k}$ to the maximum value.

Let us choose a fixed number $\delta \in (\frac{1}{2}, \frac{c+d+5}{2(c+d+4)})$ once and for all, where the numbers c and d are the parameters of $W_{a,b,c,d}$. Define $n' = |n - \lfloor \frac{N}{2} \rfloor|$ and $k' = |k - \lfloor \frac{N}{4} \rfloor|$ to be the distances from the maximum. The next lemma shows how we can estimate the other values of $S_{n,k}$.

Lemma 2.2. *Using the above definitions of n', k' and δ we have:*

- a) *If $n' + k' < N^\delta$ then $S_{n,k} \tilde{S}_N^{-1} = \exp(-\frac{\pi}{N}(n'^2 + 2n'k' + 2k'^2)) + \mathcal{O}(N^{3\delta-2})$, as $N \rightarrow \infty$.*
- b) *There are $C, \epsilon > 0$ such that if $n' + k' \geq N^\delta$ then $S_{n,k} \tilde{S}_N^{-1} < C \exp(-\epsilon N^{2\delta-1})$*

In lemma 3 the asymptotics of the maximum value \tilde{S}_N are expressed using the Lobachevski function $\Lambda(\theta) = -\int_0^\theta \log |2 \sin(x)| dx$.

Lemma 2.3. $\tilde{S}_N \sim \exp\left(\frac{4N}{\pi}\Lambda\left(\frac{\pi}{4}\right) - \frac{1}{2}\log 2N\right)$, $N \rightarrow \infty$

The asymptotics of $J_{N,a,1,c,d}$ is reduced to that of \tilde{S}_N by the following lemma. By CS we mean the constant defined in the statement of the main theorem.

Lemma 2.4. *There is a nonzero constant $C \in \mathbb{C}$ such that:*

$$J_{N,a,1,c,d} \sim CN^{(c+d+3)/2} \tilde{S}_N^{c+d} e^{\frac{iCS}{2\pi}}, \quad N \rightarrow \infty$$

There is a similar lemma for the case $b \geq 2$. We confine ourselves to the odd-colored Jones polynomials, since the even ones are 0 in $e^{\frac{2\pi i}{N}}$. In lemma 5 we reduce the asymptotics of the odd colored Jones polynomial to those of the maximal term \tilde{S}_N :

Lemma 2.5. *For $b \geq 2$ and N odd we have: $J_{N,a,b,c,d} \sim$*

$$\exp\left(- (c+d)\log\sqrt{2} + (4a+3c-3d)\pi i/4\right) N^{(c+d+2b)/2} \tilde{S}_N^{c+d} e^{\frac{iCS}{2\pi}}$$

Postponing the proofs of these lemmas to the next subsection we can now prove the main theorem.

Proof. (of the main theorem)

Using an explicit decomposition of the complement into ideal octahedra it can be shown that $\text{Vol}(W_{a,b,c,d}) = 8(c+d)\Lambda\left(\frac{\pi}{4}\right)$, see [V0]. Let us first suppose that $b = 1$. According to lemma 4 there is a constant C' such that we have:

$$J_{N,a,1,c,d} \sim \exp\left(\log(\tilde{S}_N^{c+d}) + \frac{c+d+3}{2}\log(N) + Ni\frac{CS}{2\pi} + C'\right)$$

Using lemma 3 we get:

$$\sim \exp\frac{1}{2\pi} ((\text{Vol}(W_{a,1,c,d}) + iCS)N + 3\pi\log(N) + E), \quad N \rightarrow \infty$$

The case $b \geq 2$ follows in the same way by combining lemma 3 and lemma 5. \triangle

2.3 Proof of the lemmas

In this section we prove the more technical lemmas 2,3,4 and 5.

Proof. (of lemma 2) The proof of this lemma hinges on the following key estimate of $S_{n,k}$ in terms of the Lobachevski function $\Lambda(x)$ that was proved in [Zh]. Define $f(x,y) = -2\Lambda(x+y) + 2\Lambda(y) + \Lambda(x)$. For integers $0 \leq n, k, n+k < N$ we have the uniform estimate

$$\log S_{n,k} = \frac{N}{\pi} f\left(\frac{n\pi}{N}, \frac{k\pi}{N}\right) + \mathcal{O}(\log N), \quad N \rightarrow \infty$$

Before we can apply this result we first need to show that inside the triangle $0 < x, y, x+y < \pi$ the function f has a unique critical point $(\frac{\pi}{2}, \frac{\pi}{4})$ and reaches

its maximum there, which equals $4\Lambda(\frac{\pi}{4})$. Moreover the Taylor expansion of f around the critical point is:

$$f\left(\frac{\pi}{2} + x, \frac{\pi}{4} + y\right) = f\left(\frac{\pi}{2}, \frac{\pi}{4}\right) - (x^2 + 2xy + 2y^2) + \mathcal{O}(|x|^3 + |y|^3)$$

Lemma 2 part a) and b) are direct consequences of these facts once we note that the difference between $S_{\lfloor \frac{N}{2} \rfloor, \lfloor \frac{N}{4} \rfloor}$ and the actual critical value $f(\frac{\pi}{2}, \frac{\pi}{4})$ becomes negligibly small as N grows.

To find the critical points of f in $0 < x, y, x + y < \pi$ we use the fundamental theorem of calculus to differentiate Λ and find the system of equations: $2\sin^2(x + y) = \sin(x)$ and $\sin(x + y) = \sin(y)$. For $0 < x, y, x + y < \pi$ this has the unique solution $(x, y) = (\frac{\pi}{2}, \frac{\pi}{4})$. To determine the nature of the critical point we differentiate again and this will be left to the reader.

The value of f at its critical point is $f(\frac{\pi}{2}, \frac{\pi}{4}) = -2\Lambda(\frac{3}{4}\pi) + 2\Lambda(\frac{\pi}{4}) + \Lambda(\frac{\pi}{2}) = 4\Lambda(\frac{\pi}{4})$ because $\Lambda(x) = -\Lambda(\pi - x)$. \triangle

The next lemma is an expanded version of a result proven in [Zh].

Proof. (of lemma 3) If we define $s_n = -\sum_{j=1}^n \log |2\sin(j\pi/N)|$ then we can write $\log \tilde{S}_N = -2s_{\lfloor N/4 \rfloor + \lfloor N/2 \rfloor} + 2s_{\lfloor N/4 \rfloor} + s_{\lfloor N/2 \rfloor}$. It was shown in [Zh] that for $0 < n < \frac{5}{6}N$ we have $s_n = \frac{N}{\pi}\Lambda(\frac{n\pi}{N}) - \frac{1}{2}\log n + \mathcal{O}(1)$, as $N \rightarrow \infty$. To prove the lemma we need to expand a little further. Assuming that $r = \lim_{N \rightarrow \infty} n/N$ exists, we show that

$$s_n = \frac{N}{\pi}\Lambda\left(\frac{n\pi}{N}\right) - \frac{1}{2}\log \frac{n \sin(r\pi)}{r\pi} + \mathcal{O}(N^{-1}), \quad N \rightarrow \infty$$

By applying the above expansion for s_n three times we find the desired expansion for \tilde{S}_N .

To prove the expansion for s_n we reason as follows: for $x \in [0, \frac{5}{6}\pi] - \{0, u\}$ we have

$$\frac{\sin(x - u)}{x - u} \frac{x}{\sin x} = 1 + \frac{-x \cos x + \sin x}{x \sin x} u + \mathcal{O}(u^2), \quad u \rightarrow 0$$

Now taking the logarithm and expanding $\log(1 + f)$ around $f = 0$ we find:

$$\log \left| \frac{\sin(x - u)}{\sin x} \right| = \log \left| \frac{x - u}{x} \right| + \frac{-x \cos x + \sin x}{x \sin x} u + \mathcal{O}(u^2)$$

Following [Zh] p.7 we set $x = j\pi/N$ and find:

$$\begin{aligned} s_n - \frac{N}{\pi}\Lambda\left(\frac{n\pi}{N}\right) &= \sum_{j=1}^n \frac{N}{\pi} \int_0^{\frac{\pi}{N}} \log \frac{\sin(j\pi/N - u)}{\sin j\pi/N} du = \\ &= -\frac{1}{2}\log n - \frac{1}{2}\log 2\pi + \sum_{j=1}^n \frac{N}{\pi} \int_0^{\frac{\pi}{N}} \frac{-(j\pi/N) \cos(j\pi/N) + \sin j\pi/N}{j\pi/N \sin j\pi/N} u du + \mathcal{O}(N^{-1}) \end{aligned}$$

The term $-\frac{1}{2}\log 2\pi$ is the constant contribution of the Stirling series used in [Zh] p.7. After integration with respect to u we can write the above sum as a Riemann sum. A computation then shows that the limit of this sum equals $\frac{1}{2}(\log r\pi - \log \sin r\pi)$. \triangle

Although the proof of lemma 4 below is quite long the main idea is simple: Use lemma 2 to estimate the value of the colored Jones polynomial in terms of the maximum value \tilde{S}_N .

Proof. (of lemma 4) For convenience we will assume throughout the proof that $c + d \geq 2$, so that the value of CS is $\frac{-4a-7c+7d}{8}2\pi^2$. The proof in the case $c + d = 1$ is completely analogous. According to lemma 1 the formula for the N -colored Jones polynomial of the one-belted Whitehead chain is

$$J_{N,a,1,c,d} = \phi_N \sum_{n=0}^{N-1} (2n+1) \chi_{N,n}^{4a-c+d} \left(\sum_{k=0}^{N-1-n} S_{n,k} \right)^{c+d}$$

Define the quotient $Q_N = J_{N,a,1,c,d} N^{-(c+d+3)/2} \tilde{S}_N^{-(c+d)} e^{\frac{4a+7c-7d}{8} N\pi i}$. We aim to show that $Q_\infty = \lim_{N \rightarrow \infty} Q_N = C$ for some nonzero complex constant.

Step 1: By expanding the $c + d$ -th power of the sum we obtain a multi-sum over all N -tuples of natural numbers $n, \mathbf{k} < N$ such that $n + k_j < N$. Define Central to be the set of all such tuples that satisfy $n + \max k_j < N^\delta$ and define Far to be the set of tuples such that $n + \max k_j \geq N^\delta$. We can then rewrite Q_N as follows: $Q_N =$

$$\begin{aligned} & \phi_N e^{\frac{4a+7c-7d}{8} N\pi i} N^{-(c+d+3)/2} \sum_{\text{Central}} (2n+1) \chi_{N,n}^{4a-c+d} S_{n,k_1} \cdots S_{n,k_{c+d}} \tilde{S}_N^{-(c+d)} \\ & + \phi_N e^{\frac{4a+7c-7d}{8} N\pi i} N^{-(c+d+3)/2} \sum_{\text{Far}} (2n+1) \chi_{N,n}^{4a-c+d} S_{n,k_1} \cdots S_{n,k_{c+d}} \tilde{S}_N^{-(c+d)} \end{aligned}$$

The Far sum converges to zero absolutely, because each tuple n, \mathbf{k} in the sum contains a k_m such that $n + k_m \geq N^\delta$. According to lemma 2b this means that $S_{n,k_m} \tilde{S}_N^{-1} = \mathcal{O}(\exp(-\epsilon N^{2\delta-1}))$. We can estimate all other factors $S_{n,k_j} \tilde{S}_N^{-1}$ by a constant and conclude that the sum of absolute values of the Far sum converges to zero since $\delta > 1/2$. So far we have shown that $Q_\infty =$

$$\lim_{N \rightarrow \infty} \phi_N e^{\frac{4a+7c-7d}{8} N\pi i} N^{-\frac{c+d+3}{2}} \sum_{\text{Central}} (2n+1) \chi_{N,n}^{4a-c+d} S_{n,k_1} \cdots S_{n,k_{c+d}} \tilde{S}_N^{-(c+d)}$$

Step 2: In the next step we replace the factor $(2n+1)$ in the expression for Q_∞ by a factor N . This is done by showing that the difference converges to zero. The absolute value of the difference is less than

$$N^{-(c+d+3)/2} \sum_{\text{Central}} |2n+1 - N| S_{n,k_1} \cdots S_{n,k_{c+d}} \tilde{S}_N^{-(c+d)}$$

For central tuples n, \mathbf{k} we have $n' < N^\delta$ and hence $2n+1 = N + \mathcal{O}(N^\delta)$. The number of terms in the sum is of order $\mathcal{O}(N^{(c+d+1)\delta})$ and the product $S_{n,k_1} \cdots S_{n,k_{c+d}} \tilde{S}_N^{-(c+d)}$ is $\mathcal{O}(1)$ by lemma 2a. Therefore the absolute value of the difference is at most of order $\mathcal{O}(N^{-(c+d+3)/2 + (c+d+2)\delta})$. Since $\delta < \frac{c+d+5}{2(c+d+4)} < \frac{c+d+3}{2(c+d+2)}$ the difference converges to zero and we have:

$$Q_\infty = \lim_{N \rightarrow \infty} \phi_N e^{\frac{4a+7c-7d}{8} N\pi i} N^{-(c+d+1)/2} \sum_{\text{Central}} \chi_{N,n}^{4a-c+d} S_{n,k_1} \cdots S_{n,k_{c+d}} \tilde{S}_N^{-(c+d)}$$

Step 3: Define the $(c + d + 1)$ -variable Gaussian function

$$g_N(x, \mathbf{y}) = \exp -\frac{\pi}{N} \left((c + d - (4a + c - d)i) \frac{x^2}{2} + 2 \sum_{j=1}^{c+d} (y_j + \frac{x}{2})^2 \right)$$

and let $\psi = \exp(\frac{4a+3c-3d}{4}\pi i)$. We will show that

$$Q_\infty = \lim_{N \rightarrow \infty} \psi N^{-(c+d+1)/2} \sum_{\text{Central}} g_N(n', \mathbf{k}')$$

Starting with the sum from step 2 we use lemma 2 to replace the factors $S_{n, k_j} \tilde{S}^{-1}$ by exponentials and error terms:

$$\lim_{N \rightarrow \infty} \phi_N e^{\frac{4a+7c-7d}{8} N \pi i} N^{-(c+d+1)/2} \sum_{\text{Central}} \chi_{N, n}^{4a-c+d} \prod_{j=1}^{c+d} \left(\exp\left(-\frac{\pi}{N}(n'^2 + 2n'k'_j + 2k'_j{}^2)\right) + \mathcal{O}(N^{3\delta-2}) \right)$$

To show that the error terms can be removed we estimate the contribution of their absolute values. There are $\mathcal{O}(N^{(c+d+1)\delta})$ terms in the sum so their contribution is of order $\mathcal{O}(N^{(c+d+1)\delta+3\delta-2-(c+d+1)/2})$. This converges to zero because $\delta < \frac{c+d+5}{2(c+d+4)}$.

Next we look at the phase factors ϕ_N and $\chi_{N, n}$. We have $\lim_{N \rightarrow \infty} \phi_N = e^{(c-d)\pi i}$. Furthermore:

$$\chi_{N, n} e^{\frac{N\pi i}{8}} = \exp\left(\frac{n'^2}{2N} - \frac{N}{8} + \frac{n}{2N} + \frac{N}{8}\right)\pi i = \exp\left(\frac{n'^2}{2N}\pi i\right) \exp\left(\frac{n}{2N}\pi i\right)$$

Since $n = \frac{N}{2} + \mathcal{O}(N^\delta)$ we have $\lim_{N \rightarrow \infty} \frac{n}{2N} = \frac{1}{4}$. If we apply this to the above sum we get the desired expression.

Step 4: It seems natural to replace the previous sum by an integral, this is done in step 4. We will show that

$$Q_\infty = \lim_{N \rightarrow \infty} \psi N^{-(c+d+1)/2} \int_{|x| + \max|y_j| < N^\delta - 1} g_N(|x|, |\mathbf{y}|) dx d\mathbf{y}$$

The strategy is to estimate the absolute value of the difference between sum and integral. First we write the sum from step 3 as follows:

$$Q_\infty = \lim_{N \rightarrow \infty} \psi N^{-(c+d+1)/2} \sum_{\text{Central}} \int_{B(n, \mathbf{k})} g_N(n', \mathbf{k}') dx d\mathbf{y}$$

where $B(n, \mathbf{k}) = [n - \frac{N}{2} - \frac{1}{2}, n - \frac{N}{2} + \frac{1}{2}] \times \prod_{j=1}^{c+d} [k_j - \frac{N}{4} - \frac{1}{2}, k_j - \frac{N}{4} + \frac{1}{2}]$. The absolute value of the difference between the sum and the proposed integral above is:

$$N^{-(c+d+1)/2} \left| \sum_{\text{central}} \int_{B(n, \mathbf{k})} g_N(n', \mathbf{k}') dx d\mathbf{y} - \int_{|x| + \max|y_j| < N^\delta - 1} g_N(|x|, |\mathbf{y}|) dx d\mathbf{y} \right|$$

The union of the disjoint blocks $B(n, \mathbf{k})$ as n, \mathbf{k} runs through Central, covers the entire integration domain $|x| + \max|y_j| < N^\delta - 1$ so we can subtract the integrals. However some blocks continue over the boundary of the domain of integration, resulting in a slight error. The terms n, \mathbf{k} such that the corresponding blocks $B(n, \mathbf{k})$ intersect the complement of the domain will be called Border terms. We can estimate the above quantity as follows:

$$\begin{aligned} &< N^{-(c+d+1)/2} \sum_{\text{Central}} \int_{B(n, \mathbf{k})} |g_N(n', \mathbf{k}') - g_N(|x|, |\mathbf{y}|)| dx d\mathbf{y} \\ &+ N^{-(c+d+1)/2} \sum_{\text{Border}} |g_N(n', \mathbf{k}')| \end{aligned}$$

Both sums will be shown to converge to zero, we start with the second one. Since the number of terms on the Border of the integration domain is $\mathcal{O}(N^{(c+d)\delta})$ and $g_N(n', \mathbf{k}') = \mathcal{O}(1)$ the second sum is of order $\mathcal{O}(N^{-(c+d+1)/2+(c+d)\delta})$. This implies that the sum converges to zero because $\delta < \frac{c+d+5}{2(c+d+4)} < \frac{c+d+1}{2(c+d)}$. For the first sum we need to estimate the integrands:

$$\begin{aligned} &|g_N(n', \mathbf{k}') - g_N(|x|, |\mathbf{y}|)| = |g_N(n', \mathbf{k}')| \left| 1 - \right. \\ &\left. \exp \frac{-\pi}{N} \left((c+d - (4a+c-d)i) \frac{|x|^2 - n'^2}{2} + 2 \sum_{j=1}^{c+d} (|y_j| + \frac{|x|}{2})^2 - (k'_j + \frac{n'}{2})^2 \right) \right| \end{aligned}$$

The last expression is of order $\mathcal{O}(N^{\delta-1})$ because $|g_N(n', \mathbf{k}')| = \mathcal{O}(1)$ and $|x|^2 - n'^2 = (|x| + n')(|x| - n')$ and $(|y_j| + \frac{|x|}{2})^2 - (k'_j + \frac{n'}{2})^2 = (|y_j| + \frac{|x|}{2} + k'_j + \frac{n'}{2})(|y_j| + \frac{|x|}{2} - k'_j - \frac{n'}{2})$. We integrate over $B(n, \mathbf{k})$ so $|n' - |x|| < 1$ and $|k'_j - |y_j|| < 1$ and all terms are central so $|x| + n' < N^\delta$ and $k'_j + |y_j| < N^\delta$. Therefore the second sum is of order $\mathcal{O}(N^{-(c+d+1)/2+\delta-1+(c+d+1)\delta})$ and thus converges to zero, because $\delta < \frac{c+d+5}{2(c+d+4)} < \frac{c+d+3}{2(c+d+2)}$.

Step 5: We make the substitution $x = \sqrt{N}w$ and $y_j = \sqrt{N}z_j$ with Jacobian $N^{(c+d+1)/2}$. This gives:

$$\begin{aligned} Q_\infty &= \lim_{M \rightarrow \infty} \psi \int_{w + \max|z_j| < \frac{(N^\delta - 1)}{\sqrt{N}}} \\ &\exp(-\pi \left((c+d - (4a+c-d)i) \frac{|w|^2}{2} + 2 \sum_{j=1}^{c+d} (|z_j| + \frac{|w|}{2})^2 \right)) dw dz \end{aligned}$$

Now $\delta > \frac{1}{2}$ and the integrand is rapidly decreasing so the limit exists and is equal to:

$$\psi \int_{\mathbb{R}^{c+d+1}} \exp(-\pi \left((c+d - (4a+c-d)i) \frac{|w|^2}{2} + 2 \sum_{j=1}^{c+d} (|z_j| + \frac{|w|}{2})^2 \right)) dw dz$$

Step 6: In this final step we need to show that $Q_\infty \neq 0$. We know that $\psi \neq 0$, but what about the complicated Gaussian integral above? We can write it as

an iterated integral and get rid of the absolute value signs by integrating 2^{c+d+1} times over the positive hyper-quadrant $w, z_j > 0$:

$$Q_\infty = \psi 2^{c+d+1} \int_0^\infty \exp(-\pi(c+d - (4a+c-d)i)\frac{w^2}{2})dw \cdot \prod_{j=1}^{c+d} \int_0^\infty \exp(-2\pi(z_j + \frac{w}{2})^2)dz_j dw$$

Using the substitutions $y_j = \sqrt{2\pi}(z_j + \frac{w}{2})$ we get the integral below. We only want to check that the integral is nonzero so all constants in front of the integral and the Jacobian are written as C .

$$Q_\infty = C \int_0^\infty \exp(-\pi(c+d - (4a+c-d)i)\frac{w^2}{2}) \cdot \prod_{j=1}^{c+d} \int_{\frac{\sqrt{\pi}w}{\sqrt{2}}}^\infty \exp(-y_j^2)dy_j dw$$

If we define the complementary error function [Wei] by

$$\operatorname{erfc}(x) = \frac{2}{\sqrt{\pi}} \int_x^\infty \exp(-y^2)dy$$

then we can write the integral more concisely as:

$$Q_\infty = C \int_0^\infty \exp(-\pi(c+d - (4a+c-d)i)\frac{w^2}{2}) \operatorname{erfc}^{c+d} \left(\frac{\sqrt{\pi}w}{\sqrt{2}} \right) dw = C \int_0^\infty \exp(-\pi(c+d)\frac{w^2}{2}) \operatorname{erfc}^{c+d} \left(\frac{\sqrt{\pi}w}{\sqrt{2}} \right) \cdot \left(\cos\left(\frac{4a+c-d}{2}\pi w^2\right) + i \sin\left(\frac{4a+c-d}{2}\pi w^2\right) \right) dw$$

After the substitution $x = \sqrt{\frac{4a+c-d}{2}}w$ we note that the imaginary part of integral is nonzero, because both the exponential function and the complementary error function are bounded and decrease monotonically and the decrease is quite rapid. Therefore the integral over the part where the sine is positive dominates the integral over its complement, showing that the integral is a positive scalar multiple of C . Note that the constant E mentioned in the main theorem equals $\log Q_\infty$. △

The same proof also works for lemma 5 but in this case it is much easier because the value of n is fixed at the maximum. The Gaussian integral at the end of step 5 is now a standard Gaussian integral so that the constant in front of lemma 5 can be computed easily.

Chapter 3

The volume conjecture for augmented knotted trivalent graphs

3.1 Introduction

The volume conjecture proposes a relation between the colored Jones invariants of a knot and the simplicial volume of its complement. In the formulation of [MM] the precise statement is as follows. Note that we use the variable A from skein theory instead of the q used in [MM] (the variables are related by $A^4 = q$).

Conjecture 3.1. *Volume conjecture [Ka2], [MM]. For any knot K we have:*

$$\lim_{N \rightarrow \infty} \frac{2\pi}{N} \log |J_N(K)(e^{\frac{\pi i}{2N}})| = \text{Vol}(\mathbb{S}^3 - K)$$

where J_N denotes the N -colored Jones invariant of K and Vol is the simplicial volume.

To gain more insight into this conjecture and to find simple examples where it holds true we seek to generalize the conjecture to the class of knotted trivalent graphs (KTGs) as defined in [DTh]. Roughly speaking a KTG is a thickened embedded graph that is allowed to have multiple edges and also edges without vertices, so that KTGs generalize framed knots and links.

Before turning to general KTGs we first discuss the generalization of the volume conjecture to links. For links the above version of the volume conjecture does not hold, because it fails for many split links [MMOTY] and it also fails in a more serious way for the Whitehead chains defined in [V1].

For a split link (a link some of whose components can be separated from each other by a sphere in the complement) the normalization of the colored Jones invariant has to be adjusted slightly. For knots the colored Jones invariant was normalized by dividing by the unnormalized invariant of the unknot. If we use this normalization for a split link then the colored Jones invariant vanishes at the root of unity as was noted in [MMOTY]. To avoid this problem we propose the following normalization. For a split link with s split components we

normalize by dividing by the unnormalized invariant of the s -fold unlink. With this normalization the normalized colored Jones invariant becomes multiplicative under distant union, see section 3.3. Since the simplicial volume is additive with respect to distant union it follows that using this normalization the volume conjecture is true for a split link if it holds for all its split components.

The above conjecture fails in a more serious way in the case of the Whitehead chains. For these links it was shown [V1] that $J_N(e^{\frac{\pi i}{2N}}) = 0$ for all even N but that the limit proposed in the volume conjecture is still valid when one restricts to odd colors N . In section 3.3 we will argue that the sequence of even colors is special and that the same failure is not as likely to occur in any other subsequence.

The above motivates the following modification of the volume conjecture that we propose to call the $\mathrm{SO}(3)$ volume conjecture. To the best knowledge of the author it still stands a chance to hold for all knots and links.

Conjecture 3.2. $\mathrm{SO}(3)$ volume conjecture

The following form of the volume conjecture holds for all knots and links L :

$$\lim_{N \rightarrow \infty} \frac{2\pi}{N} \log |J_N(L)(e^{\frac{\pi i}{2N}})| = \mathrm{Vol}(L)$$

where N runs over the odd numbers only and J_N is normalized as described above.

The name $\mathrm{SO}(3)$ is chosen because we restrict ourselves to odd colors N , i.e. representations of the Lie group $\mathrm{SO}(3)$ instead of the Lie algebra $\mathfrak{sl}(2)$. The restriction to odd N is natural because Kashaev's original invariant for triangulated links in \mathbb{S}^3 was also defined for odd N only, see condition (3.12) in [Ka1]. One might also argue more generally that the odd colors correspond to the spherical representations of $\mathfrak{sl}(2)$.

Now we would like to generalize the volume conjecture even further to the class of knotted trivalent graphs (KTGs). A motivation for this generalization is that such graphs show up naturally in the computation of the colored Jones invariant when one applies fusion. Another motivation is that very simple graphs such as planar graphs will have relatively simple Jones invariants and a complement that is easy to triangulate. Considering graphs in their own right will furthermore clarify the role of six-j symbols, since they are the $\mathfrak{sl}(2)$ -invariants of the tetrahedral graph. In order to obtain a volume conjecture in the case of a KTG we need to define both the colored Jones invariant of a KTG and the volume of a KTG.

The generalization of the colored Jones invariant to KTGs is fairly straightforward and is based on the Kauffman bracket, see section 3.3. The idea is to connect the three incoming Jones–Wenzl idempotents in a trivalent vertex in the only possible planar way. Alternatively one can think of a trivalent vertex as a Clebsch–Gordan injector of the representation on the incoming strand into the tensor product of the representations of the two outgoing strands. We need a slight extension of the usual formalism to deal with half twisted edges such as a Möbius band. It is well known that this procedure yields a Laurent polynomial when or KTG is a knot or a link. For general KTG's this will not be the case and we obtain an invariant that is a quotient of Laurent polynomials.

The definition of the volume of a KTG is more complicated and will be treated in detail in section 3.4. Here we give a brief overview of the ideas

involved. The boundary of the exterior of a graph is a closed surface of high genus so if the exterior is to be hyperbolic then the boundary cannot be a cusp but we can require it to be a totally geodesic boundary as in [Fr]. However very different graphs can have homeomorphic exteriors because the structure of edges and vertices is lost. To fix this we exclude annuli and tori around the edges from the boundary so that they become cusps and the remaining punctured spheres become a geodesic boundary. This version of the exterior will be called the outside of the graph. It is shown in [Fr] that rigidity still holds for such structures provided that we use a system of closed curves on the boundary to keep track of where the cusps should be.

To deal with non-hyperbolic graphs we can no longer use the simplicial volume as was done for knots and links. This is because it was shown in [Jun] that the simplicial volume of a hyperbolic manifold with geodesic boundary does not agree with its hyperbolic volume when the boundary is non-empty. To get around this we use the JSJ-decomposition and define the volume as the sum of the volumes of the hyperbolic pieces in the decomposition. For links this definition is known to agree with the simplicial volume.

Having defined the colored Jones invariant and the volume of a KTG, the above statement of the $SO(3)$ volume conjecture also makes sense for KTGs. Indeed, we propose that with this interpretation of volume and Jones invariant Conjecture 3.2 should be true for all KTGs.

Conjecture 3.3. *The $SO(3)$ volume conjecture holds for all knotted trivalent graphs.*

To provide some evidence for this claim we will prove the $SO(3)$ volume conjecture for the class of augmented KTGs defined below. This will be the main purpose of the paper.

To describe the construction of augmented KTGs and to organize the calculations it is convenient to have a way to generate all KTGs by simple operations that we define now. For now let us think of a KTG as a thickened embedding of a graph whose edges are ribbons and whose vertices are disks. A more detailed treatment can be found in section 3.2.

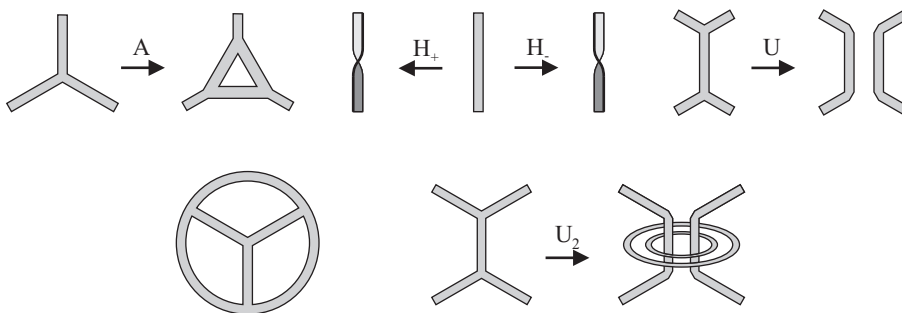


Figure 3.1: First row: the four KTG moves triangle A , positive and negative half twists H_{\pm} and Unzip U . Second row: the standard tetrahedron and the n -unzip U_n (we have drawn the case $n = 2$).

Definition 3.1. *The following four operations on KTGs will be called the KTG moves, see figure 3.1. The triangle move A replaces a vertex by a triangle, the positive half twist move H_+ inserts a positive half twist into an edge, the negative half twist H_- inserts a negative half twist and finally the unzip move U takes an edge and splices it into two parallel edges.*

We also define the following variations on the unzip move called the n -unzip U_n . This is the unzip together with the addition of n parallel rings encircling the two unzipped strands.

The four KTG moves defined above are sufficient to generate all KTGs starting from the standard tetrahedron graph shown in figure 3.1.

Theorem 3.1. *Any KTG can be obtained from the standard tetrahedron using the KTG moves only.*

According to this theorem we can work with KTGs by studying sequences of KTG moves. Of course there are many inequivalent ways to produce the same KTG using the KTG moves, see section 3.2.

Now we can define the notion of an augmented KTG.

Definition 3.2. *Let S be a sequence of KTG moves. Define the singly augmented KTG corresponding to S to be the KTG obtained from the standard tetrahedron by the moves of S except that all unzip moves are to be replaced by 1-unzip moves. We will denote the singly augmented KTG corresponding to S by Γ'_S .*

Likewise the n -augmented KTGs corresponding to S are defined to be all the KTGs that can be produced from the standard tetrahedron by the moves of S except that every unzip move is to be replaced by an m -unzip move, where $m \geq n$. Note that one may choose a different m for all unzip moves in S .

Let Γ_S be the KTG obtained from a sequence of KTG moves S and let Θ be an n -augmented KTG corresponding to S . Then Γ_S is contained in Θ and $\Theta - \Gamma_S$ is an r -fold unlink. Here is r the number of rings that were added to Γ_S to obtain the augmented KTG Θ . The number r is called the number of augmentation rings of Θ .

With all definitions in place we can now formulate the main theorem of this paper.

Theorem 3.2. (Main Theorem)

Let S be a sequence of KTG moves. There exists an $n \in \mathbb{N}$ such that all n -augmented KTGs Γ corresponding to S satisfy the following.

- 1) Let t be the number of triangle moves in S and let r be the number of augmentation rings of Γ . Let θ be the number of half twists counted with sign and define the following numbers.

$$\phi_N = (-1)^{\frac{N-1}{2}} e^{\frac{N^2-1}{4N}\pi i} \quad \text{and} \quad \text{sixj}_N = \sum_{k=0}^{\frac{N-1}{2}} \left[\begin{matrix} \frac{N-1}{2} \\ k \end{matrix} \right]^4 (e^{\frac{\pi i}{2N}})$$

The normalized N -colored Jones invariant of Γ satisfies:

$$J_N(\Gamma)(e^{\frac{\pi i}{2N}}) = \begin{cases} \phi_N^\theta N^r \text{sixj}_N^{t+1} & \text{if } N \text{ is odd} \\ 0 & \text{if } N \text{ is even} \end{cases}$$

- 2) The JSJ-decomposition of the outside of Γ consists of the outside of Γ'_S and a Seifert fibered piece for every n -unzip used in the construction of Γ such that $n \geq 2$. It follows that $\text{Vol}(\Gamma) = \text{Vol}(\Gamma'_S)$

Moreover the outside of Γ'_S is hyperbolic with geodesic boundary and can be obtained explicitly by gluing $2t + 2$ regular ideal octahedra.

- 3) Γ satisfies the $\text{SO}(3)$ volume conjecture, but not the original volume conjecture.

The quantum binomial coefficients used in the above definition of sixj_N are defined in section 3.3. For a definition of the colored Jones invariant of a KTG, see section 3.3. The outside of a graph is defined in section 3.4, it plays the role of the complement but it is a manifold with boundary pattern [Ma]. We will also define the volume of such manifolds. In section 3.4.2 we will show how to obtain the explicit glueing of octahedra mentioned above.

The proof of parts 1) and 2) of the main theorem will be given in sections 3.3 and 3.4, but it is easy to see how part 3) follows from the first two parts. The key ingredient is the following observation about the numbers sixj_N . It was shown in [Co1] that $\lim_{N \rightarrow \infty} \frac{2\pi}{N} \log |\text{sixj}_N| = 2\text{Vol}(\text{Oct})$, where $\text{Vol}(\text{Oct})$ means the hyperbolic volume of the regular ideal octahedron. Plugging in the formula for the colored Jones from part 1) gives:

$$\lim_{N \rightarrow \infty} \frac{2\pi}{N} \log |J_N(\Gamma)(e^{\frac{\pi i}{2N}})| = 2(t+1)\text{Vol}(\text{Oct})$$

as a limit over all the odd numbers N . According to part 2) of the main theorem this is exactly the volume of Γ since $\text{Vol}(\Gamma) = \text{Vol}(\Gamma'_S)$ and $\text{Vol}(\Gamma'_S)$ equals $(2t+2)\text{Vol}(\text{Oct})$. The original volume conjecture does not hold because the even values of N give a colored Jones of 0. This concludes the proof of part 3) assuming the first two parts of the main theorem.

Now let us note some immediate corollaries.

Corollary 3.1. For every KTG Γ there is a KTG Θ containing Γ such that $\Theta - \Gamma$ is an unlink and Θ satisfies the $\text{SO}(3)$ volume conjecture. If Γ happens to be a link then so is Θ .

Corollary 3.2. *The $SO(3)$ volume conjecture holds for all KTGs that can be constructed from the standard tetrahedron using the triangle move and the half twist move only. The original volume conjecture fails for such KTGs.*

The final corollary has nothing to do with the volume conjecture, but gives an alternative proof of a result by Baker [Bak] on arithmetic links. A link is said to be arithmetic if the fundamental group of its complement allows a faithful representation into $PSL(2, \mathbb{C})$, whose image is commensurable with $PSL(2, \mathcal{O})$, where \mathcal{O} is the ring of integers in an imaginary quadratic number field.

Corollary 3.3. *Every link is a sublink of an arithmetic link.*

Proof. The singly augmented link corresponding to the given link is an arithmetic hyperbolic 3-manifold, since it is obtained from glueing regular ideal octahedra by symmetries of the tiling of hyperbolic space by regular ideal octahedra, see [Th]. △

The organization of the paper is as follows. In section 3.2 we discuss KTGs, KTG diagrams and KTG moves. The subject of section 3.3 is skein theory. Here we define the colored Jones invariant of a KTG and show how it can be expressed in terms of six-j symbols. Specializing to the N -th root of unity and making use of the special properties of augmentation yields part 1) of the main theorem. In section 3.4 we give a definition of the volume of a 3-manifold with boundary and we study the geometry of the outside of an augmented KTG. Here we prove part 2) of the main theorem. Section 3.5 is a short summary and a conclusion.

Acknowledgement. I would like to thank Dave Futer, Rinat Kashaev, Jessica Purcell, Nicolai Reshetikhin and Dylan Thurston for enlightening conversations and the organizers of the conferences, workshops and seminars in Hanoi, Strasbourg, Basel, Aarhus and Geneva for giving me the opportunity to present parts of this work there.

3.2 Knotted Trivalent Graphs

In this section we state some general facts about knotted trivalent graphs (KTGs). We discuss the extra Reidemeister moves that are necessary to relate isotopic KTG diagrams and describe how every KTG can be generated from the standard tetrahedron by the KTG moves.

Definition 3.3. *A fat graph is a 1-dimensional simplicial complex together with an embedding into a surface as a spine.*

A knotted trivalent graph (KTG) is a trivalent fat graph embedded as a surface into \mathbb{S}^3 and considered up to isotopy.

By a diagram of a KTG we will mean a regular projection of its spine KTG onto the plane together with the usual crossing information and small diagonal lines indicating where an edge of a KTG makes a half twist. Except for the locations in the diagram where there is a half twist the surface of the KTG is assumed to be parallel to the projection plane as in the blackboard framing. The half twist pictures are necessary because a KTG such as the Möbius band cannot be given

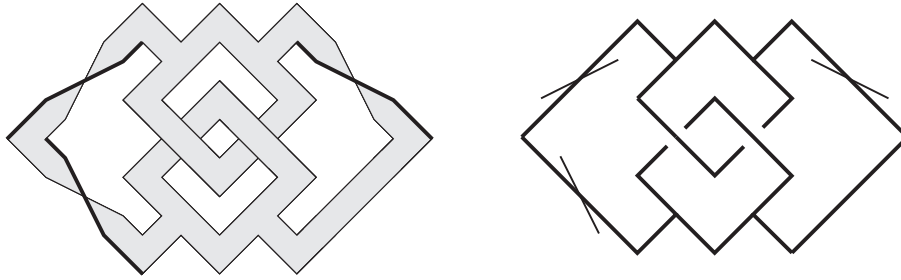


Figure 3.2: A KTG and its diagram.

the blackboard framing. See Figure 3.2 for an example of a KTG together with its diagram.

Next we consider the moves that relate diagrams of isotopic KTGs. We will call these moves the trivalent isotopy moves. In addition to the usual Reidemeister moves for framed links we have moves related to the trivalent vertex and the half-integral framing. These additional moves are called the fork slide, trivalent twist, twist slide and addition of twists, see figure 3.3.

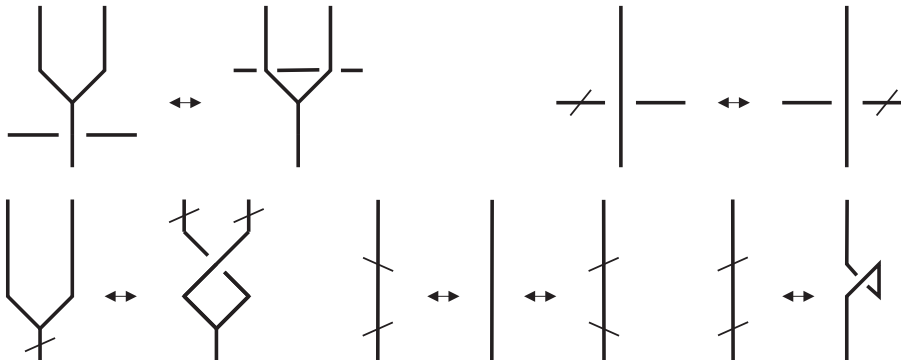


Figure 3.3: The additional trivalent isotopy moves on a KTG diagram. First row: the fork slide and the twist slide. Second row: the trivalent twist and the addition of twists (multiple cases).

Definition 3.4. *The trivalent isotopy moves are the Reidemeister moves for framed links and the following four moves on KTG diagrams:*

1. *Let the fork slide be the move where a strand is slid over or under a trivalent vertex (first picture of figure 3.3).*
2. *One can slide a half twist past a crossing (second picture of figure 3.3). This is called the twist slide.*
3. *The trivalent twist is the move where a single half twist is moved past a trivalent vertex. It starts on one edge, passes the vertex, creates a crossing and one half twist on the other two edges (third picture of figure 3.3). The*

sign of the initial half twist equals the sign of the crossing and the two ensuing half twists.

4. *One may cancel or create two half twists of opposite sign on the same edge. Two half twists of equal sign on the same edge may be replaced by a curl of the same sign on that edge (last pictures of figure 3.3). This is called addition of twists.*

The same arguments that are used in the proof of Reidemeister's theorem can be employed to prove the following theorem, see also [Tu].

Theorem 3.3. *Two KTG diagrams define isotopic KTGs if and only if the diagrams are related by trivalent isotopy moves.*

3.2.1 KTG moves

We now take a closer look at the KTG moves defined in the introduction (Definition 3.1). We will give a proof of Theorem 3.1 that states that any KTG can be generated from the standard tetrahedron (see figure 3.1) using the KTG moves.

It is important to note that the result of an unzip move is determined by the number of half twists present on the edge. Technically such half twists have to be pushed off the edge before one can perform the unzip. In practice it is however much easier to remember that n half twists on an edge give rise to n crossings between the two parallel edges produced by the unzip. This follows from the trivalent isotopy moves defined above. Alternatively it can be checked physically by cutting a twisted band into two pieces along its core.

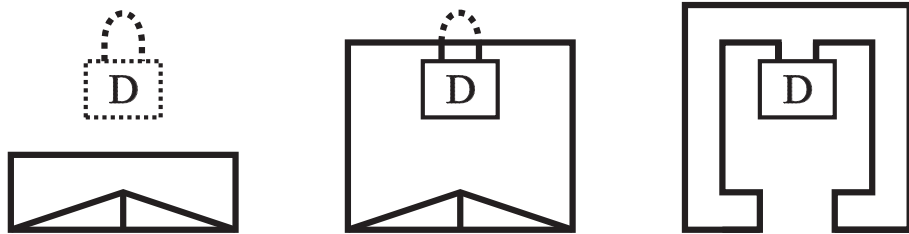


Figure 3.4: Generating an arbitrary diagram D from the tetrahedron by sweep-out.

Proof. (of Theorem 3.1). We start with the diagram D of the KTG that we want to generate drawn hatched in the first picture of figure 3.4. Below it we draw a standard tetrahedron in black. The hatched part of the picture still needs to be generated and the black part is already done.

We generate the diagram D from the topmost edge of the tetrahedron step by step using the elementary steps depicted in figure 3.5. The edge of the tetrahedron moves upwards over the hatched diagram D and at every step we delete the hatched part of D that is covered and regenerate it by one of the moves indicated in figure 3.5.

The elementary moves A , H_{\pm} and U in figure 3.5 are the KTG moves, and the moves B and C are a composition of KTG moves, see figure 3.6 for a proof.

The last step in the derivation of the move C consists of unzipping the half twisted edge. To do this one can either cut the edge along its core or first isotope the half twist up to get a crossing. Compare figure 3.3.

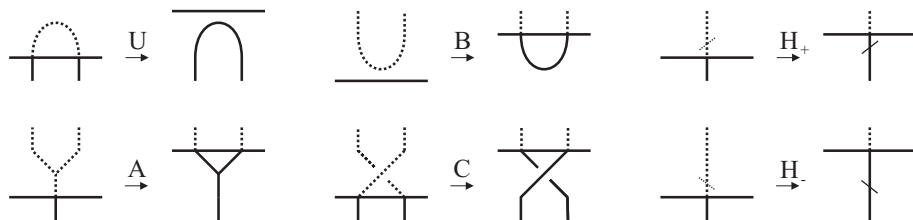


Figure 3.5: The elementary steps encountered by the edge of the tetrahedron. The hatched parts are only meant to indicate the course of action, these parts are not actually there. With this in mind one recognizes the U in the first picture as the unzip move.

We stop the sweep-out process right before reaching the last hatched maximum of D , as indicated in the middle picture in figure 3.4. To close the diagram we remove this maximum and unzip the three vertical edges of the tetrahedron to obtain the required diagram, see the last picture in figure 3.4.

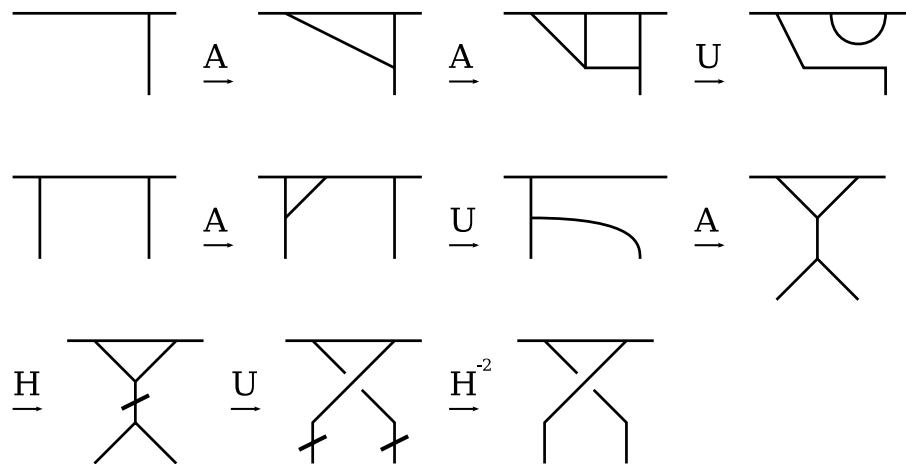


Figure 3.6: A derivation of the move B from the KTG moves (first row) and a derivation of C from the KTG moves (second and third row).

△

There are many ways to produce the same KTG using the KTG moves. For example if one starts with a single trivalent vertex and applies the triangle move then one can proceed in two ways to produce the same diagram. Either perform a single triangle move on the top vertex, or do two triangle moves on the two lower vertices followed by an unzip on the middle edge at the bottom.

3.3 The colored Jones invariant of a KTG

Our definition and calculation of the colored Jones invariant will be based on the Kauffman bracket and its skein relation. We have chosen this language over the more general representation theoretic language because its formulas do not require a preferred direction in the projection plane. Throughout we will make use of the variable A from skein theory. It is related to the q from the introduction by $A^4 = q$.

3.3.1 Möbius Skein Theory

To be able to include diagrams with half twisted edges we need to extend the usual skein theory a little. We propose to introduce the following extra relations called the half twist relations. A single edge with a positive half twist is equal to $(-A^3)^{1/2}$ times an untwisted edge. A single edge with a negative half twist is equal to $(-A^3)^{-1/2}$ times an untwisted edge. This definition is consistent with the value of the curl in ordinary skein theory and also with the trivalent isotopy move addition of twists from section 3.2.

$$\begin{array}{c}
 \left(\begin{array}{c} \diagup \diagdown \\ \diagdown \diagup \end{array} \right) = A \left(\begin{array}{c} \text{---} \\ \text{---} \end{array} \right) + A^{-1} \left(\begin{array}{c} \text{---} \\ \text{---} \end{array} \right) \quad \left(\begin{array}{c} | \\ | \end{array} \right) = (-A^3)^{1/2} \left(\begin{array}{c} | \\ | \end{array} \right) \\
 \\
 \left(\begin{array}{c} \bigcirc \\ \square \text{ D} \end{array} \right) = (-A^2 - A^{-2}) \left(\begin{array}{c} \square \text{ D} \end{array} \right) \quad \left(\begin{array}{c} | \\ | \end{array} \right) = (-A^3)^{-1/2} \left(\begin{array}{c} | \\ | \end{array} \right)
 \end{array}$$

Figure 3.7: The Kauffman relations and the additional twist relations together make up Möbius Skein Theory.

Definition 3.5. Let \mathcal{R} be the quotient field of the ring of rational Laurent polynomials in $A^{1/2}$. Define the Möbius skein of a surface Σ to be the \mathcal{R} -vector space of KTG diagrams without vertices in Σ modulo the Kauffman bracket relations and the half twist relations shown in figure 3.7.

The surface is allowed to have marked points on its boundary but in this case we only allow diagrams that have edges ending at all the boundary points.

Note that the above definition coincides with the usual definition of a skein space except for the half twist relations. A KTG diagram without vertices or half twists can be given the blackboard framing and its value in the Möbius skein will be exactly its value in the ordinary skein space.

We can now define the colored Jones invariant of a KTG using the notion of a Jones–Wenzl idempotent and a trivalent skein vertex, see [MV].

Definition 3.6. Define the unnormalized N -colored Jones invariant $\langle \Gamma \rangle_N(A)$ of a KTG Γ to be the Kauffman bracket of the Möbius skein element obtained from a diagram of Γ in the plane by replacing every edge by $(N - 1)$ parallel edges joined by a $(N - 1)$ -th Jones–Wenzl idempotent and every vertex by a trivalent skein vertex.

More generally we also define the bracket of a KTG diagram with integer labels on the edges to be the bracket of the skein element obtained by replacing an edge labeled B by a $(B - 1)$ -th Jones–Wenzl idempotent and the vertices by the appropriate trivalent skein vertices.

With this definition $\langle \Gamma \rangle_2$ coincides with the usual Kauffman bracket. As an example we note that if M is the positive Möbius band then

$$\langle M \rangle_3 = -(A^8 + A^4 + 1)$$

Note that replacing an N -colored edge with a half twist by parallel strands will cause the $(N - 1)$ parallel edges to be intertwined and individually half twisted so that we get additional crossings and half twists.

Since there is no planar way to connect an odd number of incoming edges, the trivalent vertex is defined to be zero when all edges have even colors. Therefore the colored Jones invariant of any KTG with at least one vertex is also zero for even N . In the next section we will see that at the $(4N)$ -th root of unity this is the case for all augmented KTGs.

For the above definition to make sense we still have to prove that the value of $\langle \Gamma \rangle_N$ does not depend on the particular KTG diagram we choose for Γ . For this we first need a fairly standard lemma on the half twist, see also the last diagram in figure 3.8.

Lemma 3.1. *A positive half twist on n bands on top of an n -th Jones–Wenzl idempotent is equal to $(-1)^{\frac{n}{2}} A^{\frac{n(n+2)}{2}}$ times the untwisted bands with the same idempotent at the bottom. For the negative half twist we get $(-1)^{-n/2} A^{-n(n+2)/2}$ in the same way.*

Proof. Because of the Jones–Wenzl idempotent there is only one way to resolve the crossings in the diagram that will give a non-zero contribution. A half twist on n parallel bands produces $n(n - 1)/2$ positive crossings yielding a contribution $A^{n(n-1)/2}$. Furthermore every strand contains a positive half twist, so the half twist relation gives another contribution of $(-1)^{n/2} A^{3n/2}$. Together this is exactly $(-1)^{n/2} A^{n(n+2)/2}$ as required. For the negative half twist the proof is the same. \triangle

Proposition 3.1. *The unnormalized N -colored Jones invariant $\langle \Gamma \rangle_N(A)$ of a KTG Γ is a well defined invariant of KTGs.*

Proof. We need to check that the value of the unnormalized colored Jones invariant is unchanged under the trivalent isotopy moves of KTG diagrams defined in definition 3.4. For the Reidemeister moves this is clear. Because a trivalent vertex is turned into a skein element without trivalent vertices or half twists, invariance under the fork slide move follows from invariance under Reidemeister II and III.

Lemma 3.1 proves the invariance of the Jones under the twist slide move and the addition of half twists. Invariance under the trivalent twist move now follows from this lemma in combination with Theorem 3 of [MV]. \triangle

Note that the above proof also shows that the bracket of a KTG whose edges are colored by any integers is an invariant. This invariant is multiplicative under distant union.

To relate our definition of the unnormalized colored Jones invariant to the ones that can be found in the literature we note that when Γ is a link it coincides with $(-1)^{N-1}$ times the value of the unnormalized Jones invariant defined in [Mas]. This follows from the remark that the bracket of a KTG diagram without half twists or vertices equals the bracket of the framed link in the usual skein theory.

The normalization of the Jones invariant that is used in the $\text{so}(3)$ volume conjecture (Conjecture 3.2) is defined as follows.

Definition 3.7. *Define the normalized colored Jones invariant of a KTG Γ with s split components to be $J_N(\Gamma) = \langle \Gamma \rangle_N / \langle U^s \rangle_N$, where U^s is the s -component unlink.*

For the volume conjecture we need to specialize to $A = \exp(\pi i/2N)$ but $\langle U^s \rangle_N = (-1)^{s(N-1)} [N]^s$, where $[N] = (A^{2N} - A^{-2N}) / (A^2 - A^{-2})$. At this value of A we have $[N] = 0$ so we have to check that we can divide out this pole and still get a well defined answer.

Proposition 3.2. *The normalized N -colored Jones invariant has a well defined value at $A = \exp(\pi i/2N)$.*

Proof. Since the unnormalized colored Jones invariant is multiplicative under distant union, the normalized colored Jones invariant also has this property. Therefore we can assume that the number of split components of our KTG Γ is 1. Let Γ be the closure of a 1–1 tangle Θ . We label the edges of Θ with N and interpret Θ as an element of the Möbius skein of a square with $2N - 2$ marked boundary points. As in the Temperley–Lieb algebra we can now write Θ as a scalar $f_N(A)$ times the $N - 1$ th Jones–Wenzl idempotent. Closing the tangle Θ we find that $\langle \Gamma \rangle_N = \langle U \rangle_N f_N(A)$.

It now remains to show that $f_N(A)$ is a quotient of Laurent polynomials in $A^{1/2}$ whose denominator is not zero at $A = \exp(\pi i/2N)$. To calculate $f_N(A)$ we expand all crossings and half twists in Θ so as to obtain an element of the Temperley–Lieb algebra and the component of the identity in this expression is $f_N(A)$. The calculation of $f_N(A)$ will involve the Jones–Wenzl idempotents, the skein relation and the half twist relations. From the recursive definition of the Jones–Wenzl idempotent it is clear that $f_N(A)$ is a quotient of Laurent polynomials in $A^{1/2}$ whose denominator does not have poles at $A = \exp(\pi i/2N)$.

△

It follows from our discussion that the normalized colored Jones invariant is multiplicative under both connected sum and distant union of KTG diagrams. To see the multiplicativity with respect to connected sum we observe that it corresponds to concatenation of 1–1 tangles and hence to multiplication of scalars.

We now move on to the problem of calculating the unnormalized colored Jones invariant of a general KTG. Theorem 3.1 tells us that all KTGs can be constructed from the standard tetrahedron by applying the KTG moves. It turns out that in skein theory the KTG moves correspond to the well known formulas shown in figure 3.8, see also [MV]. We will show below that these formulas can be used to calculate the colored Jones polynomial of any KTG from a sequence of KTG moves generating it.

To be able to write down the formulas for the six- j symbols shown in figure 3.8 we first recall the definition of a quantum integer $[n] = \frac{A^{2n} - A^{-2n}}{A^2 - A^{-2}}$. The value

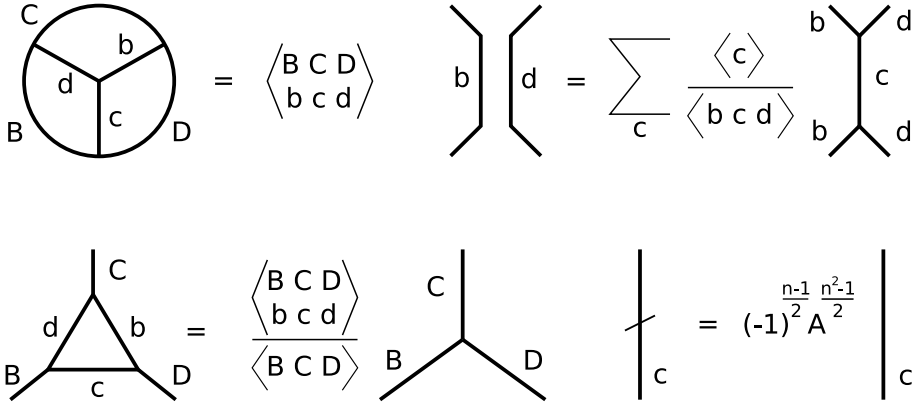


Figure 3.8: The value of the skein of the labeled standard tetrahedron is the six-j symbol defined below. The fusion formula reverses the unzip move, the half twist formula undoes the half twist move and the triangle formula undoes the triangle move.

of the unknot is $\langle U \rangle_N = \langle N \rangle = (-1)^{N-1} [N]$. Quantum factorials and binomial coefficients are defined in the usual way in terms of the quantum integers.

Given six integer labels j_1, \dots, j_6 on the edges of a tetrahedron as in figure 3.8 such that all trivalent vertices are non-zero, define V_1, V_2, V_3, V_4 to be a half times the sums of the three labels around each of the four vertices. For example $V_1 = (j_1 + j_2 + j_3)/2$. Also define $\square_1, \square_2, \square_3$ to be a half of the sums of the labels in the three squares (pairs of opposite edges). According to [MV] the value of the tetrahedron is:

$$\left\langle \begin{array}{ccc} j_1 & j_2 & j_3 \\ j_4 & j_5 & j_6 \end{array} \right\rangle \quad \text{where} \quad \left\langle \begin{array}{ccc} j_1 + 1 & j_2 + 1 & j_3 + 1 \\ j_4 + 1 & j_5 + 1 & j_6 + 1 \end{array} \right\rangle =$$

$$\frac{\prod_{m,n} (\square_m - V_n)}{\prod_{k=1}^6 [j_k]!} \sum_{z=\max V_i}^{\min \square_j} \frac{(-1)^z [z+1]!}{\prod_r [\square_r - z]! \prod_s [z - V_s]!}$$

The value of the labeled theta graph is given by $\langle a \ b \ c \rangle$, where

$$\langle a + 1 \ b + 1 \ c + 1 \rangle = (-1)^s \frac{[s+1]! [s-a]! [s-b]! [s-c]!}{[a]! [b]! [c]!} \quad \text{where} \quad s = \frac{a+b+c}{2}$$

The sum in the upper right equation in figure 8 ranges over all possible triples for which the trivalent vertex is nonzero, that is all c such that $|a-b| \leq c \leq a+b$ and $a+b+c$ is odd. It should be remarked that since we replace an edge labeled b by a $b-1$ -th Jones-Wenzl idempotent while they are replaced by b -th Jones-Wenzl idempotents in [MV] there is a slight shift of indices.

The formulas in figure 3.8 suffice to give a formula for the colored Jones invariant of any KTG in terms of the six-j symbols. By theorem 3.1 we know that any KTG Γ can be constructed from the tetrahedron by a sequence S of KTG moves. To calculate $\langle \Gamma \rangle_N$ we start with the diagram corresponding to S and label all edges by N . Now we reverse the KTG moves in S move by move. At every step we keep track of the newly produced edge labels in the diagrams

that we get. The formulas in figure 3.8 tell us that we get a six-j symbol when we reverse the triangle move A , a summation with so called fusion coefficients from the unzip move U and a factor from the half twist moves H_{\pm} . In the next subsection we will use this knowledge to calculate the colored Jones of an augmented KTG at the relevant root of unity.

Finally note that it is well known that the colored Jones invariant of knots and links is a Laurent polynomial. For KTGs this is generally not the case. The colored Jones invariant (normalized or not) of a KTG is merely a quotient of Laurent polynomials in $A^{1/2}$. As an example let us calculate the normalized colored Jones invariant of the theta graph θ . From the formula in figure 3.8 we get:

$$J_N(\theta) = (-1)^{3k} \frac{[3k+1]![k]!^3}{[2k]!^3[2k+1]} \quad N = 2k + 1$$

By considering the zeros of the numerator and the denominator it is clear that this is not a Laurent polynomial for odd N greater than 3. For example we can look at the number of zeros at $A = \exp(i\pi/4k)$.

3.3.2 Asymptotics and augmentation

We have seen that the unnormalized N -colored Jones invariant takes the form of a multi-sum of products and quotients of quantum integers. Every unzip contributes a summation with fusion coefficients, every triangle move produces a six-j symbol and every half twist move contributes a power of A .

It is not trivial to determine the asymptotics of such a multisum formula. To circumvent this difficulty we augment the KTG. Adding extra unknotted ring-like components actually simplifies the sum at the relevant root of unity because of the following formula from skein theory [Li], see figure 3.9. The value of a $k-1$ -th Jones-Wenzl idempotent encircled by a closed $N-1$ -th idempotent is $(-1)^{N-1}[kN]/[k]$ times the idempotent.

$$\text{---} \overset{N}{\bigcirc} \text{---} \underset{k}{\text{---}} = (-1)^{N-1} \frac{[N \ k]}{[k]} \text{---} \underset{k}{\text{---}}$$

Figure 3.9: The effect of adding a ring to a labeled edge. Note that every edge is replaced by a Jones-Wenzl idempotent.

The following lemma gives a calculation of the above value at our root of unity.

Lemma 3.2. *In skein theory adding a ring labeled N encircling an edge labeled k is the same as multiplying the edge by $(-1)^{N-1}[kN]/[k]$. The value of this constant is*

$$\lim_{A \rightarrow e^{\pi i/2N}} (-1)^{N-1} \frac{[kN]}{[k]} = \begin{cases} (-1)^{N-1+k-k/N} N & \text{if } N \mid k \\ 0 & \text{if } N \nmid k \end{cases}$$

Proof. The value of $(-1)^{N-1}[kN]/[k] = (-1)^{N-1} \frac{A^{2kN} - A^{-2kN}}{A^{2k} - A^{-2k}}$ at $A = e^{\pi i/2N}$ depends on whether or not the denominator vanishes. The numerator is always

zero but the denominator is zero if and only if $N \mid k$, therefore the value is 0 if N does not divide k . Using l'Hospital's rule we calculate the value in case $N \mid k$.

$$\begin{aligned} \lim_{A \rightarrow e^{\pi i/2N}} (-1)^{N-1} \frac{[kN]}{[k]} &= \lim_{A \rightarrow e^{\pi i/2N}} (-1)^{N-1} \frac{2kNA^{-1}}{2kA^{-1}} \frac{A^{2kN} + A^{-2kN}}{A^{2k} + A^{-2k}} = \\ &(-1)^{N-1} \frac{2(-1)^k}{2(-1)^{k/N}} N = (-1)^{N-1+k-k/N} N \end{aligned}$$

△

The above lemma suggests that we can use an edge with a ring as a kind of delta function. In other words we can try to pick only the term $k = N$ from a sum over edges labeled k by adding a ring to the edge. This will turn the expression of the colored Jones invariant into a single term thus making an asymptotic analysis possible. To make this idea precise we need to be careful because of poles in the six-j symbols and the possibility of several multiples of N dividing k . This is done in the proof of part 1) of the main theorem that we will now present.

Proof. (of part 1) of the main theorem (theorem 3.2)) Let us fix a sequence S of KTG moves and let Θ be the KTG generated by S starting from the tetrahedron. In the previous subsection we have seen that it is possible to express the colored Jones invariant of Θ in terms of the sequence S and the formulas from figure 3.8 by reversing the KTG moves one by one until one reaches the tetrahedron. From the formulas in figure 3.8 one sees that the unnormalized colored Jones invariant can be written as a multisum of products and quotients of quantum integers.

Let n be a fixed integer that is at least one more than the maximum number of poles at $A = e^{\pi i/2N}$ in the summands of the expression of the unnormalized N colored Jones of our KTG Θ . It is very important to note that one can choose such an n to be independent of N . To see this we write out all the six-j symbols in the expression for the colored Jones invariant to see that it is a multisum of quotients of quantum factorials. Moreover there is a number a depending only on S such that if $[r]$ occurs in a summand of the expression for the colored Jones then $r \leq aN$. Since the number of zeros of $[r]!$ at $A = \exp(2\pi i/2N)$ is $\lfloor r/N \rfloor$ we know that all terms $[r]!$ that occur have less than a zeros. It follows that the number of poles in a summand of the multi-sum is less than a times the number of quantum factorials present in the denominator. Suppose that the number of quantum factorials is at most f then we can set $n = af + 1$. Note that f is independent of N as well.

Now let Γ be an n -augmented KTG. If we calculate the unnormalized colored Jones invariant then we get the same multisum as we did for Θ except that according to lemma 3.2 we have at least n factors $(-1)^{N-1} \binom{[kN]}{[k]}$ for every unzip move, where k is the summation variable created by the formula for reversing the unzip in skein theory, see figure 3.8. By lemma 3.2 and the construction of n only those summands of the multisum for Γ for which the summation variables are multiples of N are non-zero at $A = \exp(2\pi i/2N)$.

Actually only the term where all summation variables are equal to N is non-zero at the root of unity. To see this suppose that we have a term where one

summation index equals uN for some integer $u > 1$. We may assume that the index whose value is uN is the first in the order of appearance of the summations in the calculation. This means that the index what created at a stage of the calculation when multiples of N other than N itself did not occur. Since labels that are not multiples of N will not contribute the only possibility is that the label came from fusing two edges labeled N . But this implies that the new summation ranges over the odd integers between 0 and $2N$. Therefore only the summand where all labels are N contributes.

Now that we know that in the multi-sum expression for the unnormalized colored Jones invariant of Γ only the term where all indices are N contributes at this root of unity, we can easily write down a closed form expression for its value. Reversing the KTG moves in S now becomes a matter of multiplying by

a particular factor. For the triangle move this factor is $\frac{\left\langle \begin{array}{ccc} N & N & N \\ N & N & N \end{array} \right\rangle}{\langle NNN \rangle}$, for the unzip it is $\frac{\langle N \rangle}{\langle NNN \rangle}$, for the half twist H_{\pm} it is $(-1)^{\pm(N-1)/2} A^{\pm(N^2-1)/2}$ and finally one factor $\left\langle \begin{array}{ccc} N & N & N \\ N & N & N \end{array} \right\rangle$ for the tetrahedron.

Taking into account the normalization and the powers of N from the augmentation we get the following formula for the normalized N -colored Jones invariant at $A = \exp(\pi i/2N)$. Note that Γ has only one split component so that we divide by $\langle U \rangle_N$ only once.

$$J_N(\Gamma)(e^{\frac{\pi i}{2N}}) = \left((-1)^{(N-1)/2} A^{\frac{N^2-1}{2}} \right)^{\theta} N^r \left(\frac{\langle N \rangle}{\langle NNN \rangle} \right)^u \times$$

$$\frac{\left\langle \begin{array}{ccc} N & N & N \\ N & N & N \end{array} \right\rangle^t \left\langle \begin{array}{ccc} N & N & N \\ N & N & N \end{array} \right\rangle}{\langle NNN \rangle^t \langle N \rangle}$$

where θ is the number of half twists counted with sign, u is the number of unzips in the sequence, t the number of triangle moves and r the number of augmentation rings.

Note that this formula is zero when N is even, because then

$$\left\langle \begin{array}{ccc} N & N & N \\ N & N & N \end{array} \right\rangle$$

is zero for generic A because the trivalent vertices do not exist.

For odd $N = 2k + 1$ we actually have $\frac{\langle NNN \rangle}{\langle N \rangle} = 1$ at $A = \exp(\pi i/2N)$. To see this, first observe that at this value of A we have $[N + j] = -[j] = -[N - j]$. For generic values of A we write:

$$\begin{aligned} \frac{\langle NNN \rangle}{\langle N \rangle} &= (-1)^{3k} \frac{[3k+1]! [k]!^3}{[2k+1][2k]!^3} = \\ &= (-1)^k \frac{[1] \cdots [k][k+1] \cdots [2k][2k+1][2k+2] \cdots [3k+1]}{([k+1] \cdots [2k])^3 [2k+1]} \\ &= (-1)^k \frac{[1] \cdots [k][2k+2] \cdots [3k+1]}{([k+1] \cdots [2k])^2} \end{aligned}$$

At $A = \exp(\pi i/2(2k+1))$ this becomes equal to 1 since $[1] \cdots [k] = [2k][2k-1] \cdots [k+1]$ and $[2k+2] \cdots [3k+1] = (-1)^k [1][2] \cdots [k]$.

The same type of calculation shows that:

$$S = \frac{\left\langle \begin{matrix} N & N & N \\ N & N & N \end{matrix} \right\rangle}{\langle N \rangle} (e^{\pi i/2N}) = \text{sixj}_N$$

where

$$\text{sixj}_N = \sum_{j=0}^{(N-1)/2} \left[\begin{matrix} (N-1)/2 \\ j \end{matrix} \right]^4 (e^{\pi i/2N})$$

To see this, note that after cancelling the factors $[N]$, the expression S at the N -th root of unity is equal to:

$$S = \sum_{j=0}^k (-1)^{3k+j} \frac{[3k+1+j] \cdots [2k+2][2k]!}{[j]!^4 [k-j]!^3}$$

This equals sixj_N since $[2k]! = [k]!^2$ and

$$[3k+1+j] \cdots [3k+2][3k+1] \cdots [2k+2] = (-1)^j [k+1-j] \cdots [k] (-1)^k [k]!$$

Therefore the formula for the colored Jones of the KTG Θ at the root of unity simplifies to:

$$J_N(\Theta)(e^{\frac{\pi i}{2N}}) = \left((-1)^{(N-1)/2} A^{\frac{N^2-1}{2}} \right)^\theta N^r \text{sixj}_N^{t+1}$$

as claimed in part 1) of the main theorem. △

3.4 The geometry of the complement of an augmented KTG

In this section we are concerned with the definition and the calculation of the volume of a KTG. The generalization to graphs is not straight forward because of the following problem. A knot is determined by its complement but a graph is not. The homeomorphism type of the complement of a graph does not say much about the graph itself. For example the standard tetrahedron and the connected sum of two theta graphs, shown in figure 10 have homeomorphic complements. From the point of view of the volume conjecture this is very inconvenient because the colored Jones invariant at the root of unity does distinguish these graphs. If the volume conjecture is to hold for KTGs then we need to add a little structure to the complement so that we can recover the adjacency matrix of the graph from its complement.

In the first subsection we will show how to assign a 3-manifold with boundary to any embedded graph such that the graph can be recovered from the 3-manifold and we still have the possibility of rigid hyperbolic structures. In the second subsection we apply these ideas to augmented KTGs very explicitly and we give a proof of the second part of the main theorem (theorem 3.2).



Figure 3.10: Two KTGs with homeomorphic complements.

3.4.1 The volume of a 3-manifold with boundary

In this section we lay down the necessary foundations that allow us to define the hyperbolic volume of a graph in \mathbb{S}^3 . We start with some general notions about hyperbolic structures on 3-manifolds with boundary following [Fr].

Definition 3.8. *A 3-manifold M is called a hyperbolic manifold with geodesic boundary if it is locally modeled on the right upper half space $\{(x, y, z) \in \mathbb{H}^3 | x \geq 0\}$.*

In the next subsection we will construct many examples of hyperbolic manifolds with geodesic boundary by glueing ideal polyhedra along some of their faces. The remaining faces will make up the boundary.

Mostow rigidity holds for finite volume hyperbolic 3-manifolds with geodesic boundary provided that the boundary is compact [Fr] but when the boundary is non-compact then it may fail. However even in the case of non-compact boundary one can save the rigidity result by considering annular cusp loops. In order to define this notion we first sketch the construction of the natural compactification of a hyperbolic 3-manifold with geodesic boundary.

Let M be an orientable, finite volume, hyperbolic 3-manifold with geodesic boundary. The double $D(M)$ of M (that is the manifold obtained by glueing two copies of M along ∂M) is hyperbolic without boundary. Therefore it consists of a compact portion together with some cusps based on Euclidean surfaces. It follows that M also consists of a compact portion together with some cusps of the form $T \times [0, \infty)$, where T is a Euclidean surface with geodesic boundary such that $(T \times [0, \infty)) \cap \partial T = \partial T \times [0, \infty)$. M now admits a natural compactification \bar{M} by adding such a surface T for each cusp. Note that the compactification \bar{M} of M is obtained by adding tori and closed annuli. The set of these annuli will be called \mathcal{A}_M .

Definition 3.9. *A loop γ in a hyperbolic 3-manifold with geodesic boundary M is called an annular cusp loop if in \bar{M} it is freely homotopic to the core of an annulus of \mathcal{A}_M .*

With this notion in place we can state the rigidity theorem for hyperbolic 3-manifolds with boundary proven in [Fr].

Theorem 3.4. *Let M and M' be two orientable finite volume hyperbolic 3-manifolds with geodesic boundary and let $\phi : \pi_1(M) \rightarrow \pi_1(M')$ be an isomorphism. Suppose that ϕ satisfies the additional requirement that $\phi(\gamma)$ is an annular cusp loop in M' if and only if γ is an annular cusp loop in M . Then ϕ is induced by an isometry between M and M' .*

The additional requirement is necessary only in the case of 3-manifolds with non-compact geodesic boundary. In the compact case the set \mathcal{A}_M is empty.

In order to save the rigidity we need to include the annular cusp loops into the structure of the manifold itself. This will be done in the context of 3-manifolds with boundary pattern that were introduced in [Joh].

Definition 3.10. *A 3-manifold with boundary pattern is a pair (M, P) where M is a 3-manifold with boundary and $P \subset \partial M$ is a one dimensional polyhedron. A homeomorphism of manifolds with boundary patterns is required to restrict to a homeomorphism between the boundary patterns.*

If M is a hyperbolic 3-manifold with geodesic boundary then we would like to include the boundary circles of the annuli \mathcal{A}_M in the natural compactification of M as a boundary pattern but of course they are not part of ∂M . Since the annuli connect in \bar{M} to ∂M we can push them inside a little to become part of ∂M .

Definition 3.11. *The boundary pattern corresponding to the hyperbolic structure with geodesic boundary on a M is defined to be the set of boundary curves of the annuli in \mathcal{A}_M , pushed inside of ∂M .*

A corollary of the above rigidity theorem is now the following:

Theorem 3.5. *Let (M, P) and (M', P') be two orientable finite volume hyperbolic 3-manifolds with geodesic boundary and let P and P' be their corresponding boundary patterns. If $f : (M, P) \rightarrow (M', P')$ is a homeomorphism of 3-manifolds with boundary pattern then f is induced by an isometry between M and M' .*

Thus the hyperbolic structure is still rigid if one takes into account the boundary patterns. Therefore we should only allow hyperbolic structures that agree with the given boundary pattern.

Definition 3.12. *A 3-manifold with boundary pattern (M, P) is said to allow a hyperbolic structure with geodesic boundary if it can be given a finite volume hyperbolic structure with geodesic boundary that turns the components of P into annular cusp loops.*

To define the volume for more general manifolds with boundary pattern we use the JSJ-decomposition and add up the volumes of the pieces allowing a hyperbolic structure with geodesic boundary. We state a version of the JSJ-decomposition for 3-manifolds with boundary pattern taken from [Ma].

Theorem 3.6. *Let (M, P) be an orientable, irreducible and boundary irreducible 3-manifold with boundary pattern. There exists a JSJ-system of annuli and tori that is unique up to admissible isotopy. The system decomposes (M, P) into three types of JSJ-chambers: simple 3-manifolds, Seifert manifolds and I -bundles.*

Note that the JSJ-chambers are also 3-manifolds with boundary pattern. In addition to the original boundary pattern of (M, P) they also inherit the adjacent boundary curves of the annuli in the JSJ-system [Ma].

Definition 3.13. *Let (M, P) be an orientable, irreducible, boundary irreducible 3-manifold with boundary pattern. We define the hyperbolic volume $\text{Vol}(M, P)$ of (M, P) to be the sum of the hyperbolic volumes of the JSJ-chambers that allow a hyperbolic structure with geodesic boundary.*

The rigidity theorem (Theorem 3.5) above and the uniqueness of the JSJ-decomposition show that the volume is a well defined invariant of orientable, irreducible and boundary irreducible 3-manifold with boundary pattern. The definition of volume can be extended further by demanding it to be additive under connected sums.

As a motivation for this definition of the hyperbolic volume of a 3-manifold with boundary pattern we note that it coincides with the simplicial volume in the case of an empty boundary [Rat]. However for manifolds with boundary this notion seems to be more appropriate. Indeed the Gromov norm no longer agrees with the volume of a hyperbolic manifold as soon as the boundary is non-empty [Jun].

The most important example for our purposes is the so called outside of a graph. This is the version of the complement of a graph that is suitable for carrying a rigid hyperbolic structure.

Definition 3.14. *Let Γ be an embedded graph in \mathbb{S}^3 , where edges without vertices and multiple edges are allowed. We define the outside O_Γ of Γ to be the 3-manifold with boundary pattern constructed as follows.*

Let $N(\Gamma)$ be the neighborhood of Γ made up from small open balls around the vertices, closed solid tori around the edges of Γ without vertices and small closed solid cylinders around the edges that intersect the closure of the balls around the adjacent vertices in disjoint disks. Define the outside O_Γ be $\mathbb{S}^3 - N(\Gamma)$. Also define the exterior E_Γ to be the closure of O_Γ as a subspace of \mathbb{S}^3 .

We will endow O_Γ with the boundary pattern P_Γ consisting of a circle around every hole on every holed sphere in its boundary.

The outside of a graph may not be irreducible because the graph might be the distant union of a number of split components. If this is the case we cut the outside along spheres and cap the spheres off with balls. The resulting pieces are outsides of non-splittable graphs. For such graphs the outside is an orientable, irreducible and boundary irreducible 3-manifold whose boundary consists spheres from which closed disks have been removed. We have one sphere for every vertex and its number of holes is equal to the valency of the vertex.

The outside of a graph is not compact and neither is its boundary. The corresponding exterior is compact and will play the role of the natural compactification mentioned above. In the next section we will investigate the geometry and decomposition of 1-augmented KTGs in greater detail.

3.4.2 The geometry of augmented KTGs

In this subsection we prove part 2) of the main theorem. Let Γ be an n -augmented KTG. Let us consider the JSJ-system of its outside O_Γ . We have one essential torus for every k -unzip move used to produce Γ , such that $k \geq 2$. The tori encircle the augmentation rings produced by the k -unzip move. Cutting along such a torus splits off a Seifert fibered JSJ-chamber of the form $(D_k \times \mathbb{S}^1, \emptyset)$, where D_k is a k -times punctured disk and k is the number of

augmentation rings produced in the k -unzip move. After removing all such Seifert pieces we are left with the outside of the singly augmented KTG Γ' corresponding to Γ . Below we will show that such a singly augmented outside is hyperbolic. It then follows that the JSJ-decomposition of the outside of Γ consists of the above Seifert fibred pieces and the outside of Γ' .

Note that by definition the hyperbolic volume of Γ is equal to the volume of Γ' , since we neglect Seifert fibered chambers in the JSJ-composition.

We aim to show that the outside of any singly augmented KTG Γ' admits a hyperbolic structure with geodesic boundary by decomposing it into regular ideal octahedra. The method of decomposition is similar to the construction for links in [FP].

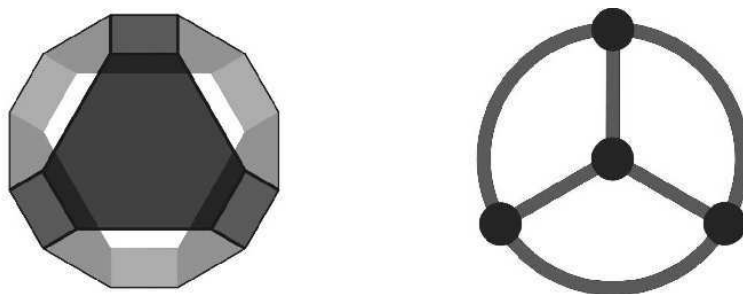


Figure 3.11: A truncated octahedron with colored faces (left). The truncated octahedron as the half space beyond the paper plus infinity (right).

The first step is to use truncated octahedra to create the exterior of the augmented KTG. The truncated octahedra we use are combinatorial closed polyhedra with eight hexagonal faces and six square truncation faces. Half of the hexagonal faces are colored blue, the other half white in an alternating fashion. The truncation faces are painted red, see figure 3.11 (left).

Lemma 3.3. *Every sequence of KTG moves S has the following properties:*

1. *The exterior E_S of the singly augmented KTG Γ'_S is homeomorphic to the space obtained by glueing together $2t + 2$ truncated octahedra, where t is the number of triangle moves in S .*
2. *If β is a sufficiently small ball around an interior point of an edge in E_S , the intersection of β and the union of the interiors of the octahedra making up E_S has either two or four components.*
3. *For each vertex of Γ'_S there is a pair of blue faces that is sent by the homeomorphism from part 1) onto the three holed sphere in the boundary of the exterior of Γ'_S corresponding to that vertex. The boundary circles of every hole are glued together from pairs of red edges of the two blue faces.*

Proof. The proof proceeds by induction on the number of KTG moves in the sequence S .

Induction basis. Let us suppose first that S is empty so that Γ'_S is the standard tetrahedron. Now take two truncated octahedra and glue their white faces together in pairs via the identity. To see how this produces the exterior

of the tetrahedron graph let us first look at a single truncated combinatorial octahedron, see figure 11 (right).

By a homeomorphism we can present the truncated octahedron as the upper half space (thought of as lying behind the paper) plus infinity with the colored faces on its boundary. The blue faces are now small blue disks in the plane, while one white face is stretched out so as to contain infinity. Now we bend the blue and red faces up as in figure 3.12. In this figure the interior of the octahedron is located directly above the blue dome-like faces in the upper half space. The horizontal plane on which the blue domes rest contains the white faces.

We can place the second octahedron in the lower half space with the blue faces pushed downwards so that it looks like the reflection of the upper octahedron in the horizontal plane. Glueing the octahedra together along the white faces thus produces a 3-manifold homeomorphic to the exterior of the tetrahedral graph. Since we used exactly two octahedra part 1) is proven.

For part 2) note that all edges of the exterior are alike so that we can concentrate on one of them. Let B be a small ball around an interior point of such an edge. The intersection of B with the interiors of the octahedra has two components, one in the upper half space and one in the lower half space.

The third part is also clear since the exterior can be arranged in such a way that the horizontal plane cuts it into mirror symmetrically arranged truncated octahedra.

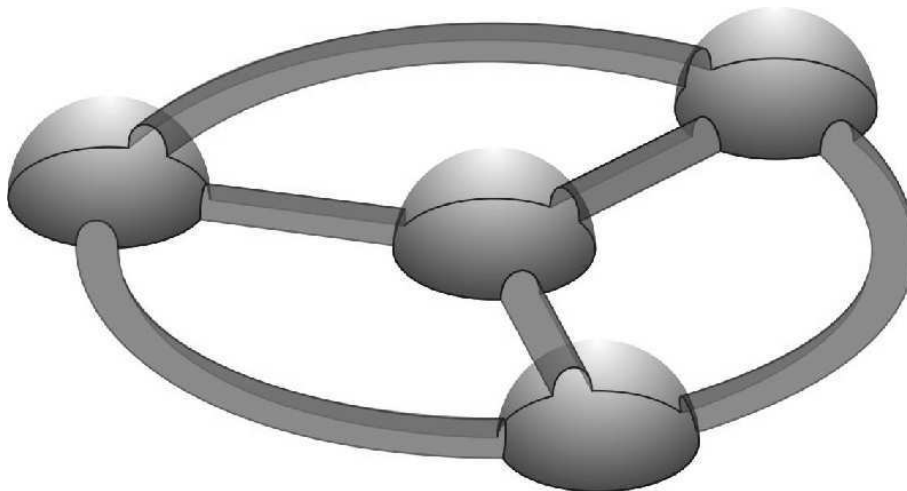


Figure 3.12: The exterior of the standard tetrahedron can be obtained by glueing two truncated octahedra. Only the upper one is shown.

Induction step. Suppose S is a sequence of KTG moves that has the properties 1,2,3 in the lemma. Let T be a sequence of KTG moves obtained by performing one of the four KTG moves directly after S . In order to show that T also has properties 1,2,3 we need to consider four cases depending on which KTG move was made: negative or positive half twist, triangle or unzip.

Half twist. If the last move was a half twist then the exteriors of Γ_S and Γ_T are homeomorphic and the number of triangle moves in producing them is

equal. We can therefore use the gluing of truncated octahedra that worked for S .

Triangle move. Since T contains one more triangle move than S we need two more truncated combinatorial octahedra to glue the exterior E_T than we needed to glue E_S . We will call the two new truncated octahedra O_1 and O_2 . Let v be the vertex of Γ_S where the triangle move was performed. By the induction hypothesis 3) we know there are two blue faces B_1 and B_2 in E_S that make up the three-holed sphere corresponding to v . The new glueing is produced from the old by decreeing that one blue face of O_i is to be identified with the face B_i . The corresponding pairs of white faces of O_1 and O_2 should be identified also.

To see that that the exterior of Γ_T is homeomorphic to the above glueing we start by bringing the truncated octahedron O_1 into the dome-like form seen in figure 3.13 (right). The chosen blue face (drawn slightly transparent) is a hemisphere and the rest of O_1 is below it. The other blue faces are small domes and the white faces are horizontal. The red faces are half tubes. Now bring O_2 into mirror symmetric position below the horizontal plane and glue them along the white faces. The result is a closed ball with three tubular entrances connecting to a triangular tunnel in the middle. It is now clear that once we glue this ball inside the three-holed sphere corresponding to the vertex v we get the exterior of Γ_T .

To check property 2) we only need to check the edges of O_1 and O_2 . For them it is clear from the mirror symmetric arrangement of O_1 and O_2 . This also proves property 3).

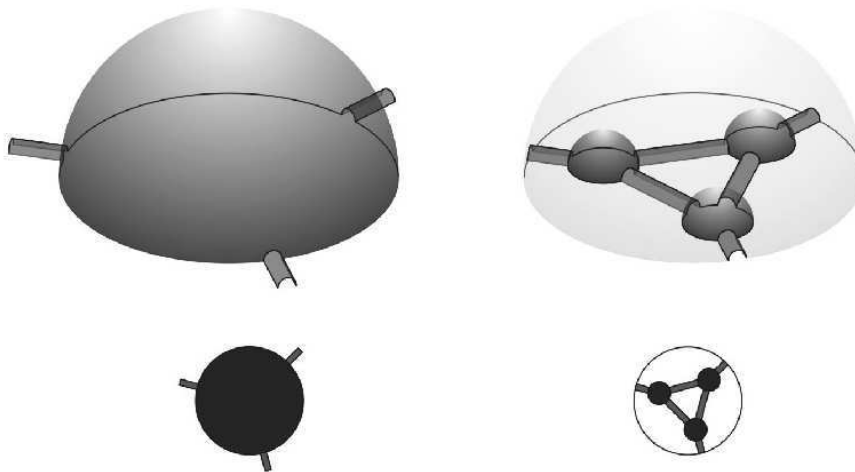


Figure 3.13: The operation corresponding to the triangle move. Only the boundary of the upper half has been depicted. The smaller pictures are a top view and should remind one of the KTG move.

Unzip. We will show that the glueing of octahedra that produces the exterior E_S also produces E_T after adding an extra identification of faces. Suppose that Γ_T is obtained from Γ_S by performing a 1-unzip move on the edge e . Take a small open ball neighborhood B in \mathbb{S}^3 of the tube around e that contains the two three-holed spheres around to the endpoints of e but does not meet any other parts of the boundary of E_S . This ball is depicted as a cylinder in

figure 3.14 (upper left). By the induction hypothesis we know that under the homeomorphism from part 1) the three-holed spheres both split up into two blue faces each in such a way that the boundary circles are glued from pairs of edges. One can thus arrange the ball B in \mathbb{R}^3 such that it is mirror symmetric with respect to the horizontal plane. Cutting along the horizontal plane produces two balls B_1 and B_2 . The boundary of one of the balls can then be flattened to look like the second picture of figure 14 (upper right).

Now let us glue together the two blue faces in B_1 . This produces the next picture in figure 3.14 (lower right). The red face in the middle of the second picture becomes a tube and the opposite red faces are joined. Now glue the blue faces of B_2 in the same way and then glue B_1 and B_2 back together. We get the ball B' seen in the last picture of figure 3.14 (lower left).

Note that when there are h half twists present on the edge e then performing an unzip produces h half twists between the resulting strands. To accommodate this feature in our glueing we cut B' open again along the two pairs of blue faces. They form a punctured disk whose boundary circle is a longitude of the newly produced ring. The disk is pierced twice by the two horizontal components of the graph that go through the ring. A half twist in these two components is produced by reglueing the disks with a half twist. This last correction gives the homeomorphism between the exterior E_T and the glueing of octahedra. When h is even then the correction has not changed the glueing, but if h is odd then we have identified the blue faces of B_1 to the diagonally opposite ones of B_2 .

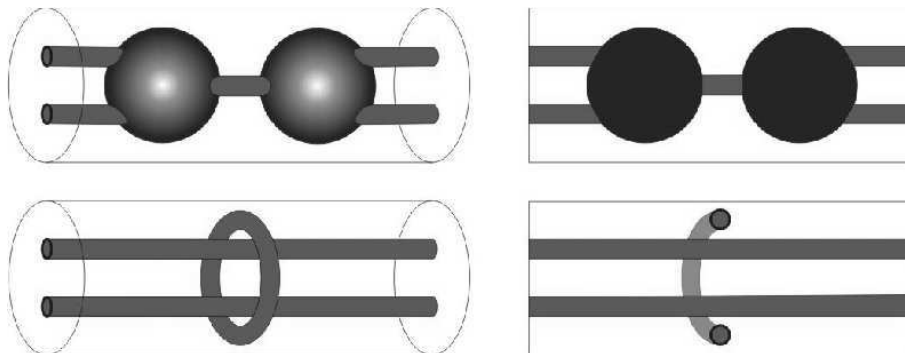


Figure 3.14: The homeomorphism corresponding to the 1-unzip.

The extra identification of faces has doubled the number of parts of octahedra coming together at some of the edges of the blue faces involved, but these were previously unglued so this settles part 2) of the lemma. Part 3) is still true because we simply deleted two vertices and left the exterior unchanged around the other ones. \triangle

Now that we have constructed the exterior of the singly augmented KTG Γ' the next step is to go back to its outside.

Lemma 3.4. *The outside $O_{\Gamma'}$ is homeomorphic as a 3-manifold with boundary pattern to the glueing of truncated octahedra that we constructed for the exterior in lemma 3.3, except that we remove all closed red square faces and endow it*

with the boundary pattern formed by lines on the unglued blue faces that are parallel to the removed red edges.

Proof. The proof of the previous lemma goes through step by step if we replace the exterior by the outside and remove the red truncation faces. It is easy to see that the homeomorphism can be made to identify the boundary patterns. \triangle

Finally we turn to hyperbolic geometry. The above gluing of truncated octahedra has the property that at each edge either two or four solid angles meet. This means that if we declare all the truncated octahedra to be regular ideal hyperbolic octahedra then we obtain a hyperbolic manifold with geodesic boundary with cusps based on the tori and annuli that used to be truncation faces [Rat].

The circles in the boundary pattern of the outside $O_{\Gamma'}$ now become annular cusp loops because in the exterior they are freely homotopic to the boundary circles of the annuli in the closure of $O_{\Gamma'}$. The exterior is exactly the natural compactification of $O_{\Gamma'}$. This finishes the construction of the hyperbolic structure on the outside of a singly augmented KTG and also the proof part 2) of the main theorem.

3.5 Conclusion

The purpose of this paper was to generalize the volume conjecture to KTGs and to prove it for augmented KTGs. In order to generalize to links and KTGs it was necessary to restrict to odd colors. For knots this seems unnecessary and in general one may ask which KTGs will satisfy the original volume conjecture.

The generalization of the volume of the complement to KTGs involved considering a specific 3-manifold with boundary pattern called the outside of a graph. This notion also makes sense for arbitrary graphs so that one may try to apply geometric techniques to questions in graph embedding. One may also hope to generalize the volume conjecture to arbitrary graphs, but then one must first be able to define the colored Jones invariant of any vertex. For trivalent vertices the colored Jones invariant has a natural meaning as a Clebsch–Gordan projector but for arbitrary vertices there is more choice.

In this paper we have proven the volume conjecture for augmented KTGs provided they had sufficiently many augmentation rings. It would be very natural to try to remove this restriction on the number of rings but this will require a more detailed analysis of the colored Jones invariant of such KTGs.

Looking back we can summarize our proof as follows. We have seen three different meanings of the KTG moves. Firstly they can be used to generate all KTGs from the tetrahedron. Secondly, reading them backwards yields an expression for the colored Jones invariant in terms of six- j symbols. Thirdly the augmented moves encode combinatorics of the triangulation by octahedra of the corresponding singly augmented KTG. The second and the third viewpoint come together once one notices that augmenting kills the summations in the expression for the Jones invariant (at least at the root of unity). Using the known asymptotics of the regular six- j symbol that remains this gives a natural and proof for the volume conjecture for augmented KTGs.

It seems that the augmented KTGs form a tractable class of KTGs that makes a good testing ground for further extensions of the volume conjecture. For example the complexified volume conjecture [MMOTY]. It is to be hoped

that with the right definition of the Chern–Simons invariant for manifolds with boundary pattern this conjecture also holds for KTGs.

A reason for the tractability of the augmented KTGs might be that they are of arithmetic type, see corollary 3.3. So far all knots links and KTGs for which the volume conjecture was proven, were of arithmetic type or not hyperbolic at all (or a combination of the two).

Chapter 4

Asymptotics of classical spin networks

4.1 Introduction

4.1.1 Spin networks and their evaluations

The paper is concerned with

- (a) an existence theorem for the asymptotics of evaluations of arbitrary spin networks (using the theory of G -functions),
- (b) a rationality property of the generating series of all evaluations with a fixed underlying graph (using the combinatorics of the chromatic evaluation of a spin network),
- (c) a complete study of the asymptotics of the so-called $6j$ -symbols in all cases: Euclidean, Plane or Minkowskian (using the theory of Borel transform),
- (d) the assignement of two numerical invariants to spin networks and cubic graphs, the spectral radius and a number field (see Definition 4.5),
- (e) an explicit illustration of our results for the regular and some flat $6j$ -symbols (using the constructive WZ method).

A (classical) *spin network* (Γ, γ) consists of a *cubic ribbon graph* Γ (i.e., an abstract trivalent graph with a cyclic ordering of the edges at each vertex) and a coloring γ of its set of edges by natural numbers.

According to Penrose, spin networks correspond to a diagrammatic description of tensors of representations of $SU(2)$, and their evaluation is a contraction of the above tensors. Spin networks originated in Racah's work in atomic spectroscopy in the late forties [Ra] and in the work of Wigner in the fifties [Wi] and their evaluations (exact or asymptotic) is a useful and interesting topic studied by Ponzano-Regge, Biedenharn-Louck and many others; see [BL1, BL2, PR, VMK]. In the past three decades, spin networks have been used in relation to classical and quantum gravity and angular momentum in 3-dimensions; see [EPR, Pe1, Pe2, RS]. On the mathematical side, q -deformations of spin networks (so called quantum spin networks) appeared in the eighties in

the work of Kirillov-Reshetikhin [KR]. *Quantum spin networks* are *knotted framed trivalent graphs* embedded in 3-space with a cyclic ordering of the edges near every vertex, and their evaluations are rational functions of a variable q . The quantum $3j$ and $6j$ -symbols are the building blocks for topological invariants of closed 3-manifolds in the work of Turaev-Viro [TV, Tu]. Quantum spin networks are closely related to a famous invariant of knotted 3-dimensional objects, the celebrated *Jones polynomial*, [J]. A thorough discussion of quantum spin networks and their relation to the Jones polynomial and the *Kauffman bracket* is given in [KL] and [CFS].

Aside from the above applications, spin networks and their evaluations have an intrinsic interest, they are formulated in terms of elementary combinatorial data and offer many challenges even for relatively simple networks such as the cube. Some examples of spin networks that will be discussed in the paper are shown in Figure 4.1.

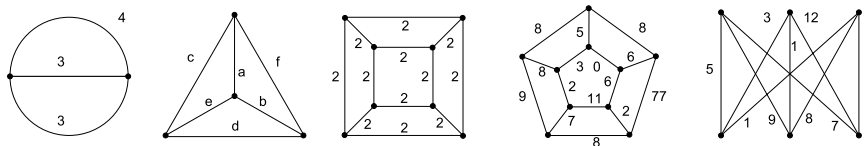


Figure 4.1: From left to right: The theta or $3j$ -symbol, the tetrahedron or $6j$ -symbol, the Cube, the 5-sided drum and the complete bipartite graph $K_{3,3}$ or $9j$ -symbol. The cyclic order of the edges around each vertex is counterclockwise.

Spin networks with underlying graph Θ or a tetrahedron are usually called $3j$ -symbols and $6j$ -symbols respectively and they form the building blocks for the evaluation of any spin network; see for example Section 4.6.1 or [BL1, BL2, PR]. We now discuss the evaluation of a spin network, introduced by Penrose in [Pe1, Pe2].

Definition 4.1. (a) We say a spin network is *admissible* when the sum of the three labels a, b, c around every vertex is even and a, b, c satisfy the triangle inequalities: $|a - b| \leq c \leq a + b$.

(b) The evaluation $\langle \Gamma, \gamma \rangle^P$ of a spin network (Γ, γ) is defined to be zero if it is not admissible. An admissible spin network is evaluated by the following algorithm.

- Use the cyclic ordering to thicken the vertices into disks and the edges into untwisted bands.
- Replace the vertices and edges by the linear combinations of arcs as shown in Figure 4.2.
- Finally the resulting linear combination of closed loops is evaluated by assigning the value $(-2)^n$ to a term containing n loops.

For example, in Figure 4.1 the Θ network and the Cube are admissible, the 5-sided drum and the $9j$ -symbol are not. Note that the admissibility condition is equivalent to saying that the strands can be connected at each vertex as in Figure 4.2. Note also that cubic ribbon graphs Γ are allowed to have multiple

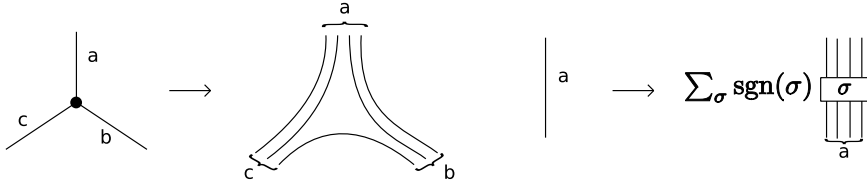


Figure 4.2: The rules for evaluating a spin network. Replace vertices and edges by linear combinations of arcs and count the number of closed loops.

edges, loops and may be disconnected with components that contain no vertices. In addition, Γ may be and non-planar (contrary to the requirement of many authors [We, Mou, KL]), as long as one fixes a cyclic ordering of the edges at each vertex. The latter condition is implicit in [Pe1]. It turns out that a different cyclic ordering on a vertex of a spin network effects its evaluation by a sign; see Lemma 4.2 below.

4.1.2 A fundamental problem

It is easy to see that if (Γ, γ) is an admissible spin network and n is a natural number, then $(\Gamma, n\gamma)$ is admissible as well. A fundamental problem is to study the asymptotic behavior of the sequence of evaluations $\langle \Gamma, n\gamma \rangle^P$ when n is large. This problem actually consists of three parts.

Problem 4.1. *Fix an admissible spin network (Γ, γ) .*

- (a) *Prove the existence of an asymptotic expansion of the sequence $\langle \Gamma, n\gamma \rangle^P$ when n is large.*
- (b) *Compute the asymptotic expansion of $\langle \Gamma, n\gamma \rangle^P$.*
- (c) *Identify the terms in the asymptotic expansion with geometric invariants of the spin network.*

Although any spin network can be evaluated in terms of $3j$ and $6j$ -symbols, a positive solution to parts (a), (b) or (c) of Problem 4.1 for $3j$ and $6j$ -symbols does *not* imply a solution to for arbitrary spin networks.

Problem 4.1 is motivated by the belief that the quantum mechanics of particles with large spin will approximate the classical theory. There is a large physics literature for Part (b); see for example [VMK]. On the other hand, the literature for Part (a) is relatively new and short, and to the best of our knowledge concerns only $3j$ and $6j$ -symbols with certain labellings. Roberts used geometric quantization techniques to prove the leading asymptotic behavior of $6j$ -symbols in the so-called Euclidean case; see [Rb1, Rb2].

In order to get an exponentially (and not factorially) growing asymptotic expansion we will rescale the evaluations of spin networks by factorials of linear forms on the labels of their edges as follows.

Definition 4.2. *We define the standard normalization of a spin network evaluation to be*

$$\langle \Gamma, \gamma \rangle = \frac{1}{Z!} \langle \Gamma, \gamma \rangle^P \quad (4.1)$$

where $\mathcal{I}!$ is defined to be the product

$$\mathcal{I}! = \prod_{v \in V(\Gamma)} \left(\frac{-a_v + b_v + c_v}{2} \right)! \left(\frac{a_v - b_v + c_v}{2} \right)! \left(\frac{a_v + b_v - c_v}{2} \right)! \quad (4.2)$$

where a_v, b_v, c_v are the colors of the edges emanating from vertex v , and $V(\Gamma)$ is the set of vertices of Γ .

There are many useful properties of this evaluation:

- $\langle G, \gamma \rangle$ is still an integer (see Theorem 4.5),
- the sequence $\langle \Gamma, n\gamma \rangle$ is exponentially bounded (see Theorem 4.1),
- the spin generating series is a rational function (see Theorem 4.5 below).

4.2 Existence of asymptotics

4.2.1 Asymptotics via G -functions

Our first result is a complete solution of Part (a) of Problem 4.1 for all spin networks, using the theory of G -functions. To state it, we need to recall the notion of a sequence of Nilsson type [Ni].

Definition 4.3. *We say that a sequence (a_n) is of Nilsson type if it has an asymptotic expansion of the form*

$$a_n \sim \sum_{\lambda, \alpha, \beta} \lambda^n n^\alpha (\log n)^\beta S_{\lambda, \alpha, \beta} h_{\lambda, \alpha, \beta}(1/n) \quad (4.3)$$

where

- the summation is over a finite set,
- the growth rates λ are algebraic numbers of equal magnitude,
- the exponents α are rational and the nilpotency exponents β are natural numbers,
- the Stokes constants $S_{\lambda, \alpha, \beta}$ are complex numbers,
- the formal power series $h_{\lambda, \alpha, \beta}(x) \in K[[x]]$ are Gevrey-1 (i.e., the coefficient of x^n is bounded by $C^n n!$ for some $C > 0$),
- K is a number field generated by the coefficients of $h_{\lambda, \alpha, \beta}(x)$ for all λ, α, β .

The above definition uses the notion of an asymptotic expansion in the sense of Poincare, given in [O, Sec.1]. In the special case where there is only one growth rate, the notation

$$a_n \sim \lambda^n n^\alpha (\log n)^\beta \sum_{k=0}^{\infty} \frac{\mu_k}{n^k}$$

means that for every $N \in \mathbb{N}$ we have

$$\lim_{n \rightarrow \infty} n^N \left(a_n \lambda^{-n} n^{-\alpha} (\log n)^{-\beta} - \sum_{k=0}^{N-1} \frac{\mu_k}{n^k} \right) = \mu_N.$$

In Section 4.7 we will prove the following.

Theorem 4.1. *For every spin network $\langle \Gamma, \gamma \rangle$, the sequence $\langle \Gamma, n\gamma \rangle$ is of Nilsson type.*

Theorem 4.1 follows from the theory of G -functions by combining Theorems 4.2 and 4.3 below. G -functions were introduced by Siegel ([Si]) in relation to transcendence problems in number theory. Many of their arithmetic and algebraic properties were established by André in [An]. G -functions appear naturally in Geometry (as Variations of Mixed Hodge Structures), in Arithmetic and most recently in Enumerative Combinatorics. For a detailed discussion, see [Ga3] and references therein. Let us recall the notion of a G -function.

Definition 4.4. *We say that series $G(z) = \sum_{n=0}^{\infty} a_n z^n$ is a G -function if*

- (a) *the coefficients a_n are algebraic numbers,*
- (b) *there exists a constant $C > 0$ so that for every $n \in \mathbb{N}$ the absolute value of every conjugate of a_n is less than or equal to C^n ,*
- (c) *the common denominator of a_0, \dots, a_n is less than or equal to C^n ,*
- (d) *$G(z)$ is holonomic, i.e., it satisfies a linear differential equation with coefficients polynomials in z .*

The following theorem is proven in Section 4.7. The proof is elementary given the results of [Ga3] and the fact that an evaluation $\langle \Gamma, n\gamma \rangle$ can be written as a multi-dimensional combinatorial sum of a balanced hypergeometric term.

Theorem 4.2. *The generating function*

$$F_{\Gamma, \gamma}(z) = \sum_{n=0}^{\infty} \langle \Gamma, n\gamma \rangle z^n \tag{4.4}$$

of an arbitrary spin network (Γ, γ) is a G -function.

The next result follows by a combination of results of André, Katz and Chudnovsky-Chudnovsky; see [An] and also [Ga3, Sec.2].

Theorem 4.3. *If $G(z) = \sum_{n=0}^{\infty} a_n z^n$ is a G -function, then (a_n) is a sequence of Nilsson type.*

Every G -function has two basic invariants: an analytic and an arithmetic one:

- the radius of convergence at $z = 0$, which equals to $|\lambda|^{-1}$ where λ is a growth rate of (a_n) as in Definition 4.3,
- a number field K corresponding to (a_n) as in Definition 4.3.

Theorem 4.2 motivates the following invariants of a spin network: its spectral radius and its number field.

Definition 4.5. *Let (Γ, γ) be a spin network.*

- (a) *The spectral radius $\rho_{\Gamma, \gamma}$ is defined to be the inverse of the radius of convergence of the generating function $F_{\Gamma, \gamma}(z)$ at $z = 0$.*
- (b) *The number field $K_{\Gamma, \gamma}$ is defined to be the number field associated to the G -function (4.4).*
- (c) *The spectral radius ρ_{Γ} and the number field K_{Γ} of a cubic ribbon graph is defined to be $\rho_{\Gamma, 2}$ and $K_{\Gamma, 2}$ respectively, where 2 denotes the admissible coloring of all edges of Γ by 2.*

4.2.2 Computation of asymptotics

The proof of Theorem 4.1 is not constructive. We know of several different methods for computing the asymptotic expansions of spin network evaluations. We will list them here briefly and illustrate them in the following sections.

- (a) The method of *Borel transform* for one-dimensional sums of balanced hypergeometric terms. This method has been developed for one-dimensional sums in [CG1, CG2, Ga6]) and gives exact formulas for the complete asymptotic expansion of such sums. The method ought to extend to multi-dimensional sums, but this still needs to be developed. Since $6j$ -symbols are given by one-dimensional sums of a balanced hypergeometric term (in all cases, Euclidean, Plane or Minkowskian), this allows us to compute exactly the leading asymptotic behavior of $6j$ -symbols.
- (b) The method of *G-functions*. We mentioned already that the generating series $F_{\Gamma, \gamma}(z)$ of (4.4) is a G -function in a non-constructive way, but more is actually true. In Theorem 4.6 we show that $F_{\Gamma, \gamma}(z)$ is the diagonal of an explicit rational function. Thus, the asymptotics of the Taylor coefficients $\langle \Gamma, n\gamma \rangle$ of $F_{\Gamma, \gamma}(z)$ can be computed in principle via Hodge theory, along the lines of [BK]; see also [PW1, PW2]. Unfortunately, Pemantle-Wilson's results require genericity assumptions that do not apply even in the case of the $K_{3,3}$ or the Cube spin network.
- (c) The method of Wilf-Zeilberger. The fundamental theorem of Wilf and Zeilberger implies that for an arbitrary spin network (Γ, γ) , the sequence $\langle \Gamma, n\gamma \rangle$ is a multi-dimensional sum of a hypergeometric term, and thus, holonomic, i.e., it satisfies a recursion relation with coefficients polynomials in n , [WZ1]. The WZ method is constructive, and has been implemented in several platforms, [PWZ, PaRi, WZ1]. WZ has been implemented for multidimensional sums, but in practice it works best for one or two dimensional sums. Using the WZ method, we compute the asymptotics of three simple examples, a Euclidean $6j$ -symbol, a Plane one and a Minkowskian $6j$ -symbol, in Section 4.10.
- (d) The ansatz for the asymptotics of hypergeometric multi-dimensional sums. In [Ga2] the first author developed a constructive ansatz for locating the

singularities of the generating series of balanced hypergeometric multi-dimensional sums. The conjecture has been confirmed for one-dimensional sums using the theory of Borel transform. For higher dimensional sums the conjecture requires a genericity assumption (finiteness of the solution set of the so-called Variational Equations) which does not seem to hold for spin networks with more than six edges. A proof of the ansatz in the higher dimensional case is expected to follow by developing further the theory of Borel transform.

The practical limitation of these methods is discussed in Section 4.12.

4.3 Asymptotics of $6j$ -symbols

4.3.1 The geometry of the tetrahedron and asymptotics of the $6j$ -symbol

In the special case of the tetrahedron graph we present a complete solution to Parts (b) and (c) of Problem 4.1 using the method of Borel transform. We can explicitly compute the asymptotic expansions for all possible colorings, even in the degenerate and non-physical cases. Moreover the quantities in the asymptotic expansion can be expressed as geometric properties of the dual tetrahedron graph interpreted as a metric polyhedron.

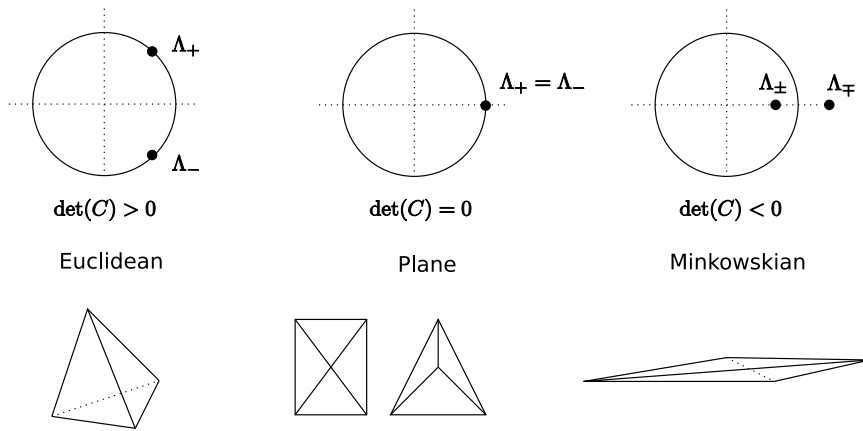


Figure 4.3: The three realizations of the dual metric tetrahedron depending on the sign of the Cayley-Menger determinant $\det(C)$. Also depicted are the two exponential growth factors Λ_{\pm} of the $6j$ -symbol.

In this section (\triangle, γ) denotes the tetrahedral spin network colored by an admissible coloring γ . Consider the planar dual graph ∇ (also a tetrahedron) with the same labelling on the edges. Regarding the labels of ∇ as edge lengths one may ask whether (∇, γ) can be realized as a metric Euclidean tetrahedron with these edge lengths. The admissibility of (\triangle, γ) implies that all faces of the dual tetrahedron ∇ satisfy the triangle inequality. A well-known theorem

of metric geometry [Bl] implies that (∇, γ) can be realized in *exactly one* of three flat geometries

- (a) Euclidean 3-dimensional space \mathbb{R}^3
- (b) Minkowskian space $\mathbb{R}^{2,1}$
- (c) Plane Euclidean \mathbb{R}^2 .

Moreover, the above trichotomy is decided by the sign of the *Cayley-Menger determinant* $\det(C)$ which is a degree six polynomial in the six edge labels; see Definition 4.14. Without loss of generality, we will assume that (\triangle, γ) is *non-degenerate* in the sense that all faces of ∇ are two dimensional (i.e., the triangle inequalities are strict). In the degenerate case, the evaluation of 6-symbol is a ratio of factorials, whose asymptotics are easily obtained from Stirling's formula. Notice that (\triangle, γ) can be degenerate only in the Plane and Minkowskian cases.

4.3.2 Numerical invariants of tetrahedra

Every sequence of Nilsson type comes with its own numerical invariants: its growth rates, exponents, nilpotency exponents, Stokes constants and number field; see Definition 4.3. Theorem 4.1 implies that 6j-symbols have such invariants. In this section we will define a set of numerical invariants of tetrahedra and in the next section we will identify those with the numerical invariants of the corresponding 6j-symbols. In this section, we will fix a nondegenerate tetrahedral spin network (\triangle, γ) .

Definition 4.6. (a) Let θ_a be the *exterior dihedral angle* corresponding to edge a of the metric realization of (∇, γ) .
(b) Consider the growth rates Λ_{\pm} defined by:

$$\Lambda_{\pm} = e^{\pm i \sum_a \theta_a \frac{a}{2}}. \quad (4.5)$$

(c) Consider the number field

$$K = \mathbb{Q}(\sqrt{-\det(C)}) \quad (4.6)$$

The next Lemma, proven in Section 4.9.2, explains the top part of Figure 4.3.

Lemma 4.1. *The growth rates Λ_{\pm} have the following properties.*

- (a) $\Lambda_+ \Lambda_- = 1$
- (b) *In the Euclidean case we have additionally that $\Lambda_- = \overline{\Lambda_+}$ and $\Lambda_+ \neq \Lambda_-$ and consequently $|\Lambda_+| = |\Lambda_-| = 1$, and $\Lambda_{\pm} \neq \pm 1$.*
- (c) *In the Plane case, we have additionally that $\Lambda_+ = \Lambda_-$ and consequently $\Lambda_{\pm} \in \{-1, 1\}$.*
- (d) *In the Minkowskian case, we have additionally that $\Lambda_{\pm} \in \mathbb{R} \setminus \{0\}$. Exactly one of Λ_{\pm} is inside and one is outside the unit circle. Let Λ denote the one inside the unit circle.*

Definition 4.7. We define the exponents α_{\pm} by

$$(\alpha_+, \alpha_-) = \begin{cases} \left(-\frac{3}{2}, -\frac{3}{2}\right) & \text{if } \gamma \text{ is Euclidean or Minkowskian} \\ \left(-\frac{4}{3}, -\frac{5}{3}\right) & \text{if } \gamma \text{ is Plane.} \end{cases} \quad (4.7)$$

Definition 4.8. (a) If γ is Euclidean, we define

$$S_{\pm} = \frac{e^{\pm i(\sum_a \frac{\theta_a}{2} + \frac{\pi}{4})}}{\sqrt{6\pi \text{Vol}}} \quad (4.8)$$

(b) If γ is Minkowskian, we define

$$S_{\pm} = \mp \frac{e^{\pm i(\sum_a \frac{\theta_a}{2})}}{\sqrt{6\pi \text{Vol}}} \quad (4.9)$$

(c) If γ is Plane, we define

$$S_{\pm} = \frac{\Gamma(4/3)(12A)^{1/3}}{\pi \prod |B_j|^{1/6}} \quad (4.10)$$

The definition of A and B_j (homogeneous polynomials in γ of degree 2 and 3 respectively) in the Plane case can be found in Section 4.9.2.

4.3.3 Asymptotics of $6j$ -symbols

In this section we will express the asymptotics of the $6j$ symbols (using the minor change $\langle \cdot \rangle^U$ in normalization explained in Definition 4.15) in terms of the numerical invariants of the previous section.

Theorem 4.4. Fix a nondegenerate tetrahedron (\triangle, γ) .

(a) If γ is Euclidean or Plane, there exist $h_{\pm} \in K[[x]]$ so that

$$\langle \triangle, n\gamma \rangle^U \sim \Lambda_+^n n^{\alpha_+} S_+ h_+ \left(\frac{1}{n}\right) + \Lambda_-^n n^{\alpha_-} S_- h_- \left(\frac{1}{n}\right) \quad (4.11)$$

(b) If γ is Minkowskian, let S be the Stokes constant corresponding to Λ . There exists $h \in K[[x]]$ so that

$$\langle \triangle, n\gamma \rangle^U \sim \Lambda^n n^{\alpha} S h \left(\frac{1}{n}\right)$$

Moreover, K is the associated number field.

Equation (4.11) implies in the Euclidean case that

$$\langle \triangle, n\gamma \rangle^U = \frac{\sqrt{2}}{\sqrt{3\pi n^3 \text{Vol}}} \cos \left(n \sum_a \frac{\theta_a}{2} + \sum_a \frac{\theta_a}{2} + \frac{\pi}{4} \right) \left(1 + O \left(\frac{1}{n} \right) \right)$$

which is the well-known *Ponzano-Regge formula* for the asymptotics of Euclidean $6j$ -symbols. In the Euclidean and Minkowskian cases these asymptotic formulas were conjectured by Ponzano-Regge [PR]. An elementary but non-rigorous proof of the Euclidean case was given in [Gu]. The Euclidean case was rigorously proven by [Rb1] but there was no proof for the Minkowskian case. The formula for the Plane case is new.

Remark 4.1. Notice that exponents α_{\pm} in the Plane case of Theorem 4.4 is not a half-integer but rather the third of an integer. This phenomenon (accompanied by the collision of the two points in the Plane case of Figure 4.3) is natural from the point of view of local monodromy of G -functions, and is often overlooked in the physics literature.

An illustration of Theorem 4.4 in all three geometries is given in Section 4.10, using the WZ method.

Remark 4.2. Using Theorem 4.4, we can compute explicitly the leading asymptotics of an infinite family of spin networks whose underlying graphs can be created from the tetrahedron graph by repeatedly replacing a vertex by a triangle. As follows from the recoupling theory discussed in Section 4.6 the corresponding spin network evaluation will change by multiplication by a certain $6j$ -symbol and a theta. We thus find the asymptotics for all these networks. In particular, this leads to spin networks with an arbitrary number of growth rates, and with associated number fields which are the composite of an arbitrary number of quadratic number fields.

4.4 A generating function for spin network evaluations

In this section we discuss the generating series S_{Γ} of a spin network evaluation for a fixed underlying graph Γ . As it turns out, S_{Γ} is a rational function. Among other things, this implies that the G -functions of Theorem 4.2 come from geometry and more precisely from a Variation of Mixed Hodge structures, much in the spirit of Bloch-Kreimer [BK].

The next definition introduces the generating series S_{Γ} of a fixed graph Γ with cyclic ordering. S_{Γ} is a formal power series in commuting variables z_e where $e \in E(\Gamma)$, the set of edges of Γ .

Definition 4.9. The spin generating function S_{Γ} of a cubic ribbon graph Γ is defined to be

$$S_{\Gamma} = \sum_{\gamma} \langle \Gamma, \gamma \rangle \prod_{e \in E(\Gamma)} z_e^{\gamma_e} \in \mathbb{Q}[[z_e, e \in E(\Gamma)]] \quad (4.12)$$

where the sum ranges over all colorings γ of the graph Γ .

We will express the spin generating function of an arbitrary graph in terms of the curve polynomial that we will define now. A *curve* in a graph Γ is a 2-regular subgraph. By definition the empty set is also a curve. The set of all curves in Γ is called C_{Γ} .

Definition 4.10. Given a cubic ribbon graph Γ and $X \subset C_{\Gamma}$ we define

(a) a polynomial

$$P_{\Gamma, X} = \sum_{c \in C_{\Gamma}} \epsilon_X(c) \prod_{e \in c} z_e. \quad (4.13)$$

where $\epsilon_X(c) = -1$ (resp. 1) when $c \in X$ (resp. $c \notin X$).

(b) We will call $P_{\Gamma, \emptyset}$ the curve polynomial of Γ .

With the above notation, we define $\iota(X)$ to be the minimal number of intersections when X is drawn on the thickened ribbon graph Γ and

$$a_X = \frac{1}{2^{|C_\Gamma|}} \sum_{Y \subset C_\Gamma} (-1)^{|X \cap Y| + \iota(Y)}. \quad (4.14)$$

The next theorem proves the rationality of S_Γ .

Theorem 4.5. *For every cubic ribbon graph Γ we have*

$$S_\Gamma = \sum_{X \subset C_\Gamma} a_X P_{\Gamma, X}^{-2} \in \mathbb{Z}[[z_\epsilon, e \in E(\Gamma)]] \cap \mathbb{Q}(z_\epsilon, e \in E(\Gamma)). \quad (4.15)$$

Corollary 4.1. *For every spin network (Γ, γ) , the evaluation $\langle \Gamma, \gamma \rangle$ is an integer number.*

Corollary 4.2. *[We] When Γ is planar with the counterclockwise orientation, then $a_X = 0$ unless X is empty, in which case $a_\emptyset = 1$. It follows that*

$$S_\Gamma = \frac{1}{P_{\Gamma, \emptyset}^2}$$

recovering an earlier theorem by Westbury [We].

The next theorem shows that the generating series $F_{\Gamma, \gamma}(z)$ of (4.4) is a *diagonal* of a rational function. Let us recall the notion of a diagonal.

Definition 4.11. *Given a power series $f(x_1, \dots, x_r) \in \mathbb{Q}[[x_1, \dots, x_r]]$ and an exponent $I = (i_1, \dots, i_r) \in \mathbb{N}_+^r$, we define the I -diagonal of f by*

$$(\Delta_I f)(z) = \sum_{n=0}^{\infty} [x^{nI}](f) z^n \in \mathbb{Q}[[z]] \quad (4.16)$$

where $[x^{nI}](f)$ denotes the coefficient of $x_1^{ni_1} \dots x_r^{ni_r}$ in f .

Theorem 4.6. *For every spin network (Γ, γ) we have*

$$F_{\Gamma, \gamma} = \Delta_\gamma S_F \quad (4.17)$$

Consequently, the G -function $F_{\Gamma, \gamma}(z)$ is the diagonal of a rational function, and thus it comes from geometry; see Lemma 4.5 below.

We end this section with the following curious proposition.

Proposition 4.1. *If Γ is a 2-connected cubic ribbon graph, then the evaluations $\langle \Gamma, \gamma \rangle$ for all γ uniquely determine Γ as an abstract trivalent graph. Moreover, we only need to use the colors 0 and 1.*

4.5 Plan of the paper

In Section 4.6 we discuss the recoupling method for evaluating spin networks which reduces the evaluation of an arbitrary spin network to the $3j$ and $6j$ -symbols. Using this method, and an explicit formula for the $3j$ and $6j$ -symbols, we evaluate the Drum and the $K_{3,3}$ graphs.

In Section 4.7 we prove that the evaluation of a spin network is given by a multi-dimensional sum of a balanced hypergeometric term. This, together with the results of [Ga3], implies Theorem 4.2 and Theorem 4.1.

In Section 4.8 we apply techniques of Borel transform (developed in [CG1, CG2, Ga6]) that give exact formulas for the leading asymptotic behavior of one-dimensional sums of hypergeometric terms. Since $6j$ -symbols are given by such sums, this allows us to compute exactly the leading asymptotic behavior of $6j$ -symbols.

Section 4.9 identifies the combinatorial leading asymptotic behavior with geometric quantities associated to the metric tetrahedron in all cases, Euclidean, Plane or Minkowskian.

In Section 4.10 we present an alternative constructive method to compute the asymptotic behavior of evaluations of spin networks, namely the WZ method.

In Section 4.11 we discuss in detail the chromatic evaluation of spin networks and obtain the integrality and rationality results of the spin generating series.

4.5.1 Acknowledgment

The results were conceived in a workshop in Aarhus, Denmark, and presented in HaNoi, Vietnam and Strasbourg, France in the summer of 2007. The authors wish to thank the organizers for their hospitality. S.G. wishes to thank D. Zeilberger for many enlightening conversations.

4.6 Evaluation of spin networks

We start by recording some elementary facts about spin network evaluations.

Lemma 4.2. *Let (Γ, γ) be a spin network.*

- (a) *Inserting a vertex colored $(0, a, a)$ in the interior of an edge of Γ colored a does not change the evaluation of the spin network.*
- (b) *Changing the cyclic ordering at a vertex whose edges are colored a, b, c changes the evaluation by a sign $(-1)^{(a(a-1)+b(b-1)+c(c-1))/2}$*

Proof. (a) The chosen normalization introduces an extra factor $1/a!$ for the new vertex labeled $(0, a, a)$, while it follows from the definition that one also inserts an extraneous summation over permutations in the pre-existing edge labeled a . Since $\sum_{\sigma \in S_a} \sum_{\tau \in S_a} \text{sign}(\sigma)\sigma \text{sign}(\tau)\tau = a! \sum_{\sigma \in S_a} \text{sign}(\sigma)\sigma$ the evaluation is unchanged.

(b) Changing the cyclic order at a vertex with edge labels a, b, c has the following effect. The alternating sum at each of the adjacent edges is multiplied by the permutation that turns the arcs in the edge by 180 degrees. This element has sign $a(a-1)/2$ in S_a . △

As a consequence of part (a) of the above lemma, an edge labeled 0 in a spin network can be removed without affecting the evaluation.

There is an alternative *bracket normalization* $\langle \Gamma, \gamma \rangle^B$ of the evaluation of a spin network (Γ, γ) which agrees with a specialization of the *Jones polynomial* and the *Kauffman bracket*.

Definition 4.12. The bracket normalization of a spin network (Γ, γ) is defined by

$$\langle \Gamma, \gamma \rangle^B = \frac{1}{\mathcal{E}!} \langle \Gamma, \gamma \rangle^P \quad (4.18)$$

where

$$\mathcal{E}! = \prod_{e \in E(\Gamma)} \gamma(e)! \quad (4.19)$$

This normalization has the property that it coincides with the Kauffman bracket (Jones polynomial) of a quantum spin network evaluated at $A = -1$ [KL]. However, $\langle \Gamma, \gamma \rangle^B$ is not necessarily an integer number, and the analogous generating series does not satisfy the rationality property of Theorem 4.5.

Proof. (of Proposition 4.1) For convenience we work with the unnormalized evaluation $\langle \Gamma, \gamma \rangle^P$. A 2-connected graph is determined up to isomorphism by its 2-regular subgraphs, simply take a polygon for every 2-regular subgraph and identify equal edges [Di]. To decide whether a set X of edges forms a 2-regular subgraph, let γ be the coloring that assigns 1 to members of X and 0 to the other edges. By definition of the spin network evaluation X is an n component 2-regular subgraph if and only if $\langle \Gamma, \gamma \rangle^P = (-2)^n$. \triangle

4.6.1 Evaluation of spin networks by recoupling

In this subsection we describe a way of evaluating spin networks by recoupling. We will reduce the evaluation of spin networks to multi-dimensional sums of $6j$ and $3j$ -symbols. The value of the $6j$ and $3j$ -symbols is given by the following lemma of [KL] and [We], using our normalization.

Lemma 4.3. (a) Let (\triangle, γ) denote a tetrahedron labeled and oriented as in Figure 4.1 or Figure 4.5 (left) with $\gamma = (a, b, c, d, e, f)$. Its normalized evaluation is given by $\langle \triangle, \gamma \rangle =$

$$\sum_{k=\max T_i}^{\min S_j} (-1)^k (k+1) \binom{k}{S_1 - k, S_2 - k, S_3 - k, k - T_1, k - T_2, k - T_3, k - T_4} \quad (4.20)$$

where, as usual

$$\binom{a}{a_1, a_2, \dots, a_r} = \frac{a!}{a_1! \dots a_r!}$$

denotes the multinomial coefficient when $a_1 + \dots + a_r = a$, and S_i are the half sums of the labels in the three quadrangular curves in the tetrahedron and T_j are the half sums of the three edges emanating from a given vertex. In other words, the S_i and T_j are given by

$$S_1 = \frac{1}{2}(a+d+b+c) \quad S_2 = \frac{1}{2}(a+d+e+f) \quad S_3 = \frac{1}{2}(b+c+e+f) \quad (4.21)$$

$$T_1 = \frac{1}{2}(a+b+e) \quad T_2 = \frac{1}{2}(a+c+f) \quad T_3 = \frac{1}{2}(c+d+e) \quad T_4 = \frac{1}{2}(b+d+f) \quad (4.22)$$

(b) Let (Θ, γ) denote the Θ spin network of Figure 4.1 admissibly colored by $\gamma = (a, b, c)$. Then we have

$$\langle \Theta, \gamma \rangle = (-1)^{\frac{a+b+c}{2}} \left(\frac{a+b+c}{2} + 1 \right) \left(\frac{a+b+c}{2}, \frac{-a+b+c}{2}, \frac{a-b+c}{2}, \frac{a+b-c}{2} \right) \quad (4.23)$$

Note that the value of a n -colored unknot is by Lemmas 4.2 and 4.3 equal to $(-1)^n(n+1)$.

Recoupling is a way to modify a spin network locally, while preserving its evaluation. This is done as in the topmost picture in Figure 4.4. This formula is called the recoupling formula and follows from the recoupling formula in [KL], using our conventions. The other two pictures in the figure show two important special cases of the recoupling formula, the bubble formula and the triangle formula.

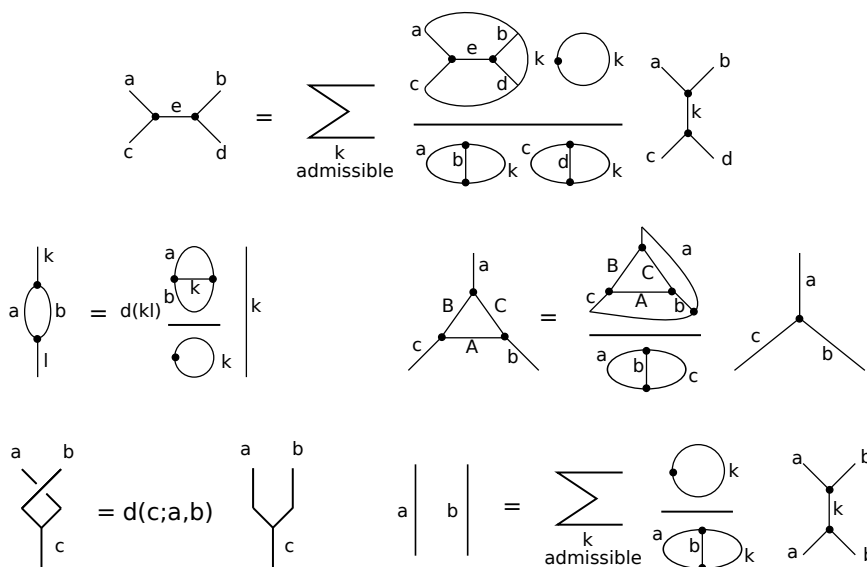


Figure 4.4: The recoupling formula (top), the bubble formula (left) and the triangle formula (right). The sum is over all k for which the network is admissible, and $\delta_{k,l}$ is the *Kronecker delta function*.

The bubble formula shown on the left of Figure 4.4 serves to remove all bigon faces. Likewise the triangle formula can be used to remove triangles. To see why the recoupling formula suffices to write any spin network as a multi sum of products of $6j$ -symbols divided by thetas we argue as follows. Applying the recoupling formula to a curve in the graph reduces its length by one. Keep going until you get a multiple edge which can then be removed by the bubble formula.

Although the triangle formula follows quickly from the bubble formula and the recoupling formula it is important enough to state on its own. This formula shows that the evaluation of the class of *triangular networks* is especially simple. The triangular networks, mentioned in Remark 4.2 are the planar graphs that

can be obtained from the tetrahedron by repeatedly replacing a vertex by a triangle. By the triangle formula any triangular network is simply a product of $6j$ -symbols divided by thetas.

To illustrate how recoupling theory works, let us evaluate the regular s -sided drum and $K_{3,3}$. Consider the s -sided drum network as shown in Equation (4.24) (for $s = 5$) where every edge is colored by the integer n . In the figure we have left out most of the labels n for clarity. By convention unlabeled edges are colored by n . Performing the recoupling move on every inward pointing edge we transform the drum into a string of bubbles that is readily evaluated.

$$\text{Drum}_s = \sum_{k \text{ admissible}} \left(\frac{\theta(n, k)}{\theta(n, k)} \right)^s \text{Cycle}(k) = \sum_{k \text{ admissible}} \left(\frac{\theta(n, k)}{\theta(n, k)} \right)^s \text{Bubble}(k) \quad (4.24)$$

Observing that if n is odd the network is not admissible (and thus evaluates to zero), and denoting the tetrahedron and the theta with one edge colored by k and the others by n by $S(n, k)$ and $\theta(n, k)$ we conclude the following formula for the n -colored s -sided drum.

Proposition 4.2. *If $n = 2N$ is even we have*

$$\langle \text{Drum}_s, 2N \rangle = \sum_{j=0}^{2N} (2j+1) \left(\frac{S(2N, 2j)}{\theta(2N, 2j)} \right)^s$$

and if n is odd we have $\langle \text{Drum}_s, n \rangle = 0$.

For small values of s the drum can be evaluated in a more straight forward way, thus providing some well known identities of $6j$ -symbols. Namely when $s = 1$ we get zero, when $s = 2$ we find some thetas and when $s = 3$ we have by the triangle formula a product of two $6j$ -symbols thus giving a special case of the Biedenharn-Elliott identity [KL]. For $s = 4$ we find a formula for the regular cube, we know of no easier evaluation in this case.

A similar computation for $K_{3,3}$ cyclically ordered as a plane hexagon with its three diagonals gives the following.

Proposition 4.3. *If $n = 2N$ is even we have*

$$\langle K_{3,3}, 2N \rangle = \sum_{j=0}^{2N} (-1)^j (2j+1) \left(\frac{S(2N, 2j)}{\theta(2N, 2j)} \right)^3$$

and if n is odd we have $\langle K_{3,3}, n \rangle = 0$.

Note the similarity between Drum_3 and $K_{3,3}$. The only difference is the sign that comes up in the calculation when one needs to change the cyclic order. The extra sign makes $\langle K_{3,3}, 2N \rangle = 0$ for all odd N . This is because changing the cyclic ordering at a vertex takes the graph into itself, while it produces a sign $(-1)^N$ when all edges are colored $2N$.

4.7 G -functions and existence of asymptotic expansions

4.7.1 Existence of asymptotic expansions

In this section we prove the existence of an asymptotic expansion for all spin networks using the theory of G -functions and the combinatorial fact that any spin network can be evaluated as a multi-dimensional sum of a balanced hypergeometric term.

Definition 4.13. An r -dimensional balanced hypergeometric term $\mathfrak{t}_{n,k}$ (in short, balanced term) in variables (n, k) , where $n \in \mathbb{N}$ and $k = (k_1, \dots, k_r) \in \mathbb{Z}^r$, is an expression of the form

$$\mathfrak{t}_{n,k} = C_0^n \prod_{i=1}^r C_i^{r_i} \prod_{j=1}^J A_j(n, k)^{\epsilon_j} \quad (4.25)$$

where C_i are algebraic numbers for $i = 0, \dots, r$, $\epsilon_j = \pm 1$ for $j = 1, \dots, J$, and A_j are integral affine linear forms in (n, k) that satisfy the balance condition

$$\sum_{j=1}^J \epsilon_j A_j = \text{constant} \quad (4.26)$$

We assume that the convex polytope $P_\mathfrak{t}$ in \mathbb{R}^r defined by $A_j(1, w) \geq 0$ for $j = 1, \dots, J$ and $w = (w_1, \dots, w_r)$ is compact.

Lemma 4.4. For every spin network (Γ, γ) there exists a balanced term $\mathfrak{t}(n, k)$ with $k = (k_1, \dots, k_r)$ such that

$$\langle \Gamma, n\gamma \rangle = \sum_{k \in nP_\mathfrak{t} \cap \mathbb{Z}^r} \mathfrak{t}(n, k) \quad (4.27)$$

for every $n \in \mathbb{N}$.

Proof. Using the recoupling formulae from the previous paragraph we can write $\langle \Gamma, \gamma \rangle$ as a multi-dimensional sum of products of $6j$ -symbols, $3j$ -symbols and unknots (i.e., $1j$ -symbols) with a denominator consisting of $3j$ -symbols. It follows from Equations (4.20) and (4.23) that the $6j$ -symbols (resp. $3j$ -symbols) are balanced 1-dimensional (resp. 0-dimensional) sums, thus the ratio of the product of the $3j$ -symbols by the product of the $3j$ -symbols is a balanced multi-dimensional sum. The unknots can be written as $(-1)^k (k+1)!/k!$ and are therefore balanced as well. It is easy to check that admissibility guarantees that the multi-dimensional sum has finite range. \triangle

Beware that the term $\mathfrak{t}(n, k)$ constructed in the proof of lemma 4.4 is neither unique nor canonical in any sense. Lemma 4.4 and the following result implies Theorem 4.1.

Theorem 4.7. [Ga3, Thm.2] (a) If (a_n) is a multi-dimensional sum of a balanced term, then the generating series

$$F(z) = \sum_{n=0}^{\infty} a_n z^n$$

is a G -function.

(b) If $F(z)$ is a G -function, its Taylor series at $z = 0$ is a sequence of Nilsson type.

Remark 4.3. *This argument implies that the sequences $\langle \Gamma, n\gamma \rangle^U$ and $\langle \Gamma, n\gamma \rangle^P$ are also asymptotic to a rational power of $n!$ times a sequence of Nilsson type. This follows from the fact that the above normalizations of the spin networks differ from Definition 4.2 by a ratio of factorials of linear forms in n , which can be asymptotically expanded using Stirling's formula.*

Let us end this section with a lemma which shows that diagonals of rational functions are G -functions that come from geometry. This is relevant to spin networks since we know from Theorem 4.6 that the generating function $F_{\Gamma, \gamma}$ for the evaluations of a spin network is a diagonal of a rational function.

Fix a power series $f(x_1, \dots, x_r) \in \mathbb{Q}[[x_1, \dots, x_r]]$ convergent at the origin and an exponent $I = (i_1, \dots, i_r) \in \mathbb{N}_+^r$ and consider the diagonal $(\Delta_I f)(z) \in \mathbb{Q}[[z]]$ as in Definition 4.11. Let \mathcal{C} denote a small r -dimensional torus around the origin. Then we have the following.

Lemma 4.5. *With the above assumptions, we have*

$$(\Delta_I f)(z) = \frac{1}{(2\pi i)^r} \int_{\mathcal{C}} \frac{f(x_1, \dots, x_r)}{x_1 \dots x_r - z} dx_1 \wedge \dots \wedge dx_r. \quad (4.28)$$

Proof. With the notation of Definition 4.16, an application of Cauchy's theorem gives for every natural number n

$$[x^{nI}](f) = \frac{1}{(2\pi i)^r} \int_{\mathcal{C}} \frac{f(x_1, \dots, x_r)}{(x_1 \dots x_r)^{n+1}} dx_1 \wedge \dots \wedge dx_r.$$

Summing up for n and interchanging summation and integration concludes the proof. \triangle

If in addition $f(x_1, \dots, x_r)$ is a rational function, then the singularities of the analytic continuation of the right hand-side of (4.28) can be analyzed by deforming the integration cycle \mathcal{C} and studying the corresponding variation of Mixed Hodge Structure as in [BK]. Such G -functions come from geometry; see [An, BK].

4.8 Computation of asymptotic expansions using Borel transform

The results of Section 4.7 are powerful but non-constructive. In this section we will use constructive results from the theory of Borel transform, known in the case of balanced terms of rank 1. These results appear in [CG1, CG2, Ga3], and in the present paper we will quote them without proofs. Let us specialize to 1-dimensional balanced terms $t_{n,k}$, that is expressions of the form

$$t_{n,k} = C_0^n C_1^k \prod_{j=1}^J A_j(n, k)!^{\epsilon_j} \quad (4.29)$$

satisfying the balancing condition (4.26). The relevant example of these is the $6j$ -symbol, Equation (4.20). Fixing a 1-dimensional balanced term $t_{n,k}$, summation over k (it is a finite sum) gives rise to a sequence

$$a_n = \sum_{k \in \mathbb{Z}} t_{n,k} \quad (4.30)$$

To describe and compute the asymptotics of such sequences we need the following notation. For affine linear forms we use the notation $A(n,k) = v_0(A)n + v_1(A)k + v(A)$ and $A(u) = v_0(A) + v_1(A)u$. Next we define the multivalued analytic functions

$$V(u) = \log C_0 + u \log C_1 + \sum_{j=1}^J \epsilon_j A_j(u) \log(A_j(u)) \quad (4.31)$$

$$W(u) = \prod_{j=1}^J A_j(u)^{\epsilon_j/2 + \epsilon_j v(A_j)} \quad (4.32)$$

V and W are analytic functions on the open interval (m, M) (which is determined by $A_j, j = 1, \dots, J$) and they have single-valued analytic continuation in the *doubly cut* complex plane $\mathbb{C} \setminus ((-\infty, m] \cup [M, \infty))$. V and W can be further analytically continued as multivalued functions in the complex plane minus a finite set of points $\mathbb{C} \setminus \{u \prod_j A_j(u) = 0\}$.

Define the constants

$$\mu = \frac{1}{2} \sum_{j=1}^J \epsilon_j, \quad \nu = \sum_{j=1}^J \epsilon_j v(A_j), \quad (4.33)$$

The set of critical points of V satisfies the Variational Equation

$$C_1 \prod_{j=1}^J A_j(u)^{\epsilon_j v_1(A_j)} = 1 \quad (4.34)$$

If u is a critical point of V , then $e^{V(u)} = \lambda(u)$ where

$$\lambda(u) = C_0 \prod_{j: A_j(u) \neq 0} A_j(u)^{\epsilon_j v_0(A_j)} \quad (4.35)$$

Let K denote the number field generated by the solutions of the Variational Equation.

Suppose that u is a critical point of order m for V , that is $V^{(j)}(u) = 0$ for $j = 1, \dots, m$ and $V^{(m+1)}(u) \neq 0$ and W is non-vanishing at u , i.e., $W(u) \neq 0$. Let

$$c_m = 2\Gamma\left(\frac{m+2}{m+1}\right) (m+1)!^{\frac{1}{m+1}}. \quad (4.36)$$

and let

$$\alpha(u) = \mu + \nu + 1 - \frac{1}{m+1} \quad (4.37)$$

and

$$S(u) = (2\pi)^\mu c_m \frac{W(u)}{(-V^{(m+1)}(u))^{\frac{1}{m+1}}} \quad (4.38)$$

We will require a modification of the above definition of the Stokes constant when u lies in one of the cuts $(-\infty, m] \cup [M, \infty)$. In that case, we define

$$S(u) = (2\pi)^\mu c_m \frac{|W(u)|}{(|V^{(m+1)}(u)|)^{\frac{1}{m+1}}} \quad (4.39)$$

Theorem 4.8. *With the above assumptions we have*

$$a_n \sim \sum_u \lambda(u)^n n^{\alpha_u} S(u) h_u \left(\frac{1}{n} \right) \quad (4.40)$$

where $h_u \in K[[x]]$ is Gevrey-1 and u runs through a subset of solutions of the Variational Equation. The selected subset can be described algorithmically and in case of the $6j$ -symbols it is discussed below.

4.9 Asymptotics of the $6j$ -symbol

The purpose of this section is to prove and explain Theorem 4.4 on the explicit expansions of the $6j$ -symbols. Since the asymptotics are phrased in terms of geometric properties of the tetrahedron dual to the spin network, we start with a section on the geometry of the tetrahedron. Next we apply Theorem 4.8 to find the asymptotic expansion and finally we work out the details in each of the geometric cases.

4.9.1 The geometry of the tetrahedron

The asymptotics of the $6j$ -symbols turn out to be intimately related to the geometry of the planar dual tetrahedron. From now on, we will assume that γ is non-degenerate, i.e. that the faces of (∇, γ) are two dimensional triangles.

Recall that the $6j$ -symbol is a tetrahedral spin network (\triangle, γ) admissibly labeled as in Figure 4.1 with $\gamma = (a, b, c, d, e, f)$. Its dual tetrahedron (∇, γ) is also labeled by γ . The tetrahedron and its planar dual, together with an ordering of the vertices and a coloring of the edges of the dual is depicted in Figure 4.5. When a more systematic notation for the edge labels is needed we will denote them by d_{ij} (or ij if there cannot arise any confusion) it follows that

$$(a, b, c, d, e, f) = (d_{12}, d_{23}, d_{14}, d_{34}, d_{13}, d_{24})$$

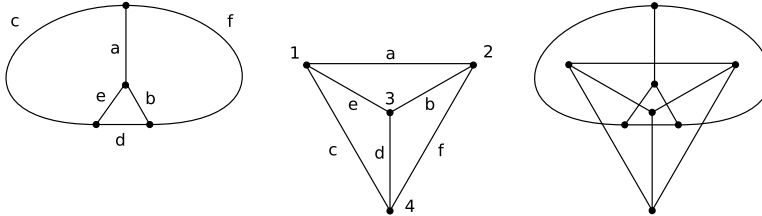


Figure 4.5: The tetrahedral spin network and its planar dual with a vertex and edge labeling.

Recall from Section 4.3.1 that we interpret the labels of the dual tetrahedron ∇ as edge lengths in a suitable flat geometry. One may now ask for a condition that allows one to realize (∇, γ) in a flat metric space such that the edge lengths equal the edge labels. Labeling the vertices of (∇, γ) as in Figure 4.5 we can formulate such a condition in terms of the Cayley-Menger determinant. This is a homogeneous polynomial of degree 3 in the six variables a^2, \dots, f^2 . We give a definition of the determinant following [Ko1].

Definition 4.14. *Given numbers d_{ij} define the (modified) Cayley-Menger matrix (C_{ij}) by $C_{ij} = 1 - d_{ij}^2/2$ for $i, j \geq 1$ and $C_{ij} = \text{sgn}(i - j)$ for when $i = 0$ or $j = 0$. In terms of the coloring $\gamma = (a, b, c, d, e, f)$ of a tetrahedron, we have*

$$C = \begin{pmatrix} 0 & -1 & -1 & -1 & -1 \\ 1 & 1 & 1 - a^2/2 & 1 - e^2/2 & 1 - c^2/2 \\ 1 & 1 - a^2/2 & 1 & 1 - b^2/2 & 1 - f^2/2 \\ 1 & 1 - e^2/2 & 1 - b^2/2 & 1 & 1 - d^2/2 \\ 1 & 1 - c^2/2 & 1 - f^2/2 & 1 - d^2/2 & 1 \end{pmatrix}. \quad (4.41)$$

We can now state the criterion for the realizability of (∇, γ) . For a proof see [Bl] or [Ko1].

Proposition 4.4. *Consider a non-degenerate tetrahedron (∇, γ) . The sign of the Cayley-Menger determinant determines in what space the tetrahedron can be realized such that the edge labels equal the edge lengths*

- If $\det(C) > 0$ then the tetrahedron is realized in Euclidean space \mathbb{R}^3 .
- If $\det(C) = 0$ then the tetrahedron is realized in the Euclidean plane \mathbb{R}^2 .
- If $\det(C) < 0$ then the tetrahedron is realized in Minkowski space $\mathbb{R}^{2,1}$.

In each case the volume of the tetrahedron is given by $\text{Vol} = \frac{1}{6} \sqrt{|\det(C)|}$.

The 6 dimensional space of non-degenerate tetrahedra thus consists of regions of Minkowskian and regions of Euclidean tetrahedra. It turns out to be a cone that is made up from one connected component of three dimensional Euclidean tetrahedra and two connected components of Minkowskian tetrahedra. The three dimensional Euclidean and Minkowskian tetrahedra are separated by Plane tetrahedra. The Plane tetrahedra also form two connected components, representatives of which are depicted in Figure 4.3. The tetrahedra in the Plane component that look like a triangle with an interior point are called *triangular* and the Plane tetrahedra from that other component that look like a quadrangle together with its diagonals are called *quadrangular*. We use the same names for the corresponding Minkowskian components. An integer representative of the triangular Plane tetrahedra is not easy to find as the smallest example is $(37, 37, 13, 13, 24, 30)$.

We finish this section with a short discussion of the dihedral angles of a tetrahedron realized in either of the three above spaces. The cosine and sine of these angles can be expressed in terms of certain minors of the Cayley-Menger matrix. Define the *adjugate matrix* $\text{ad}(C)$ whose ij entry is $(-1)^{i+j}$ times the determinant of the matrix obtained from C by deleting the i -th row and the j -th column. Define C_{iijj} to be the matrix obtained from C by deleting both the i -th row and column and the j -th row and column.

The Law of Sines and the Law of Cosines are well-known formulae for a triangle in the Euclidean plane. The next Lemma is the *Law of Sines* and the *Law of Cosines* for a tetrahedron in all three flat geometries.

Lemma 4.6. *Let θ_{kl} be the exterior dihedral angle at the opposite edge ij . The following formula is valid for all non-degenerate tetrahedra*

$$\exp(\theta_{kl}i) = \frac{\text{ad}(C)_{kl} + \sqrt{-\det(C) \det(C_{kkll})}}{\sqrt{\text{ad}(C)_{kk} \text{ad}(C)_{ll}}}$$

Proof. See [K01] for a proof in the Euclidean and Plane case. The Minkowskian case is entirely analogous once one uses the right conventions on angles [SP]. Given a Minkowskian tetrahedron the angle between two outward pointing normal vectors has the form $n\pi + i\omega$, where $n \in \mathbb{N}$ and $\omega \in \mathbb{R}$. Since the normal vectors are time-like they can either be in the same sheet or in different sheets of the unit hyperboloid. If they are in the same sheet then ω is defined to be the length the hyperbolic line between them and $n = 0$. If they are in opposite sheets then $-\omega$ is the length of the line between one and the reflection of the other in the horizontal plane and $n = 1$. △

4.9.2 Asymptotics of the $6j$ -symbol

We now start to apply Theorem 4.8 to determine the asymptotics of the non-degenerate $6j$ -symbol. In this section it is convenient to use the following normalization $\langle \Gamma, \gamma \rangle^U$ for spin networks.

Definition 4.15. *We define the unitary normalization $\langle \Gamma, \gamma \rangle^U$ of a spin network evaluation $\langle \Gamma, \gamma \rangle$ to be*

$$\langle \Gamma, \gamma \rangle^U = \frac{1}{\Theta(\gamma)} \langle \Gamma, \gamma \rangle$$

where

$$\Theta(\gamma) = \prod_{v \in V(\Gamma)} \sqrt{|\langle \Theta, a_v, b_v, c_v \rangle|}$$

and a_v, b_v, c_v are the colors of the edges at vertex v .

As it turns out, with this normalization the asymptotics of the $6j$ -symbols matches the corresponding geometry well. Since the theta is a quotient of factorials one can use Stirling's formula [O] to find its asymptotics and hence one can see how the new choice in normalization effects the asymptotic expansion. For later use we record the asymptotic expansion of the normalization factor in the case of a $6j$ -symbol.

Let us define

$$\lambda_{abc} = \frac{(-a+b+c)^{(-a+b+c)/4} (a-b+c)^{(a-b+c)/4} (a+b-c)^{(a+b-c)/4}}{(a+b+c)^{(a+b+c)/4}}$$

$$s_{abc} = \frac{((-a+b+c)(a-b+c)(a+b-c)(a+b+c))^{1/4}}{a+b+c}$$

Lemma 4.7. *Let γ be an admissible coloring of a tetrahedron. Then we have*

$$\Theta(n\gamma)^{-1} \sim (2\pi)^2 s_{abe} s_{acf} s_{ced} s_{bdf} (\lambda_{abe} \lambda_{acf} \lambda_{ced} \lambda_{bdf})^n \left(\sum_{l=0}^{\infty} \frac{\mu_l}{n^l} \right)$$

where $\mu_0 = 1$ and $\mu_l \in \mathbb{Q}(\gamma)$ for all l .

Thus, the asymptotics of $\langle \underline{\Delta}, \gamma \rangle^U$, is reduced to the study of the asymptotics of $\langle \underline{\Delta}, \gamma \rangle$. Since this is a 1-dimensional sum of a balanced term given by Equation (4.20), we can apply Theorem 4.8 to find its asymptotic expansion. Equation (4.20) implies that the balanced term is given by

$$t_{n,k} = \frac{(-1)^k (k+1)!}{\prod_i (nS_i - k)! \prod_j (k - nT_j)!} \quad (4.42)$$

With the notation of Theorem 4.8 we have $J = 8$, and the linear forms $A_j(n, k)$ are given by

$$\begin{aligned} A_1(n, k) &= k+1, & A_2(n, k) &= nS_1 - k, & A_3(n, k) &= nS_2 - k, & A_4(n, k) &= nS_3 - k, \\ A_5(n, k) &= k - nT_1, & A_6(n, k) &= k - nT_2, & A_7(n, k) &= k - nT_3, & A_8(n, k) &= k - nT_4 \end{aligned}$$

and $\epsilon_1 = 1, \epsilon_2 = \dots \epsilon_8 = -1$. It follows that

$$\nu = 1, \quad \mu = -3. \quad (4.43)$$

The functions V and W from Theorem 4.8 in this case are

$$V(u) = u \log(-1) + u \log u - \sum (S_i - u) \log(S_i - u) - \sum (u - T_j) \log(u - T_j) \quad (4.44)$$

$$W(u) = u^{3/2} (\prod (S_i - u) \prod (u - T_j))^{-1/2}. \quad (4.45)$$

V and W are analytic functions on the open interval

$$(m, M) = (\max\{0, T_j\}, \min\{S_i\})$$

and they have single-valued analytic continuation in the doubly cut complex plane $\mathbb{C} \setminus ((-\infty, \max\{0, T_j\}] \cup [\min\{S_i\}, \infty))$. V and W can be further analytically continued as multivalued functions in $\mathbb{C} \setminus \{0, S_i, T_j\}$.

The possible critical values of $V(u)$ that determine the growth rate are given by

$$\lambda_v = \frac{\prod_{j=1}^4 (v - T_j)^{T_j}}{\prod_{i=1}^3 (S_i - v)^{S_i}} \quad (4.46)$$

here v is a solution of the variational equation which is the equation

$$-u \prod (S_i - u) \prod (u - T_j)^{-1} = 1 \quad (4.47)$$

At first sight, the above equation appears to be a quartic equation for u . However, the coefficients of u^4 and u^3 is zero because $\sum S_j = \sum T_i$. Thus, Equation (4.47) is quadratic in u , with coefficients which are polynomial in a, \dots, f . It

is convenient to introduce a fourth number $S_4 = 0$. We can then write the Variational Equation (4.47) in the form

$$E(u) = -\prod(S_i - u) + \prod(u - T_j) = Au^2 + Bu + C' = 0 \quad (4.48)$$

where A , B and C' are homogeneous polynomials in γ of degrees 2, 3 and 4 respectively. A calculation gives that

$$\begin{aligned} A &= \frac{1}{2}(ad + bc + ef) & (4.49) \\ B &= -\frac{1}{4}(bc(b+c) + ad(a+d) + ef(e+f) + abc + abd + acd + bcd \\ &\quad + bce + ade + cde + acf + bcf + adf + bdf + aef + bef + cef + def) \end{aligned}$$

The next Lemma identifies the number field generated by the Variational Equation (4.48) in terms of the Cayley-Menger determinant.

Lemma 4.8. *Let D be the discriminant of the Variational Equation (4.47). Then we have*

$$D = -\det(C)/4 \quad (4.51)$$

where C is the Cayley-Menger matrix. The number field K generated by the solutions to the Variational Equation (4.48) is given by

$$K = Q(\sqrt{-\det(C)}). \quad (4.52)$$

Proof. The proof follows from an explicit calculation, keeping in mind that D and $\det(C)$ are homogeneous polynomials in γ of degree 6. \triangle

The next Lemma determines the order of vanishing of V at the solutions of Equation (4.47).

Lemma 4.9. *Let D be the discriminant of the Variational Equation (4.47).*

- (a) *The tetrahedron is degenerate iff there is a solution to the variational equation that equals S_i , or T_j for some i, j .*
- (b) *Assume the tetrahedron is non-degenerate. The two solutions v_+, v_- to the variational equation satisfy*

$$-\prod(v_{\pm} - T_j)V''(v_{\pm}) = \pm\sqrt{D}$$

- (c) *If in addition $D = 0$ then the two solutions coincide, $V''(v_{\pm}) = 0$ and we have*

$$\prod(v - T_j)V'''(v) = -2A$$

where A is given in (4.49).

- (d) *In the Euclidean or Plane case, v_{\pm} does not lie in the double cut $(-\infty, m] \cup [M, \infty)$. In the Minkowskian case, v_{\pm} are real and exactly one of them (call it v) lies in the double cut $(-\infty, m] \cup [M, \infty)$.*

Proof. In the proof it is convenient to define $S_4 = 0$ so that all indices run from 1 to 4. This convention will only be used in this proof. (a) If the tetrahedron is degenerate then there are i, j such that $S_i = T_j$. Plugging in this value for u will set both terms in the equation to zero as required. On the other hand if $v = T_j$ is a solution to the variational equation then $\prod_i (S_i - T_j) = 0$, so that $T_j = S_i$ for some i and likewise when $v = S_i$.

(b) Note that $A = (ad + bc + ef)/2 > 0$ since all edge labels are positive so that a solution always exists. By (a) we know that the solutions to the variational equation are not equal to S_i or T_j .

By differentiating V we find that $-V''(v_\pm) = \sum \frac{1}{S_i - v_\pm} + \sum \frac{1}{v_\pm - T_j}$. Using the variational equation $\prod(S_i - u) = \prod(u - T_j)$ we can write

$$-\prod(v_\pm - T_j)V''(v_\pm) = \prod(S_i - v_\pm) \sum \frac{1}{S_j - v_\pm} + \prod(v_\pm - T_i) \sum \frac{1}{v_\pm - T_j} \quad (4.53)$$

We see that $-\prod(v_\pm - T_j)V''(v_\pm) = E'(v_\pm)$. Now choose the solutions such that $v_\pm = (-B \pm \sqrt{D})/2A$ so that $E'(v_\pm) = 2Av_\pm + B = \pm\sqrt{D}$.

(c) Since $D = 0$ the solutions v_\pm coincide and will be written as v . Differentiating we find $V'''(v) = -\prod(S_i - v)^{-2} + \prod(v - T_j)^{-2}$. On the other hand $D = 0$ and we assumed that our tetrahedron is non-degenerate, so by part (a) $V''(v) = 0$. Therefore

$$\frac{1}{(S_i - v)^2} + \sum_{j \neq i} \frac{1}{(S_i - v)(S_j - v)} + \sum_k \frac{1}{(S_i - v)(v - T_k)} = \frac{V''(v)}{S_i - v} = 0$$

Adding these to similar equations for $\frac{V''(v)}{v - T_j}$ implies

$$V'''(v) = 2 \sum_{i \neq j} \frac{1}{(S_i - v)(S_j - v)} - \frac{1}{(v - T_i)(v - T_j)}$$

Multiplying through by the variational equation $\prod(v - T_j) = \prod(S_i - v)$ we get

$$\prod(v - T_j)V'''(v) = 2 \sum_{i \neq j} (S_i - v)(S_j - v) - (v - T_i)(v - T_j) = -2A,$$

where A is given in Equation (4.49).

(d) The Euclidean or Plane case follows from (b). For the Minkowskian case, there are connected components (types) of Minkowskian tetrahedra: the rectangular type where $T_j < v_\pm$ and the *triangular type* where we have $T_1, T_2, T_3 < v_\pm < T_4$ where T_4 is the distinguished triangle of the triangular tetrahedron. This fact is in turn proven by continuity. It is true by explicit computation (using the WZ method of Section 4.10) for the two examples

$$(3, 4, 4, 3, 5, 5), \quad (37, 37, 13, 13, 24, 30)$$

of rectangular type and triangular type respectively. The result follows by continuity for all Minkowskian nondegenerate tetrahedra, since $v_\pm = T_j$ only for degenerate tetrahedra. \triangle

From now on we will always assume that our $6j$ -symbols are non-degenerate. Using Lemma 4.7 and Theorem 4.8, it follows that the possible growth rates in

the asymptotic expansion of $\langle \triangle, \gamma \rangle^U$ are given by

$$\Lambda_{\pm} = \lambda_{abe} \lambda_{acf} \lambda_{ced} \lambda_{bdf} \lambda_{v_{\pm}}$$

We close this subsection with a lemma connecting these growth rates to the dihedral angles in the tetrahedron.

Lemma 4.10. *Let θ_a be the dihedral angle corresponding to the edge labeled a as introduced in Section 4.9.1.*

(a) *The growth rate Λ_{\pm} satisfies*

$$\Lambda_{\pm} = e^{\pm i \sum_a \theta_a \frac{\alpha}{2}} \quad (4.54)$$

(b) *Moreover,*

$$(s_{abe} s_{acf} s_{cde} s_{bdf} W_t(v_{\pm}))^2 = \frac{-e^{\pm i \sum_a \theta_a i}}{\prod_j (v_{\pm} - T_j)} \quad (4.55)$$

Proof. (a) The strategy is to collect equal powers in Λ_{\pm} . It follows that we can write Λ_{\pm} as a product

$$\Lambda_{\pm} = \prod_{i < j} (h_{ij\pm})^{d_{ij}/2}$$

where we define

$$h_{ij\pm} = \frac{(v_{\pm} - (ij + ik + jk)/2)(v_{\pm} - (ij + il + jl)/2)(ij - ik + jk)}{((ij + kl + ik + jl)/2 - v_{\pm})((ij + kl + jk + il)/2 - v_{\pm})} \times \quad (4.56)$$

$$\frac{(ij + ik - jk)(ij - il + jl)(ij + il - jl)}{\sqrt{K_l K_k}}$$

and

$$K_l = (-ij + ik + jk)(ij - ik + jk)(ij + ik - jk)(ij + ik + jk)$$

Now we will show that $h_{ij\pm} = e^{\pm \theta_{kl} i}$. Since $\det(C_{kkl}) = d_{ij}^2$ and $4\text{ad}_l(C) = K_l$ we can clear denominators in the expression for $e^{\pm \theta_{kl} i}$ from Lemma 4.6 and the expression for $h_{ij\pm}$. Equality of the numerators is then shown by direct calculation using Equation (4.51). Equation (4.54) follows.

(b) To show Equation (4.55), first note that $s_{ij} s_{ik} s_{jk} = \frac{(K_l)^{1/4}}{ij + ik + jk}$ and hence

$$(s_{abe} s_{acf} s_{cde} s_{bdf} W_t(v_{\pm}))^2 = \frac{v_{\pm}^3 \sqrt{K_1 K_2 K_3 K_4}}{\prod (S_i - v_{\pm}) \prod (v_{\pm} - T_j) (T_1 T_2 T_3 T_4)^2}$$

In the product of the h_{ij} we can also collect like terms together in the form K_j in the denominator. We get

$$\prod_{i < j} h_{ij} = \frac{(K_1 K_2 K_3 K_4)^{3/2}}{(T_1 T_2 T_3 T_4)^2 K_1 K_2 K_3 K_4} \frac{\prod (v_{\pm} - T_j)^3}{\prod (S_i - v_{\pm})^4}$$

Using the variational equation and $h_{ij\pm} = e^{\pm \theta_{kl} i}$ proves part (b). \triangle

Lemmas 4.10 and 4.9 prove Lemma 4.1 regarding the properties of the growth rates.

Combining our results, we can finally prove Theorem 4.4 by reading off the numerical invariants from Theorem 4.8. First of all the growth rates Λ_{\pm} are identified with the dihedral angles by Lemma 4.10. In the Euclidean and the Plane case both rates contribute, whereas in the Minkowskian case we include only the contribution of Λ , corresponding to the distinguished solution v of the Variational Equation that lies in the cut; see part (d) of Lemma 4.9. In the terminology of Section 4.9.1 and Lemma 4.9 we have $\Lambda = \Lambda_+$ in the triangular component and $\Lambda = \Lambda_-$ in the quadrangular component, and always $|\Lambda| < 1$.

Next the exponent in the leading power of n is given by Equation (4.37) and the order of vanishing is determined by Lemma 4.9. We have $m = 1$ in the Euclidean and Minkowskian cases and $m = 2$ in the Plane cases.

Lemma 4.8 identifies the number field generated by the solutions to the Variational Equation with K from Definition 4.6.

Finally we consider the Stokes constants in all three cases. The Stokes constant is computed from Theorem 4.8 using Lemmas 4.10 and 4.9. In the Euclidean case we have to refine Lemma 4.10 (b) to choose the right square root of the left hand side. This is done by considering the simple example of the regular tetrahedron and extending by continuity. We thus find

$$S_{\pm} = (2\pi)^{-1/2} s_{abe} s_{acf} s_{cde} s_{bdf} \frac{W_t(v_{\pm})}{\sqrt{V_t''(v_{\pm})}} = (2\pi)^{-1/2} \frac{\pm i \prod_a e^{\pm \theta_a i/2}}{\sqrt{-\prod(v_{\pm} - T_j) V''(v_{\pm})}}$$

Now applying part (b) of Lemma 4.9 and Lemma 4.8, we can rewrite the above as

$$S_{\pm} = (2\pi)^{-1/2} \frac{\pm i e^{\pm i \sum_a \theta_a/2}}{\sqrt{\pm i \sqrt{|\det(C)|}/2}} = \frac{e^{\pm i(\sum_a \theta_a/2 + \pi/4)}}{\sqrt{6\pi \text{Vol}}}$$

In the Minkowskian case we have to choose the Stokes constant corresponding to Λ . This is computed as in the Euclidean case except that the solutions to the variational equation lie in the cut. We therefore use Equation (4.39) so that we take absolute values everywhere. This explains the sign in (4.9). It makes the Stokes constant positive by canceling the real part of the Minkowskian angle sum, which is 3π in the triangular case and 4π in the quadrangular case.

Finally in the Plane case we have by Lemma 4.9 that $v \neq T_j$ and we know that $V''(v) = 0$. Furthermore $c_2 = \Gamma(4/3)6^{1/3}$, so

$$S = \frac{\Gamma(4/3)6^{1/3}}{\pi} s_{abe} s_{acf} s_{ced} s_{bdf} \frac{|W(v)|}{|V'''(v)|^{1/3}} = \frac{\Gamma(4/3)6^{1/3} |e^{i \sum_a \theta_a/2}|}{\pi |\prod_j (v - T_j)|^{1/2} |V'''(v)|^{1/3}} = \frac{\Gamma(4/3)6^{1/3}}{\pi |\prod_j (v - T_j)|^{1/6} (2A)^{1/3}}$$

where we used part (c) of Lemma 4.9 and the fact that the dihedral angles are real. Since the tetrahedron is Plane, we have $\sqrt{D} = 0$, so $v = -B/2A$ with the notation of (4.48). Therefore we can take out the $2A$ terms to get

$$S = \frac{\Gamma(4/3)(12A)^{1/3}}{\pi \prod |B + 2AT_j|^{1/6}}$$

Recall from Equations (4.22), (4.49) and (4.50) that T_j , A and B are homogeneous polynomials of γ . A calculation shows that $B_j := B + 2AT_j$ is a homogeneous polynomial of degree 3. It is unclear to us what is the geometric interpretation of the rational function $A^2 / \prod_{j=1}^4 B_j \in \mathbb{Q}(\gamma)$.

4.10 Computation of asymptotic expansions using the WZ method

In this section we will compute the asymptotic expansion of three representative $6j$ -symbols using the WZ method. The main observation is that a $6j$ -symbol is given by one-dimensional sum of a balanced hypergeometric term; see Equation (4.20) and Definition 4.13. The fundamental theorem of Wilf-Zeilberger implies that such sums are holonomic, i.e., they satisfy linear recursion relations with coefficients polynomials in n . The WZ method is constructive and works well for one-dimensional sums, implemented in several platforms, see [PaRi, PWZ, WZ1]. Given a recursion relation for the evaluation of the $6j$ -symbols, together with the fact that it is a sequence of Nilsson type, allows us to compute explicitly its asymptotic expansion.

The three examples we consider are the simplest representatives of the three geometric types of $6j$ -symbols. Consider the sequences

$$\begin{aligned} (a_n) &= \langle \triangle, n \gamma_{\text{Euclidean}} \rangle^U & \gamma_{\text{Euclidean}} &= (2, 2, 2, 2, 2, 2) \\ (b_n) &= \langle \triangle, n \gamma_{\text{Minkowskian}} \rangle^U & \gamma_{\text{Minkowskian}} &= (4, 4, 4, 4, 6, 6) \\ (c_n) &= \langle \triangle, n \gamma_{\text{Plane}} \rangle^U & \gamma_{\text{Plane}} &= (3, 4, 4, 3, 5, 5) \end{aligned}$$

The explicit formulas for these sequences are as follows:

$$\begin{aligned} a_n &= \frac{n!^6}{(3n+1)!^2} \sum_{k=3n}^{4n} \frac{(-1)^k (k+1)!}{(k-3n)!^4 (4n-k)!^3} \\ b_n &= \frac{n!^2 (2n)!^2 (3n)!^2}{(6n+1)!^2} \sum_{k=6n}^{7n} \frac{(-1)^k (k+1)!}{(k-6n)!^4 (7n-k)! (8n-k)! (9n-k)!} \\ c_n &= \frac{n!^2 (3n)!^4}{(7n+1)!^2} \sum_{k=7n}^{8n} \frac{(-1)^k (k+1)!}{(k-7n)!^4 (8n-k)! (10n-k)!^2} \end{aligned}$$

The command

```
<< zb.m
```

loads the package of [PaRi] into *Mathematica*. The command

```
teucl[n_, k_] := n!^6 / (3n+1)!^2 (-1)^k (k+1)! / ((4n-k)!^3 (k-3n)!^4)
```

defines the summand of the sequence (a_n) , and the command

```
Zb[teucl[n, k], {k, 3n, 4n}, n, 2]
```

computes the following second order linear recursion relation for the sequence (a_n)

$$\begin{aligned} & -9(1+n)(2+3n)^2(4+3n)^2(451+460n+115n^2)a[n] + \\ & (3+2n)(319212+1427658n+2578232n^2+2423109n^3+1255139n^4+340515n^5+37835n^6)a[1+n] - \\ & 9(2+n)(5+3n)^2(7+3n)^2(106+230n+115n^2)a[2+n] = 0 \end{aligned}$$

This linear recursion has two formal power series solutions of the form

$$\begin{aligned} a_{\pm,n} &= \frac{1}{n^{3/2}} \Lambda_{\pm}^n \left(1 + \frac{-432 \pm 31i\sqrt{2}}{576n} + \frac{109847 \mp 22320i\sqrt{2}}{331776n^2} + \right. \\ &+ \frac{-18649008 \pm 4914305i\sqrt{2}}{573308928n^3} + \frac{14721750481 \pm 45578388960i\sqrt{2}}{660451885056n^4} + \\ &+ \frac{-83614134803760 \pm 7532932167923i\sqrt{2}}{380420285792256n^5} \\ &\left. + \frac{-31784729861796581 \mp 212040612888146640i\sqrt{2}}{657366253849018368n^6} + O\left(\frac{1}{n^7}\right) \right) \end{aligned}$$

where

$$\Lambda_{\pm} = \frac{329 \mp 460i\sqrt{2}}{729}$$

are two complex numbers of absolute value 1. These growth rates Λ_{\pm} computed with the WZ method match those of Theorem 4.4. Indeed, the Theorem states that

$$\Lambda_{\pm} = e^{\mp i6 \arccos(1/3)}$$

An algebraic calculation confirms that

$$e^{\pm i6 \arccos(1/3)} = \frac{329 \pm 460i\sqrt{2}}{729}.$$

The coefficients of the formal power series $a_{\pm,n}$ are in the number field $K = \mathbb{Q}(\sqrt{-2})$ and the Cayley-Menger determinant is $\det(C) = 2^5$ confirming Lemma 4.8 and Theorem 4.4.

More is actually true. Namely, the sequence (a_n) generates two new sequences $(\mu_{+,n})$ and $(\mu_{-,n})$ defined by

$$a_{\pm,n} = \frac{1}{n^{3/2}} \Lambda_{\pm}^n \sum_{l=0}^{\infty} \frac{\mu_{\pm,l}}{n^l}$$

where $\mu_{\pm,0} = 1$. Each of the sequences $(\mu_{\pm,n})$ are factorially divergent. However, the generating series $\sum_{n=0}^{\infty} z^n \mu_{\pm,n+1}/n!$ are G -functions (as follows from [An]), and the sequences $(\mu_{\pm,n+1}/n!)$ are of Nilsson type, with exponential growth rates $\Lambda_{\pm} - \Lambda_{\mp}$. The asymptotics of each sequence $(\mu_{\pm,n+1}/n!)$ gives rise to finitely many new sequences, and so on. All those sequences span a finite dimensional vector space, canonically attached to the sequence (a_n) . This is an instance of resurgence, and is explained in detail in [GM, Sec.4].

The second order recursion relation for the Plane and the Minkowskian examples has lengthy coefficients, and leads to the following sequences $(b_{\pm,n})$ and $(c_{\pm,n})$

$$\begin{aligned}
b_{+,n} &= \frac{1}{n^{4/3}} \Lambda_+^n \left(1 - \frac{1}{3n} + \frac{3713}{46656n^2} - \frac{25427}{2239488n^3} + \frac{9063361}{17414258688n^4} \right. \\
&\quad \left. - \frac{109895165}{104485552128n^5} + \frac{1927530983327}{2437438960041984n^6} + \dots \right) \\
b_{-,n} &= \frac{1}{n^{5/3}} \Lambda_-^n \left(1 - \frac{37}{96n} + \frac{3883}{46656n^2} - \frac{13129}{4478976n^3} - \frac{5700973}{8707129344n^4} \right. \\
&\quad \left. - \frac{14855978561}{3343537668096n^5} + \frac{2862335448661}{2437438960041984n^6} + \dots \right) \\
c_{\pm,n} &= \frac{1}{n^{3/2}} \Lambda_{\pm}^n \left(1 + \frac{336 \mp 1369\sqrt{2}}{4032n} + \frac{1769489 \mp 831792\sqrt{2}}{1806336n^2} + \right. \\
&\quad \frac{67925105712 \mp 66827896993\sqrt{2}}{21849440256n^3} + \frac{5075437500833257 \mp 2589265090380768\sqrt{2}}{176193886224384n^4} \\
&\quad + \frac{100978405759997442992 \mp 98904713360431641651\sqrt{2}}{552544027199668224n^5} \\
&\quad \left. + \frac{685103512739058526758457 \mp 349782631602887151717776\sqrt{2}}{247539724185451364352n^6} + \dots \right)
\end{aligned}$$

where in the Plane case we have

$$\Lambda_- = \Lambda_+ = -1, \quad K = \mathbb{Q}, \quad \det(C) = 0$$

and in the Minkowskian case we have

$$\begin{aligned}
\Lambda_+ &= \frac{696321931873 - 111529584108\sqrt{2}}{678223072849} = 0.794127\dots \\
\Lambda_- &= \frac{696321931873 + 111529584108\sqrt{2}}{678223072849} = 1.25924\dots \\
K &= \mathbb{Q}(\sqrt{2}), \quad \det(C) = -2^5 3^4.
\end{aligned}$$

again in agreement with Theorem 4.4.

4.11 Chromatic evaluation of spin networks

The purpose of this section is to prove the rationality statement of the spin generating function stated in Theorem 4.5 of Section 4.4. We will use the *chromatic evaluation method* which goes back to [Pe2]. Our proof builds on earlier work by [We] and [KL] on planar spin networks.

The chromatic method for the evaluation of a spin network is based on introducing a generalized evaluation $\langle \Gamma, \gamma \rangle_N^P$ following the algorithm of Definition 4.1, with the exception that a collection of n loops is assigned the value N^n instead of $(-2)^n$. Therefore,

$$\langle \Gamma, \gamma \rangle_{-2}^P = \langle \Gamma, \gamma \rangle^P.$$

Now the crucial observation is that $\langle \Gamma, \gamma \rangle_N^P$ is a polynomial in N with integer coefficients, so that $\langle \Gamma, \gamma \rangle^P$ is determined once we know the values of $\langle \Gamma, \gamma \rangle_N^P$ for all positive N .

For positive N there exists an alternative interpretation of $\langle \Gamma, \gamma \rangle_N^P$ as a contraction of tensors. For convenience we will orient the edges of Γ . Let V be an N dimensional vector space and for $\sigma \in S_n$ define the following permutation operators $\sigma : V^{\otimes n} \rightarrow V^{\otimes n}$, $\sigma(e_{i_1} \otimes \cdots \otimes e_{i_n}) = e_{\sigma(i_1)} \otimes \cdots \otimes e_{\sigma(i_n)}$. At every edge colored n we can now speak of the map $\sum_{\sigma \in S_n} \text{sgn}(\sigma) \sigma$. Note that the single arcs in the expanded diagram for (Γ, γ) now correspond to copies of V . The systems of arcs at the vertices indicate how to contract (compose) the tensors on the edges. Since all the tensors involved are linear combinations of Kronecker deltas we can for each choice of permutations count the number of contracted deltas and this will exactly contribute a term $\pm N^k$ for some k since the trace of a delta is simply N . This coincides with the counting and evaluation of loops in every state, since a contracted delta represents a loop. However there is also another way to carry out this tensor calculation.

We can also calculate $\langle \Gamma, \gamma \rangle_N^P$ by writing out the contraction of tensors into the single contributions of basis elements in the various tensor products. This will yield an explicit formula for the evaluation of a general spin network in terms of so called curve configurations on Γ . Recall that a curve is a 2-regular subgraph of Γ and a curve configuration is a function from the set C of all curves to the natural numbers, $\mathcal{L} : C \rightarrow \mathbb{N}$. For such functions we define $|\mathcal{L}|$ to be the sum of the function values. Define sign $(-1)^{\iota(\mathcal{L})}$, where for any subset $\iota(\mathcal{L})$ is the minimal number of intersections one can have when drawing $\mathcal{L}(c)$ copies of c for every curve on the thickened ribbon graph Γ .

Lemma 4.11. *For every spin network (Γ, γ) we have*

$$\langle \Gamma, \gamma \rangle = \sum_{\gamma_{\mathcal{L}} = \gamma} (-1)^{\iota(\mathcal{L}) + |\mathcal{L}|} (|\mathcal{L}| + 1) \binom{|\mathcal{L}|}{\mathcal{L}} \in \mathbb{Z}.$$

This implies in particular that the generating series S_{Γ} of Definition 4.9 satisfies $S_{\Gamma} \in \mathbb{Z}[[z_e, e \in E(\Gamma)]]$ proving one part of Theorem 4.5.

Proof. (of Lemma 4.11) We will calculate $\langle \Gamma, \gamma \rangle_N^P$ by writing out the contraction of tensors into the single contributions of basis elements in the various tensor products. Given a choice of permutations we place tensor products of basis elements $e_{i_1} \otimes \cdots \otimes e_{i_n}$ on every edge. Such a term contributes 0 if some basis vectors on the same strand are unequal or the same basis element occurs twice in a tensor product corresponding to an edge. Otherwise the contribution is always $(-1)^{\#\text{crossings}}$.

To enumerate the non-zero states in an orderly fashion including the signs of their contributions we proceed in three stages. First we choose which sets of arcs get labeled by the same base vector. Then we assign base vectors to the loops in the curves. Finally we count the number of such labeled states.

In the first stage we choose the collections of all loops that are labeled by the same base vector. For non-zero states these collections are necessarily 2-regular subgraphs of Γ , also known as curves. We will view curves both as sets of the loops they contain and as subgraphs of Γ . This first stage of the calculation is summarized in the concept of a curve configuration. To every curve $c \in C_{\Gamma}$ we assign the number of distinct base vectors it occurs with. The curve configuration \mathcal{L} determines the total coloring of the spin network γ . However there may be many curve configurations yielding the same coloring γ .

Note that all states with the same curve configuration contribute the same sign. This is because of planarity of the (multiple) annulus neighborhood of the curve: two loops in the same curve can only cross an even number of times. The common sign is determined by the cyclic ordering of the graph and equals $(-1)^{\iota(\mathcal{L})}$. This follows directly from a count of the number of intersections of such states.

In the second stage we choose base vectors and we assign them to the loops such that all the loops with the same base vector constitute exactly one copy of a curve. First we need to choose which base vectors to use. There are $\binom{N}{|\mathcal{L}|}$ ways to do this. Then we need distribute these over the various curves, assigning $\mathcal{L}(c)$ base vectors to the curve c in no particular order. There are $\binom{|\mathcal{L}|}{\mathcal{L}}$ ways to do this.

In the last stage we need to count how many arrangements of loops are possible given a curve configuration with base vectors at every loop. As was shown in [KL] there are $\mathcal{I}!$ ways to do this. Their argument does not make use of planarity but for completeness sake we still reproduce the argument here. If we ignore the labelling by base vectors we will count exactly $\frac{1}{\mathcal{I}!}$ of the possible states. However if we also choose to ignore the fact that in contributing states the loops cannot self intersect, then counting possibly zero states will multiply our count by the same factor $\mathcal{L}!$. To see why, note that to modify a zero state takes one permutation per curve.

Recall that $\mathcal{I}!$ corresponds to a choice of a permutation on the arcs on each side of every vertex in the ribbon graph. We will show that there are exactly $\mathcal{I}!$ (possibly zero) states corresponding to a given curve configuration. First choose one such a state S . We will show that all others can be reached by inserting a unique permutation at every side of every vertex, with the appropriate modification. At any rate there cannot be more than $\mathcal{I}!$ such states, because arcs belonging to one side of a vertex can never be permuted to become part of another side, because that would destroy the curve configuration. Even inserting a permutation at the side of a vertex may destroy the curve configuration, but in this case this can be compensated as follows. Choose an edge adjacent to the chosen side of the vertex and insert the inverse of the part of the permutation swapping arcs belonging to different curves. Exactly because of the fact that this compensating permutation involves only arcs corresponding to unequal curves this does not interfere with any other inserted permutations at the sides of vertices or their compensations.

Summarizing, we get

$$\langle \Gamma, \gamma \rangle_N^P = \sum_{\gamma_{\mathcal{L}} = \gamma} (-1)^{\iota(\mathcal{L})} \binom{N}{|\mathcal{L}|} \binom{|\mathcal{L}|}{\mathcal{L}} \mathcal{I}!$$

and rescaling we get

$$\langle \Gamma, \gamma \rangle_N = \sum_{\gamma_{\mathcal{L}} = \gamma} (-1)^{\iota(\mathcal{L})} \binom{N}{|\mathcal{L}|} \binom{|\mathcal{L}|}{\mathcal{L}}$$

Finally setting $N = -2$ provides a general formula for spin network evaluation as given in the lemma. \triangle

To find a generating function for these evaluations, we first introduce a more general generating function.

Definition 4.16. Define the curve generating function CG_Γ of a graph Γ by

$$CG_\Gamma = \sum_{\mathcal{L}} \langle \mathcal{L} \rangle \prod_{c \in C} w_c^{\mathcal{L}(c)}$$

where CG_Γ is a function of $|C_\Gamma|$ variables, one for each curve in Γ . The exponents of these variables encode a curve configuration, and the evaluation $\langle \mathcal{L} \rangle$ of a curve configuration \mathcal{L} is given by

$$\langle \mathcal{L} \rangle = (-1)^{\iota(\mathcal{L}) + |\mathcal{L}|} (|\mathcal{L}| + 1) \binom{|\mathcal{L}|}{\mathcal{L}}$$

The spin generating function S_Γ can be recovered from the curve generating function CG_Γ by substituting $w_c = \prod_{e \in c} z_e$, because the color of an edge is the sum of the number of curves (with multiplicity) containing that edge.

Proof. (Of Theorem 4.5) Our goal now is to write CG_Γ and hence S_Γ as a rational function. As a first step we note that if we drop the term $(-1)^{\iota(\mathcal{L})}$ then we can sum the resulting series using the binomial series and the multinomial theorem to get

$$\begin{aligned} \sum_{\mathcal{L}} (-1)^{|\mathcal{L}|} (|\mathcal{L}| + 1) \binom{|\mathcal{L}|}{\mathcal{L}} w^{\mathcal{L}} &= \frac{1}{(1 + w_1 + \dots + w_{C_\Gamma})^2} \\ &= Q(w_1, \dots, w_{C_\Gamma}) = \sum_{\mathcal{L}} b_{\mathcal{L}} w^{\mathcal{L}} \end{aligned}$$

Using this together with the Fourier expansion of $(-1)^{\iota(\mathcal{L})}$ viewed as a function on the group $(C_2)^{C_\Gamma}$ as

$$(-1)^{\iota(\mathcal{L})} = \sum_{X \subset C_\Gamma} a_X (-1)^X$$

we find

$$CG_\Gamma = \sum_{\mathcal{L}} (-1)^{\iota(\mathcal{L})} b_{\mathcal{L}} w^{\mathcal{L}} = \sum_{X \subset C_\Gamma} a_X \sum_{\mathcal{L}} (-1)^{X \cap \mathcal{L}} b_{\mathcal{L}} w^{\mathcal{L}} = \sum_{X \subset C_\Gamma} a_X Q_X$$

where $Q_X(w_1, \dots, w_{C_\Gamma}) = Q(v_1, \dots, v_{C_\Gamma})$ and $v_i = \epsilon_X(c_i) w_i$. △

4.12 Challenges and future directions

In this section we list some challenges and future directions. Recall from Definition 4.5 that every spin network (Γ, γ) (and consequently every ribbon graph) has a spectral radius $\rho_{\Gamma, \gamma}$ and a number field $K_{\Gamma, \gamma}$. Our first problem implies the existence of an upper bound of the spectral radius in terms of Γ alone. This is phrased more conveniently in terms of the unitary evaluation of Definition 4.15.

Problem 4.2. Show that the unitary evaluation of a spin network (Γ, γ) satisfies

$$|\langle \Gamma, \gamma \rangle^U| \leq 1$$

This problem may be proven using unitarity and locality in a way similar to the proof that the Reshetikhin-Turaev invariants of a closed 3-manifold grow at most polynomially with respect to the level; see [Ga5, Thm.2.2].

Recall the spectral radius of a cubic ribbon graph from Definition 4.5; it is a nonnegative algebraic number. Our next problem is a version of the Volume Conjecture for classical spin networks with all edges colored by 2.

Problem 4.3. *Show that the spectral radius of a cubic ribbon graph with $2n$ vertices equals to 3^{3n} .*

Theorem 4.4 confirms this problem for the following ribbon graphs: the Θ , the tetrahedron, the 3-faced drum and more generally for the infinite family of ribbon graphs of Remark 4.2. There is convincing numerical evidence for the above problem in the case of the $K_{3,3}$ and the Cube.

Recall the generating series $F_{\Gamma,\gamma}(z)$ of Equation (4.4). Problem 4.3 motivates the next problem.

Problem 4.4. *Give a geometric meaning to the finitely many singularities of the generating series $F_{\Gamma,\gamma}(z)$ for a spin network (Γ, γ) .*

At the moment, we do not know the answer to Problem 4.4 for the Cube with all edges colored by 2. Numerical evidence suggests that there are 12 equally spaced singularities in the boundary of the disk of convergence of $F_{\text{Cube},2}(z)$.

The next problem is a computational challenge to all the known asymptotic methods, and shows their practical limitations.

Problem 4.5. *Compute the asymptotics of the evaluation $\langle K_{3,3}, 2n \rangle$ (given explicitly in Proposition 4.3) and $\langle \text{Cube}, 2n \rangle$.*

Problem 4.6. *Give a geometric interpretation of the number field $K_{\Gamma,\gamma}$ of a spin network (Γ, γ) .*

In Theorem 4.4 we identified the Stokes constants of the $6j$ -symbol with geometric quantities of the associated metric tetrahedron.

Problem 4.7. *Give a geometric meaning to the Stokes constants of the sequence $\langle \Gamma, n\gamma \rangle$.*

The next problem is motivated by the examples involving the WZ method, discussed in Section 4.10. A positive answer can give an independent proof of Theorem 4.4.

Problem 4.8. *Prove that for every coloring γ of the tetrahedron spin network (\triangle, γ) , the sequence $\langle \triangle, n\gamma \rangle$ satisfies a second order recursion relation with coefficients polynomials in n . Can you compute the coefficients of this recursion from γ alone?*

Our last problem concerns an integrality property of quantum spin networks. Our paper discusses four normalizations $\langle \Gamma, \gamma \rangle^P$, $\langle \Gamma, \gamma \rangle$, $\langle \Gamma, \gamma \rangle^B$ and $\langle \Gamma, \gamma \rangle^U$ for the evaluation of a classical spin network (Γ, γ) ; see Definitions 4.1, 4.2, 4.12 and 4.15. With the notation of these definitions, these normalizations are related by

$$\langle \Gamma, \gamma \rangle^P = \mathcal{I}! \langle \Gamma, \gamma \rangle, \quad \langle \Gamma, \gamma \rangle^B = \frac{\mathcal{I}!}{\mathcal{E}!} \langle \Gamma, \gamma \rangle, \quad \langle \Gamma, \gamma \rangle^U = \frac{1}{\Theta(\gamma)} \langle \Gamma, \gamma \rangle. \quad (4.57)$$

On the other hand, if (Γ, γ) is a quantum spin network, the Kauffman bracket evaluation $\langle \Gamma, \gamma \rangle^B$ makes sense, and in general it is a rational function of the bracket parameter A ; see Definition 4.12 and [KL]. The following problem is a first step towards the categorification of the evaluation of a quantum spin network.

Problem 4.9. *Show that for every quantum spin network (Γ, γ) , the evaluation $\langle \Gamma, \gamma \rangle^B \mathcal{E}!/\mathcal{I}!$ lies in $\mathbb{Z}[A^{\pm 1}]$.*

One can show that the above problem holds for the Θ and the tetrahedron spin networks, or more generally for the class of quantum spin networks of Remark 4.2.

Let us end this section with a remark. The main results of our paper can be extended to evaluations of spin networks corresponding to higher rank Lie groups. This will be discussed in a later publication.

Chapter 5

Asymptotics of quantum spin networks at a fixed root of unity

5.1 Introduction

5.1.1 History

Spin networks originally arose from calculations of angular momentum in quantum mechanics [VMK]. They were formalized in the sixties by Penrose [Pe1, Pe2] in attempt to quantize gravity combinatorially. Similar ideas were developed by Ponzano and Regge who related the semi-classical expansion of 3D gravity to the Regge action, [BL1, BL2, PR, Wi]. In recent years, spin networks have played an important role in the development of loop quantum gravity; see [BC, EPR, Pz, Ro] and references therein. In the eighties, quantum spin networks were used by Reshetikhin, Turaev and Viro as building blocks of combinatorially defined invariants of knotted 3-dimensional objects; see [Tu, TV]. Those topological invariants that are collectively called TQFT generalize the famous Jones polynomial of a knot [J].

A key problem in classical and quantum spin networks is their asymptotic behavior for large spins. In the case of the $6j$ -symbols Ponzano-Regge conjectured the leading term of an explicit asymptotic expansion and gave ample numerical evidence; see [PR]. The Ponzano-Regge conjecture was proven by Roberts [Rb1] using methods of geometric quantization. The existence of a general asymptotic expansion for all classical spin networks (to all orders in perturbation theory, in a constructive way) was recently obtained by the authors in [GV]. The method of [GV] was to convert the problem of asymptotic expansions to questions in Algebraic Geometry and Number Theory, and use the highly developed theory of G -functions. An important part in this conversion was the use of holonomic functions, developed by Zeilberger.

5.1.2 Classical spin networks

A *classical spin network* consists of a ribbon graph Γ (i.e., an abstract graph with a cyclic ordering of the vertices around each edge) and an admissible coloring γ of its edges by natural numbers. The standard evaluation $\langle \Gamma, \gamma \rangle$ of a spin network is an integer number. In a previous paper [GV], we proved an existence theorem for the asymptotics of the sequence $\langle \Gamma, n\gamma \rangle$ of an arbitrary trivalent classical spin network when the coloring of its edges is scaled by a large natural number n . In addition, we presented several ways (algebraic-geometric, combinatorial, and numerical) for computing the asymptotics of $\langle \Gamma, n\gamma \rangle$ for large n .

The goal of the present paper is to extend the results of [GV] to the case of quantum spin networks at a fixed root of unity. As in the case of classical spin networks, our proofs use the theory of G -functions of André. There are two new ingredients which allow us to use the theory of G -functions. They come from the theory of holonomic and q -holonomic functions of Wilf-Zeilberger:

- (a) Theorem 5.4 which states that the derivative of a q -holonomic sequence with respect to q is q -holonomic.
- (b) Theorem 5.5 which states that the evaluation of a q -holonomic sequence at a fixed root of unity is holonomic.

5.1.3 Quantum spin networks

Quantum spin networks differ from their classical versions in two ways:

- (a) the underlying graphs Γ are knotted (i.e., embedded in S^3) and not abstract,
- (b) their evaluations are polynomials of q , and not simply integer numbers.

Recall that a *knotted ribbon graph* is an embedded framed graph in S^3 , of arbitrary valency, together with a cyclic ordering of the edges around each vertex. We will restrict ourselves to integer framings so that thickening the graph gives rise to an orientable surface. A *quantum spin network* consists of a knotted ribbon graph Γ together with a pair of functions $\gamma = (\gamma_E, \gamma_V)$. Here $\gamma_E : \text{Edges}(\Gamma) \rightarrow \mathbb{N}$ is an admissible coloring γ of its edges, and $\gamma_V : \text{Vert}(\Gamma) \rightarrow \{\text{projectors}\}$ a choice of a local projector at each vertex of Γ . Local projectors are explained in detail in Section 5.2, and can be ignored in case Γ is a trivalent graph.

The *standard evaluation* $\langle \Gamma, \gamma \rangle(q)$ of a quantum spin network is a rational function of $q^{1/4}$; see [Tu]. Recently, Costantino [Co2] obtained an integrality result for the standard evaluation of a quantum spin network, namely:

$$\langle \Gamma, \gamma \rangle(q) \in q^{\frac{n}{4}} \mathbb{Z}[q^{\pm \frac{1}{2}}] \quad (5.1)$$

For some n depending on the network. Our first result deals with fixing the fractional power of q .

Proposition 5.1. *For every quantum spin network (Γ, γ) there exist a $\mathbb{Z}/4\mathbb{Z}$ -valued quadratic form $Q(\gamma)$ such that*

$$\langle \Gamma, \gamma \rangle(q) = q^{\frac{1}{4}Q(\gamma)} \langle\langle \Gamma, \gamma \rangle\rangle(q), \quad \langle\langle \Gamma, \gamma \rangle\rangle(q) \in \mathbb{Z}[q^{\pm 1}]. \quad (5.2)$$

The above proposition allows us to define a modified evaluation $\langle\langle \Gamma, \gamma \rangle\rangle(\zeta) \in \mathbb{C}$ that can be evaluated at a *fixed root of unity* ζ . To make $\langle\langle \Gamma, \gamma \rangle\rangle$ well defined we use the convention that $0 \leq Q(\gamma) \leq 3$. When $\zeta = 1$, it follows from the definitions that $\langle\langle \Gamma, \gamma \rangle\rangle(1)$ equals the classical evaluation and is hence independent of the embedding of Γ in 3-space. The goal of this paper is to extend the results of [GV] to the case of the standard evaluation of a quantum spin network at a *fixed* root of unity ζ .

5.1.4 Sequences of Nilsson type and G -functions

To state our results, we need to recall what is a G -function and what is a sequence of *Nilsson type*. These were discussed in detail in [GV], and reproduced here for the convenience of the reader.

Definition 5.1. *We say that a sequence (a_n) is of Nilsson type if it has an asymptotic expansion of the form*

$$a_n \sim \sum_{\lambda, \alpha, \beta} \lambda^n n^\alpha (\log n)^\beta S_{\lambda, \alpha, \beta} h_{\lambda, \alpha, \beta} \left(\frac{1}{n} \right) \quad (5.3)$$

where

- (a) the summation is over a finite set of triples (λ, α, β)
- (b) the growth rates λ are algebraic numbers of equal absolute value,
- (c) the exponents α are rational and the nilpotency exponents β are natural numbers,
- (d) the Stokes constants $S_{\lambda, \alpha, \beta}$ are complex numbers,
- (e) the formal power series $h_{\lambda, \alpha, \beta}(x) \in K[[x]]$ are Gevrey-1 (i.e., the coefficient of x^n is bounded by $C^n n!$ for some $C > 0$),
- (f) K is a number field generated by the coefficients of $h_{\lambda, \alpha, \beta}(x)$ for all λ, α, β .

Definition 5.2. *We say that series $G(z) = \sum_{n=0}^{\infty} a_n z^n$ is a G -function if*

- (a) the coefficients a_n are algebraic numbers,
- (b) there exists a constant $C > 0$ so that for every $n \in \mathbb{N}$ the absolute value of every conjugate of a_n is less than or equal to C^n ,
- (c) the common denominator of a_0, \dots, a_n is less than or equal to C^n (where the common denominator d of a_0, \dots, a_n is the least natural number such that da_i is an algebraic integer for $i = 1, \dots, n$),
- (d) $G(z)$ is holonomic, i.e., it satisfies a linear differential equation with coefficients polynomials in z .

The following connection between sequences of Nilsson type and G -functions was observed in [Ga3, Prop.2.5].

Theorem 5.1. [Ga3, Prop.2.5] *If $G(z) = \sum_{n=0}^{\infty} a_n z^n$ is a G -function, then (a_n) is a sequence of Nilsson type.*

The above existence theorem has a valuable, effective corollary.

Corollary 5.1. *If $G(z) = \sum_{n=0}^{\infty} a_n z^n$ is a G -function, and suppose that we are given either (a) a linear differential equation for $G(z)$ with coefficients in $L[x]$ for some number field L , or (b) a linear recursion for (a_n) with coefficients in $L[n]$, then one can effectively compute λ, α, β and $h_{\lambda, \alpha, \beta}(x) \in K[[x]]$ for a number field K such that the asymptotic expansion (4.3) holds, for some unknown Stokes constants $S_{\lambda, \alpha, \beta}$.*

In other words, a linear recursion for (a_n) or a linear differential equation for $G(z)$ allows us to compute the asymptotic expansion (4.3) to all orders in $1/n$, up to a finite set of unknown Stokes constants. For explicit illustrations of the above corollary, see [FS, WZ2] and also [GV, Sec.10] where the authors discuss in detail effective asymptotic expansions of evaluations of classical spin networks.

5.1.5 Statement of our results

Let $f^{(r)}(q) = d^r/dq^r f(q)$ denote the r -th derivative of a Laurent polynomial $f(q) \in \mathbb{Z}[q^{\pm 1}]$.

Theorem 5.2. *For every quantum spin network (Γ, γ) , every complex root of unity ζ and every natural number $r \geq 0$, the sequence $\langle\langle \Gamma, n\gamma \rangle\rangle^{(r)}(\zeta)$ is of Nilsson type.*

Theorem 5.2 follows from Theorem 5.1 and the following theorem.

Theorem 5.3. *For every quantum spin network (Γ, γ) , every complex root of unity ζ and every natural number r , the generating function*

$$F_{\Gamma, \gamma, \zeta, r}(z) = \sum_{n=0}^{\infty} \langle\langle \Gamma, n\gamma \rangle\rangle^{(r)}(\zeta) z^n \quad (5.4)$$

is a G -function.

Theorem 5.3 follows from Theorems 5.4, 5.5 and 5.6 below, which involve structural properties of the classes of holonomic and q -holonomic sequences and may be of independent interest. To state them, recall that a sequence (f_n) of complex numbers is *holonomic* if it satisfies a linear recursion of the form

$$c_d(n)f_{n+d} + \cdots + c_0(n)f_n = 0 \quad (5.5)$$

for all n where $c_j(n) \in K[n]$ are polynomials in n with coefficients in a number field K for $j = 0, \dots, d$ with $c_d \neq 0$. Likewise, a sequence $(f_n(q))$ of rational functions of q is *q -holonomic* if it satisfies a linear recursion of the form

$$c_d(q^n, q)f_{n+d}(q) + \cdots + c_0(q^n, q)f_n(q) = 0 \quad (5.6)$$

for all n where $c_j(u, v) \in K[u, v]$ are polynomials in two variables u and v for $j = 0, \dots, d$ with $c_d \neq 0$. Holonomic and q -holonomic sequences were studied in detail by Zeilberger; see [Z, WZ1].

Theorem 5.4. *The derivative with respect to q of a q -holonomic sequence is q -holonomic.*

Theorem 5.5. *For every q -holonomic sequence $f_n(q) \in \mathbb{Z}[q^{\pm 1}]$ and every complex root of unity ζ , the evaluation $f_n(\zeta)$ is a holonomic sequence which is exponentially bounded.*

Let us make some remarks.

Remark 5.1. *Theorem 5.5 fails when ζ is not a complex root of unity. For example, $f_n(q) = q^{n^2}$ is q -holonomic and satisfies the recursion $f_{n+1}(q) - q^{2n+1}f_n(q) = 0$. On the other hand, $f_n(\omega)$ is holonomic only when ω is a complex root of unity. Theorem 5.5 is another manifestation of the importance of roots of unity in Quantum Topology. See also Section 5.3.*

Remark 5.2. *Theorems 5.4 and 5.5 presumably hold for multi-variable q -holonomic sequences $f_{n_1, \dots, n_r}(q) \in \mathbb{Z}[q^{\pm 1}]$. Multi-variable holonomic and q -holonomic sequences were introduced and studied in [Z, WZ1]. In the present paper, we will not use them. However, the reader should keep in mind that for every quantum spin network (Γ, γ) the multi-variable sequence $\gamma \mapsto \langle \Gamma, \gamma \rangle(q)$ is q -holonomic. This follows from Section 5.2.3 where it is shown that $\langle \Gamma, \gamma \rangle(q)$ is a multi-sum of a q -proper hypergeometric term. By the fundamental theorem of WZ-theory (see [WZ1]), $\langle \Gamma, \gamma \rangle(q)$ is q -holonomic in all γ -variables.*

Remark 5.3. *The q -holonomic sequence $f_n(\zeta)$ in Theorem 5.5 need not be exponentially bounded. For example,*

$$f_n(q) = \prod_{k=1}^n \frac{1 - q^k}{1 - q} \in \mathbb{Z}[q]$$

satisfies the linear recursion

$$(q - 1)f_{n+1}(q) - (q^{n+1} - 1)f_n(q) = 0.$$

Thus, $f_n(q)$ is q -holonomic. Its evaluation at $\zeta = 1$ is given by $f_n(1) = n!$ which is holonomic, since it satisfies the linear recursion

$$f_{n+1}(1) - (n + 1)f_n(1) = 0$$

However, $n!$ is not exponentially bounded.

Despite the above remark, the evaluations of quantum spin networks at a fixed root of unity is exponentially bounded.

Theorem 5.6. *For every quantum spin network (Γ, γ) , every complex root of unity ζ and every natural number r , there exists $C > 0$ (which depends on Γ, γ and r) such that*

$$|\langle \langle \Gamma, n\gamma \rangle \rangle^{(r)}(\zeta)| \leq C^n \tag{5.7}$$

for all $n \in \mathbb{N}$.

Finally we would like to propose a conjecture concerning the growth rates of a quantum spin network at a primitive N -th root of unity. Conjecturally their absolute values are determined by the classical growth rates at $q = 1$. The latter depend on the abstract graph Γ and not on its particular embedding in 3-space. This phenomenon is contrast with the Volume Conjecture, where the relevant growth rates depend non-trivially on the embedding of Γ in 3-space, [Ka2]. In view of the above theorems we choose to phrase the conjecture in the more general setting of holonomic sequences.

Conjecture 5.1. *Let Λ_N denote the absolute value of the growth rates of the sequence $(\Gamma, n\gamma)(e^{\frac{2\pi i s}{N}})$. Then, we have*

$$\Lambda_N^N = \Lambda_1$$

5.1.6 Acknowledgment

The paper was conceived during a conference on *Interactions Between Hyperbolic Geometry, Quantum Topology and Number Theory* held in Columbia University, New York, in June 2009. The authors wish to thank the organizers, A. Champanerkar, O. Dasbach, E. Kalfagianni, I. Kofman, W. Neumann and N. Stoltzfus for their hospitality. In addition, we wish to thank F. Costantino, G. Kuperberg and D. Zagier for enlightening conversations.

5.2 Evaluation of quantum spin networks

5.2.1 Local projectors

We start by defining classical spin networks of arbitrary valency using the notion of a local projector. A *classical spin network* will be a pair (Γ, γ) of an abstract ribbon graph Γ (of arbitrary valency), together with a pair of functions $\gamma = (\gamma_E, \gamma_V)$ where $\gamma_E : \text{Edges}(\Gamma) \rightarrow \mathbb{N}$ is an admissible coloring γ of its edges, and $\gamma_V : \text{Vert}(\Gamma) \rightarrow \{\text{projectors}\}$ a choice of a local projector at each vertex of Γ . A local projector is defined as follows. Given an admissible coloring (c_1, \dots, c_d) of the d edges around a vertex v of a ribbon graph, place a collection of $c_1 + \dots + c_d$ points on a disk. A *local projector* is a planar way to connect these points with *disjoint arcs* on the disk and *no U-turns*, as in the following example:

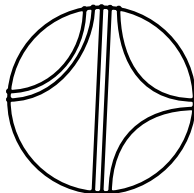


Figure 5.1: An example of a projector for a degree 4 vertex with edge coloring $(2, 5, 2, 3)$.

Note that if p is a local projector and n is a natural number, then there is there is a canonical choice of a local projector np by cabling each arc of p into n arcs. In [Ku, p.118], Kuperberg uses the term *clashed web space* $W(c_1, \dots, c_d)$ which has a basis the local projectors defined above. Local projectors are a pictorial way to encode dual canonical bases for \mathfrak{sl}_2 , as was shown in [FK]. However, clashed web spaces and dual canonical bases do *not* coincide for \mathfrak{sl}_3 ; see [KK]. Finally note that there are alternative methods of defining multi-valent vertices, for example [Yo],[Ba]. However our definition using projectors works without change for Lie algebras of arbitrary rank.

5.2.2 The standard evaluation of a quantum spin network

Recall from the introduction that a quantum spin network is a pair (Γ, γ) where Γ is a framed ribbon graph embedded in S^3 and $\gamma = (\gamma_E, \gamma_V)$ as in the classical case. We allow Γ to have multiple edges and loops and it may be disconnected. Knots and links are quantum spin networks with zero vertices. However we restrict ourselves to integral framings of Γ . In this section we define the evaluation of quantum spin networks in terms of the Kauffman bracket. Recall that the *quantum integer* $[n]$ and the balanced *quantum factorial* $[n]!$ is defined by

$$[n] = \frac{A^{2n} - A^{-2n}}{A^2 - A^{-2}}, \quad [n]! = \prod_{k=1}^n [k] \quad (5.8)$$

where

$$A^4 = q. \quad (5.9)$$

The *Kauffman bracket* evaluation is determined by the following rules:

$$\begin{aligned} \begin{array}{c} \diagup \quad \diagdown \\ \diagdown \quad \diagup \end{array} &= A \begin{array}{c} \frown \\ \smile \end{array} + A^{-1} \begin{array}{c} \smile \\ \frown \end{array} \\ \bigcirc \cup D &= -[2] \cdot D \end{aligned}$$

To emphasize the similarity to the evaluation of classical spin networks we use the explicit expression for the Jones-Wenzl idempotent from [KL, Chpt.3]. This is defined as the following formal sum of braids:

$$A^{b(b-1)} \sum_{\sigma \in S_b} A^{-3\ell(\sigma)} \beta_\sigma$$

Here b is the label of the edge, and for any permutation σ we denote by β_σ the unique negative (with respect to orientation downwards) permutation braid corresponding to σ . By $\ell(\sigma)$ we mean the minimal length of σ written as a product of transpositions. Note that we leave out the quantum factorial $[b]!$ that is used in [KL].

Definition 5.3. (a) We say a quantum spin network is *admissible* if for every vertex v the projector $\gamma_V(v)$ matches the labels of the edges given by γ_E .
(b) The evaluation $\langle \Gamma, \gamma \rangle^P$ of a quantum spin network (Γ, γ) is defined to be zero if it is not admissible. An admissible quantum spin network is evaluated by the following algorithm.

- Use the ribbon structure to thicken the vertices into disks and the edges into untwisted bands.
- Replace each vertex v by the pattern of the projector $\gamma_V(v)$ and replace each edge by the linear combination of braids as shown in Figure 5.2.
- Finally the resulting linear combination of links is evaluated calculating the Kauffman bracket.

In the case $A = -1$ this definition agrees with the Penrose evaluation defined in [GV]. For general A the definition agrees with that given in [MV, KL, CFS] except for the missing quantum factorial $[b]!$ in the denominator, one for every

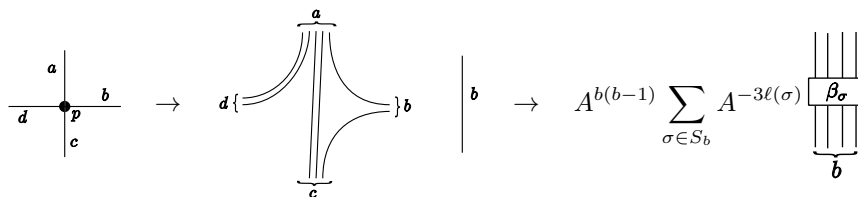


Figure 5.2: The rules for evaluating a quantum spin network. Replace vertices and edges to get a linear combination of links that is evaluated using the Kauffman bracket.

edge. The reason for leaving out this factor is that there is a better way to normalize (see Definition 5.4 below) which results in Laurent polynomials in $q^{1/4}$ (as opposed to rational functions in $q^{1/4}$) while the value of $\langle \Gamma, n\gamma \rangle(q)$ at a fixed root of unity q grows at most exponentially with respect to n , see Theorem 5.6.

Definition 5.4. *The standard evaluation of a quantum spin network is defined by*

$$\langle \Gamma, \gamma \rangle = \frac{1}{[\mathcal{I}]!} \langle \Gamma, \gamma \rangle^P$$

Here $[\mathcal{I}]! = \prod_v [\gamma_V(v)]!$, where for a projector $[p]!$ means grouping all strands connecting the same two edges and forming the product of the quantum factorials of these numbers.

Note that with this normalization subdividing an edge colored a into two edges colored a connected by a vertex whose third edge is colored 0 does not change the value of the evaluation. This is the way in which the value of the unknot should be interpreted in order to obtain the correct value $(-1)^a [a + 1]$ instead of its quantum factorial.

We end this section by proving that any quantum spin network evaluation actually reduces to a trivalent quantum spin network evaluation. Hence all results previously known in the trivalent case extend to the general case.

Lemma 5.1. *Let (Γ, γ) be a quantum spin network. There exists a trivalent quantum spin network (Γ', γ') such that for all $n \in \mathbb{N}$*

$$\langle \Gamma, n\gamma \rangle = \langle \Gamma', n\gamma' \rangle$$

Proof. It is convenient to take a slightly different view of the evaluation algorithm defined in 5.3. Instead of expanding out the linear combination at every edge, we view the Jones-Wenzl idempotent as box with arcs coming out. After expanding the vertices the whole network becomes a number of boxes connected by arcs. The idea is to add extraneous boxes and to reinterpret the result as the evaluation of a trivalent quantum spin network. The key property that makes this work is the fundamental fact that once one includes the factor $\frac{1}{[b]!}$ in a box with b strands, it becomes an idempotent [MV]. Since we're not using this normalization we get that adding an extra box to b parallel adjacent arcs coming out of a box multiplies the evaluation by $[b]!$. This factor will cancel with the

the normalization factor due to the trivalent vertices that will be created in the process.

Let us first describe how to modify a single half-edge pointing into a multivalent vertex v with projector p . The arcs coming into v from half edge e are grouped into a_j parallel arcs according to the projector p . To the box that already marks the beginning of e we now add an extra stack of boxes as shown in the middle of Figure 5.3. This will multiply the Penrose evaluation of Γ by a factor $a_e = ([a_2]! \dots [a_n]!)([a_1 + a_2 \dots + a_{n-1}]! \dots [a_1 + a_2]![a_1]!)$

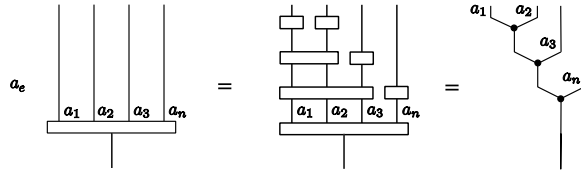


Figure 5.3: Turning an edge into a trivalent network.

Doing this for every half edge gives just enough boxes to split into a trivalent quantum spin network Γ' as shown in the above figure. However the smallest boxes at the tip of the tree meet another equal sized box on the other side which are not there in the evaluation of Γ' . Therefore we have to remove those boxes again, which reduces the Penrose evaluation by exactly a factor $[\mathcal{I}]! = [\mathcal{I}(\Gamma)]!$. Therefore,

$$\langle \Gamma, \gamma \rangle^P \prod_e a_e = [\mathcal{I}]! \langle \Gamma', \gamma' \rangle^P$$

And hence passing to the standard normalization we find:

$$\langle \Gamma, \gamma \rangle = \frac{\langle \Gamma, \gamma \rangle^P}{[\mathcal{I}]!} = \frac{\langle \Gamma', \gamma' \rangle^P}{\prod_e a_e} = \langle \Gamma', \gamma' \rangle$$

concluding the proof. \triangle

5.2.3 Evaluation of spin networks using the shadow formula

In this subsection we describe a way of evaluating spin networks in terms of the shadow formula. We restrict ourselves to trivalent Γ . Since Γ is supposed to be orientable, we can choose a blackboard framed diagram D of Γ .

The shadow formula expresses the evaluation in terms of a multi-dimensional sum of $1j$, $3j$ and $6j$ -symbols. The latter are the evaluations of three basic spin networks, shown in Figure 5.4.

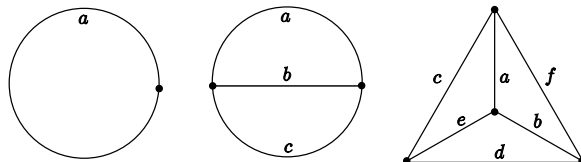


Figure 5.4: Three basic spin networks.

Let

$$\left[\begin{array}{c} a \\ a_1, a_2, \dots, a_r \end{array} \right] = \frac{[a]!}{[a_1]! \dots [a_r]!} \quad (5.10)$$

denote the multinomial coefficient when $a_1 + \dots + a_r = a$. The value of the $1j$, $3j$ and $6j$ -symbols is given by the following lemma of [KL] (see also, [MV, We]), using our normalization.

Lemma 5.2. (a) We have

$$\langle \bigcirc, a \rangle = (-1)^a [a + 1]$$

(b) Let (Θ, γ) denote the Θ spin network admissibly colored by $\gamma = (a, b, c)$ as in Figure 5.4. Then we have

$$\langle \Theta, \gamma \rangle = (-1)^{\frac{a+b+c}{2}} \left[\frac{a+b+c}{2} + 1 \right] \left[\begin{array}{c} \frac{a+b+c}{2} \\ -\frac{a+b+c}{2}, \frac{a-b+c}{2}, \frac{a+b-c}{2} \end{array} \right] \quad (5.11)$$

(c) Let (\triangle, γ) denote a tetrahedron labeled and oriented as in Figure 5.4 and admissibly colored by $\gamma = (a, b, c, d, e, f)$. Then we have $\langle \triangle, \gamma \rangle =$

$$\sum_{k=\max T_i}^{\min S_j} (-1)^k [k + 1] \left[\begin{array}{c} k \\ S_1 - k, S_2 - k, S_3 - k, k - T_1, k - T_2, k - T_3, k - T_4 \end{array} \right] \quad (5.12)$$

where S_i are the half sums of the labels in the three quadrangular curves in the tetrahedron and T_j are the half sums of the three edges emanating from a given vertex. In other words, the S_i and T_j are given by

$$S_1 = \frac{1}{2}(a + d + b + c) \quad S_2 = \frac{1}{2}(a + d + e + f) \quad S_3 = \frac{1}{2}(b + c + e + f) \quad (5.13)$$

$$T_1 = \frac{1}{2}(a + b + e) \quad T_2 = \frac{1}{2}(a + c + f) \quad T_3 = \frac{1}{2}(c + d + e) \quad T_4 = \frac{1}{2}(b + d + f) \quad (5.14)$$

In addition to the three basic spin networks above, we choose to consider a variant of the tetrahedron that represents a crossing. The crossing can be reduced to a $6j$ -symbol using the half twist formula, [MV].

$$\begin{array}{c} r_1 \\ \bigcirc \\ a \\ b \\ r_3 \\ r_4 \end{array} = (-1)^{\frac{-r_1 - r_3 + r_2 + r_4}{2}} q^{\frac{-r_1(r_1+2) - r_3(r_3+2) + r_2(r_2+2) + r_4(r_4+2)}{8}} \begin{array}{c} r_1 \\ \bigcirc \\ b \\ a \\ r_3 \\ r_4 \end{array}$$

We are now ready to explain how to evaluate a spin network using the shadow formula. A blackboard framed diagram of Γ gives rise to a planar graph D , whose edges are colored by γ and whose vertices are either vertices of Γ or crossings. Let V, E, F, C denote the sets of trivalent vertices, edges, faces and crossings (4-valent vertices) of D . We will express the evaluation of the quantum spin network as a sum over all admissible colorings of F by natural numbers. Here admissible means that for any two faces colored r_1, e, r_2 and separated by edge e , the numbers $(r_1, r_2, \gamma(e))$ satisfy the triangle inequalities. Moreover the outer face should get color 0.

$$\langle \Gamma, \gamma \rangle = \sum_r \prod_{f \in F} \bigcirc \prod_{e \in E} \Theta^{-1} \prod_{v \in V} \triangle \prod_{c \in C} \otimes \quad (5.15)$$

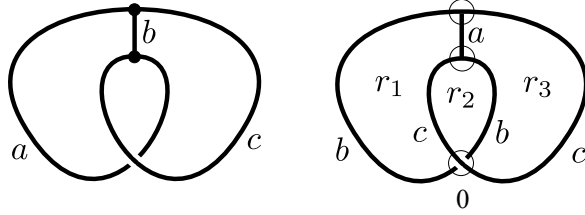


Figure 5.5: An example spin network Γ, γ (left) and its diagram with encircled crossings and vertices and a coloring of the regions.

The sum is over admissible colorings r of the faces F and the labels of the symbols in the formula are found from the coloring and γ as follows. The $1j$ symbol gets the color of the face it corresponds to. The theta gets the color of the edge it corresponds to plus the two colors of the faces it bounds. For every vertex the corresponding $6j$ symbol is colored by the three adjacent faces and the three adjacent edge labels. Finally every crossing is counted by a skew $6j$ -symbol obtained by encircling the crossing and coloring according to the faces one crosses. For a more elaborate discussion see [Co2].

Consider the following simple example of a spin network evaluation using the shadow formula.

Note that one can find the contributing $6j$ -symbols from the diagram by encircling the vertices and crossings. This is useful in keeping track of the labels. Similarly one could also encircle the edges and faces to obtain the $3j$ and $1j$ -symbols.

$$\langle \Gamma, a, b, c \rangle = \sum_{r_1, r_2, r_3} \frac{\text{Diagram 1} \cdot \text{Diagram 2} \cdot \text{Diagram 3}}{\Theta(0, b, r_1)\Theta(0, c, r_3)\Theta(r_1, c, r_2)\Theta(r_2, b, r_3)\Theta(r_1, a, r_3)}$$

Since the sum is over admissible colors only, we see that in this special case there is quite some simplification. The fact that the outside color is 0 forces $r_1 = b$, $r_2 = c$. Actually one can check that after substituting the formulas for the $6j$, $3j$ and $1j$ -symbols one gets that the answer is 0 unless $a = 0$ and $b = c$ in which case we get a twisted unknot.

5.2.4 Integrality

In [Co2] it was shown that $\langle \Gamma, \gamma \rangle \in A^f \mathbb{Z}[A^{\pm 2}]$ for some f depending on (Γ, γ) . In this subsection we use the shadow formula to extend this result to prove that actually $\langle \Gamma, \gamma \rangle \in A^{Q(\gamma)} \mathbb{Z}[A^{\pm 4}]$. Here $Q(\gamma)$ is a quadratic form depending on Γ in the labels γ , that takes values in $\mathbb{Z}/4\mathbb{Z}$. The proof below will indicate how to obtain an expression for $Q(\gamma)$ from an admissible coloring of the faces of a diagram of Γ . The form itself is independent of the choice of diagram, and coloring. By identifying $\mathbb{Z}/4\mathbb{Z}$ with $\{0, 1, 2, 3\}$ we have defined $\langle \Gamma, \gamma \rangle = A^{-Q(\gamma)} \langle \Gamma, \gamma \rangle$ precisely.

Proof. (of Proposition 5.1). Note that by Lemma 5.1 we can restrict ourselves

to trivalent Γ . Pick any blackboard framed diagram D of (Γ, γ) and consider applying the shadow formula (5.15). Since by Costantino's result [Co2] we already know the evaluation is a polynomial in A we can look at the degree of the terms in the sum.

Now define $\phi : \mathbb{Z}[A^{\pm 1}] \rightarrow \mathbb{Z}/4\mathbb{Z}$ to be a function such that we have $P(a) \in A^{\phi(P)}\mathbb{Z}[A^{\pm 4}]$. As a first step we calculate ϕ for the building blocks of the shadow formula. By dividing the leading powers of the denominator in the formulas for the $6j$ -symbol we see that:

$$\begin{aligned} \phi([k]) &= 2k - 2 \\ \phi(\Theta, a, b, c) &= a^2 + b^2 + c^2 \\ \phi(\triangleleft, \gamma) &= \sum_i \gamma_i^2 + \sum_{i < j} \gamma_i \gamma_j \\ \phi\left(\begin{array}{c|c} r_1 & r_2 \\ \hline r_4 & r_3 \end{array}\right) &= \frac{-r_1^2 - r_3^2 + r_2^2 + r_4^2}{2} - r_1 - r_3 + r_2 + r_4 + \phi(\triangleleft) \end{aligned}$$

It suffices to show that every term in the shadow formula has the same value of ϕ (modulo 4). In order to check this we consider the effect on ϕ of a term when we increase one of the variables r by two. This is sufficient since a simple argument shows that any state can be reached from any other state by repeatedly increasing or decreasing one of the variables by two.

So let $\phi(r)$ be the value of ϕ on a particular summand in which we ignore the terms not containing r . With respect to the region labeled r we make a distinction between the edges and regions directly adjacent to it (notation: $e|r$ or $r_i|r$) and those edges and regions transverse to the region r (notation: $e \perp r$). See also Figure 5.6.

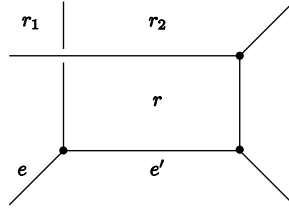


Figure 5.6: The region labeled r . The region r_1 the edge e are transverse to r . The region r_2 and the edge e' are adjacent to r .

Let C denote the number of crossings next to r , counted with sign σ . Looking at the above formulae for ϕ we get the following expression for $\phi(r)$. Here we abused the notation to make r_i denote both the face and its value and $\sigma(r_i)$ is the sign of the corresponding crossing between r and r_i .

$$\phi(r) = r^2(\#\text{adjacent edges} + \#\text{adjacent vertices} + \frac{C}{2} + \#\text{unsigned crossings}) +$$

$$r(2 + 2 \sum_{e|r} \gamma(e) + 2 \sum_{r_i|r} r_i + \sum_{e \perp r} \gamma(e) + \sum_{r_i \perp r} r_i + \sigma(r_i))$$

We will show that $\Delta = \phi(r+2) - \phi(r)$ is divisible by 4. Since modulo 4 we have

$$\Delta \equiv 2((r+1)\#\text{crossings} + \sum_{e \perp r} \gamma(e) + \sum_{r_i \perp r} r_i + \sigma(r_i)) \pmod{4}$$

we need to check that the term in brackets is even. To do so we use admissibility and write congruences modulo 2. By admissibility of the labels at the trivalent vertices and admissibility of the thetas coming from the edges in the shadow formula respectively we have:

$$\gamma(e) \equiv \gamma(e') + \gamma(e'') \quad r_i \equiv \gamma(e_1) + \gamma(e_2) + r \pmod{2}$$

Here e, e', e'' are the edges at a vertex and e_1, e_2, r, r_i are the edges and two opposite regions at a crossing. Summing all these identities we see that every edge adjacent to r appears exactly twice, which shows that

$$\sum_{e \perp r} \gamma(e) + \sum_{r_i \perp r} r_i \equiv r\#\text{crossings} \pmod{2}$$

Finally $\sum_{r_i \perp r} \sigma(r_i) \equiv \#\text{crossings}$, therefore Δ is divisible by 4 and the proof is complete. \triangle

5.3 Proof of Theorems 5.3, 5.4, 5.5 and 5.6

5.3.1 Behavior of q -holonomic sequences under differentiation

In this section we prove Theorem 5.4.

Proof. Consider a q -holonomic sequence $f_n(q) \in \mathbb{Q}(q)$ that satisfies a linear recursion relation

$$\sum_{j=0}^d a_j(q^n, q) f_{n+j}(q) = 0$$

where $a_j(u, v) \in \mathbb{Q}[u, v]$ for $j = 0, \dots, d$. Differentiate with respect to q . We obtain that

$$\sum_{j=0}^d a_j(q^n, q) f'_{n+j}(q) + nq^{n-1} \sum_{j=0}^d a_{j,u}(q^n, q) f_{n+j}(q) + \sum_{j=0}^d a_{j,v}(q^n, q) f_{n+j}(q) = 0 \quad (5.16)$$

where $a_{j,u} = \partial a_j / \partial u$, $a_{j,v} = \partial a_j / \partial v$ and $f'(q) = df(q)/dq$. Recall now that the product and the $\mathbb{Q}[q]$ -linear combination of two q -holonomic sequences is q -holonomic; see [Z, WZ1]. Lemma 5.3 implies that for every j , the sequences $(nq^{n-1} a_{j,u}(q^n, q) f_{n+j}(q))$ and $(a_{j,v}(q^n, q) f_{n+j}(q))$ are q -holonomic. It follows that the second and third sum in Equation (5.16) is q -holonomic, i.e., it satisfies a linear recursion relation with coefficients in $\mathbb{Q}[q^n, q]$. Substituting in this linear recursion the first sum of Equation (5.16), it follows that the sequence $f'_n(q)$ is q -holonomic. \triangle

Lemma 5.3. *For every fixed integer c , the sequence (nq^{cn}) is q -holonomic.*

Proof. It is easy to verify that the sequence $f_n(q) = nq^{cn}$ satisfies linear recursion relation

$$f_{n+2}(q) - 2q^c f_{n+1}(q) + q^{2c} f_n(q) = 0$$

△

5.3.2 Evaluations of q -holonomic sequences a fixed root are holonomic

Consider a q -holonomic sequence $f_n(q) \in \mathbb{Z}[q^{\pm 1}]$ that satisfies a linear recursion relation of the form

$$c_d(q^n, q)f_{n+d}(q) + \cdots + c_0(q^n, q)f_n(q) = 0 \quad (5.17)$$

for all n where $c_j(u, v) \in \mathbb{Q}[u, v]$ are polynomials in two variables for $j = 0, \dots, d$. The field \mathbb{Q} of coefficients does not matter here and can be replaced by \mathbb{C} without any change. Fix a complex root of unity ζ . The idea of the proof consists of a lucky case, and a general case which reduces to a lucky case after sufficient differentiation. The differentiation trick appears in an efficient algorithm to compute the Kashaev invariant of some knots in [GL1], and was also inspired by conversations of the first author with D. Zagier.

Let us first discuss the proof of Theorem 5.5 when $\zeta = 1$. In the lucky case, the set

$$S = \{j \mid 0 \leq j \leq d, c_j(1, 1) \neq 0\}$$

is non-empty. In that case, expand (5.17) as a power series in $q - 1$. The vanishing of the constant term implies that $f_n(1)$ satisfies a non-trivial linear recursion with constant coefficients

$$\sum_{j \in S} c_j(1, 1) f_{n+j}(1) = 0$$

Thus, the sequence $(f_n(1))$ is holonomic. In the general case, there exists a unique natural number $s \geq 0$ such that $c_j(q^n, q) = \gamma_j(q - 1)^s + O((q - 1)^{s+1})$ and some γ_j is nonzero. In other words, $c_j(q^n, q)$ vanish to order $s - 1$ at $q = 1$ for all i , and some $c_j(q^n, q)$ does not vanish to order s at $q = 1$. In that case, observe that

$$\sum_{j \in S'} c_j^{(s)}(1, 1) f_{n+j}(1) = 0$$

where

$$S' = \{j \mid 0 \leq j \leq d, \gamma_j \neq 0\} \neq \emptyset$$

and $c_j^{(s)}(1, 1) \in \mathbb{Q}[n]$. This concludes the proof of Theorem 5.5 when $\zeta = 1$.

Suppose now that ζ is a complex root of unity of order N . The problem is that $c_j^{(s)}(\zeta^n, \zeta)$ is no longer a polynomial of n even when $s = 0$. To remedy this, we consider n to be in a fixed arithmetic progression modulo N . In other words, fix i with $0 \leq i \leq N - 1$ and replace n by $Nn + i$ in (5.17). Then, $c_j(q^{Nn+i}, q)$ can be expanded in powers of $q - \zeta$ with coefficients in $\mathbb{Q}(\zeta)[n]$ for all i and j . In other words, for all i, j we have $c_{ij}(q) := c_j(q^{Nn+i}, q) \in \mathbb{Q}(\zeta)[n][[q - \zeta]]$. Let us consider the column vector $x_n = (f_{Nn}(\zeta), \dots, f_{Nn+N-1}(\zeta)) \in \mathbb{C}^N$. If $c_{i,j}(\zeta) \neq 0$, then $f_{Nn+i+j}(\zeta)$ is a $\mathbb{Q}(\zeta)[n]$ -linear combination of $f_{Nn+i+j'}(\zeta)$ for $j' \neq j$. Of course, $f_{Nn+i+j}(\zeta)$ is the k -th coordinate of x_n where $k \equiv i + j \pmod{N}$.

Now we consider two cases. In the lucky Case 1, the following set

$$S = \{(i, j) \in [0, N - 1] \times [0, d] \mid c_{i,j}(\zeta) \neq 0\}$$

is non-empty. S defines a graph $G(S)$ defined as follows. It has vertex set $\{0, 1, \dots, N - 1\}$, and an edge e between vertices k and k' if and only if there exist $(i, j), (i, j') \in S$ such that $k \equiv i + j \pmod{N}$ and $k' \equiv i + j' \pmod{N}$. We consider two subcases. In the very lucky Case 1.1, $G(S)$ is connected. The above discussion implies that the vector x_n and finitely many of its translates, put together in a column vector y_n satisfy a first order linear recursion of the form

$$y_{n+1} = A(n)y_n$$

for a square matrix $A(n)$ with coefficients in the field $\mathbb{Q}(\zeta)(n)$. The cyclic vector Lemma 5.4 below implies that every coordinate of y_n is holonomic. It follows that $(f_{Nn+i}(\zeta))$ is holonomic (with respect to n) for every fixed $i \in [0, N - 1]$. Since (a_n) is holonomic if and only if (a_{Nn+i}) is holonomic for all $i \in [0, N - 1]$ (see [PWZ]), it follows that $f_n(\zeta)$ is holonomic in the very lucky Case 1.1.

In the not-so-lucky Case 1.2, the set S is non-empty but the graph $G(S)$ is disconnected. In that case, differentiate (5.17) once and consider the pair of column vectors $x_n^r = (f_{Nn}^{(r)}(\zeta), \dots, f_{Nn+N-1}^{(r)}(\zeta)) \in \mathbb{C}^N$ for $r = 0, 1$. Consider also the set

$$S^r = \{(i, j) \in [0, N - 1] \times [0, d] \mid c_{i,j}^{(r)}(\zeta) \neq 0\}$$

for $r = 0, 1$. $S^0 \cup S^1$ gives rise to a graph $G(S^0 \cup S^1)$ with vertices pairs (r, k) for $r = 0, 1$ and $k = 0, \dots, N - 1$. There is an edge between (r, k) and (r', k') if there exist $(i, j) \in S^r, (i, j') \in S^{r'}$ such that $k \equiv i + j \pmod{N}$ and $k' \equiv i + j' \pmod{N}$. Note that by assumption, $S^0 = S$ is non-empty, and there is a natural inclusion of $G(S)$ into $G(S^0 \cup S^1)$. In the not-so-lucky Case 1.2, the graph $G(S^0 \cup S^1)$ is connected. The argument of Case 1.1 shows that $f_n(\zeta)$ is holonomic. If $G(S^0 \cup S^1)$ is disconnected, differentiate (5.17) once more. It is easy to see that after a finite number t of differentiations, the graph $G(S^0 \cup \dots \cup S^t)$ will be connected and consequently $f_n(\zeta)$ is holonomic. Differentiating (5.17) t times and using induction implies that $f_n(\zeta)$ is holonomic.

This concludes the proof of Theorem 5.5 when S is non-empty. In the unlucky Case 2 where all functions $c_{i,j}(q)$ vanish to first order at $q = \zeta$, there is a natural number s such that $c_{i,j}^{(s')}(\zeta) = 0$ for all $s' < s$ and all i, j and in addition $c_{i,j}^{(s)}(\zeta) \neq 0$ for some i, j . In that case, replace S by the set

$$S' = \{(i, j) \mid 0 \leq j \leq d, 0 \leq i < N - 1, c_{i,j}^{(s)}(\zeta) \neq 0\}$$

and repeat the above proof. Finally, to complete the proof of Theorem 5.5 we need to show that $f_n(\zeta)$ grows at most exponentially. This follows from [GL2, Thm.15].

Theorem 5.7. [GL2, Thm.15] *If $f_n(q) \in \mathbb{Q}[q^{\pm 1}]$ is a q -holonomic sequence, then the span of $f_n(q)$ is $O(n^2)$, the L^1 -norm of the coefficients of $a_n(q)$ are $O(C^n)$.*

Lemma 5.4. *Consider a sequence of vectors $x_n \in \mathbb{C}^l$ that satisfy a first order linear recursion of the form*

$$x_{n+1} = A(n)x_n$$

where $A(n)$ is an $l \times l$ matrix with coefficients in $\mathbb{C}[n]$. Then every coordinate of x_n is a holonomic sequence.

Proof. Consider the operators ν and N which act on a sequence (a_n) by

$$(\nu a)_n = na_n, \quad (Na)_n = a_{n+1}.$$

These operators satisfy the commutation relation $N\nu = \nu N + N$ and generate an Ore ring $R = \mathbb{C}[\nu]\langle N \rangle$. The matrix $A(n)$ defines an R -module M as in [VPS]. The lemma follows from the *cyclic vector theorem* applied to the module M ; see [VPS, Prop.2.9] and also [Kz]. The proof is constructive and can be implemented for example in [AB]. \triangle

This finishes the proof of Theorem 5.5. \triangle

Note that Theorem 5.5 fails when q is not a root of unity. For example, consider the q -holonomic sequence $a_n(q) = q^{n^2}$ and fix $q = \omega$, a complex number which is not a root of unity. Suppose that the sequence $b_n = \omega^{n^2}$ is holonomic. So for all natural numbers n we have

$$\sum_{k=0}^d c_k(n)b_{n+k} = 0$$

where $c_j(n) \in \mathbb{Q}[n]$. Dividing by b_n we get

$$\sum_{k=0}^d c_k(n)\omega^{2nk+k^2} = 0$$

Collecting the coefficients of a fixed power of n , we find that there are coefficients $C_1 \dots C_D \in \mathbb{C}$ such that

$$\sum_{k=0}^D C_k \omega^{nk} = 0$$

In other words, for all n , ω^n is a root of the polynomial $\sum_{k=0}^D C_k x^k$. It follows that $\omega^m = 1$ for some m .

5.3.3 Proof of Theorem 5.6

In this section we prove Theorem 5.6. Recall from Remark 5.3 that this theorem is special to the quantum spin network evaluations and not valid for general q -holonomic sequences.

The main ideas that go into the proof of Theorem 5.6 are the following:

- (a) its validity for the local building block of quantum spin networks (namely the quantum $6j$ -symbol),
- (b) a state-sum formula for the evaluation of an arbitrary quantum spin network where the summand is a product of quantum $6j$ -symbols divided by quantum $3j$ -symbols,
- (c) a lemma for the growth rate of the coefficients of inverse quantum factorials, in the spirit of [GL2, Thm.15].

Let us begin with the first ingredient.

Lemma 5.5. *Theorem 5.6 holds for the quantum $6j$ -symbols.*

Proof. Equation (4.20) shows that $f_n(q) = \langle \triangleleft, n\gamma \rangle$ is a Laurent polynomial in $q^{1/2}$ which is written as a 1-dimensional sum. Let $\|h(q)\|_1$ denote the sum of the absolute values of a Laurent polynomial in $q^{1/4}$. It is well known that the quantum binomial coefficient (5.10) is a Laurent polynomial in $q^{1/2}$ with nonnegative integer coefficients. Moreover, its evaluation at $q = 1$ is the usual multinomial coefficient. The sum of the latter is at most r^a . It follows that

$$\left\| \begin{matrix} a \\ a_1, a_2, \dots, a_r \end{matrix} \right\| = \frac{a!}{a_1! \dots a_r!} \leq r^a.$$

Equation (4.20) and the above inequality conclude the proof of the lemma. \triangleleft

Now consider an arbitrary quantum spin network (Γ, γ) and its evaluation $f_N(q) = \langle \Gamma, N\gamma \rangle(q)$. Viewing $1j$ -symbols as special cases of $6j$ -symbols and crossings as a power of q times a $6j$ -symbol, the shadow state-sum formula (5.15) expresses $f_N(q)$ by

$$f_N(q) = \sum_{k \in NP} \frac{M(k)}{D(k)} \quad (5.18)$$

where the summation is over the set of lattice points of NP (for some rational convex polytope P) and $M(k)$ is a product a power of q and of quantum $6j$ -symbols at linear forms of k , and $D(k)$ is a product of quantum factorials at linear forms of k . The fact that D is a product of quantum factorials only follows from the formula for the $3j$ -symbol, see Equation (4.23). We know that $f_N(q) \in \mathbb{Z}[q^{\pm 1/4}]$ by Proposition 5.1. Theorem 5.5 implies that the exponents of q in $\langle \Gamma, N\gamma \rangle(q)$ are bounded above and below by quadratic functions of N .

Let $(q)_n = \prod_{j=1}^n (1 - q^j)$ for $n \in \mathbb{N} \cup \{\infty\}$. It is well-known that

$$\frac{1}{(q)_\infty} = \sum_{k=0}^{\infty} p_k q^k$$

where $p_k \in \mathbb{N}$ is the number of partitions of k ; see [Aw]. Moreover, for every k and n , the coefficient of q^k in $1/(q)_n$ is a natural number which is at most p_k . In addition, we have

$$p_k \leq e^{Ck^{1/2} + o(1)}$$

where $C = \pi\sqrt{2/3}$; see [Aw]. It follows that the coefficient of q^n in $1/D(k)$ is exponentially bounded by n^2 , and since $n = O(N^2)$, the coefficient is exponentially bounded by N . Since the number of k -summation terms in the state-sum (5.18) is bounded by a polynomial function of N , this completes the proof of Theorem 5.6. \triangleleft

Remark 5.4. *The above proof is similar in spirit with the proof of [GL2, Thm.15].*

5.3.4 Proof of Theorem 5.3

Fix a quantum spin network (Γ, γ) . It follows from the shadow state sum in Section 5.2.3 and Lemma 5.1 that the standard evaluation $\langle \Gamma, n\gamma \rangle(q)$ is a sum of a balanced q -hypergeometric term. Hence, by the fundamental theorem of WZ theory (see [WZ1]), it follows that $\langle \Gamma, n\gamma \rangle(q)$ is q -holonomic. Since $\langle\langle \Gamma, n\gamma \rangle\rangle(q) = q^{Q(n\gamma)/4} \langle \Gamma, n\gamma \rangle(q)$ and $Q(n\gamma)$ is periodic, $\langle\langle \Gamma, n\gamma \rangle\rangle(q)$ is q -holonomic as well.

Fix a complex root of unity ζ , and a natural number $r \geq 0$, and let $a_n = \langle\langle \Gamma, n\gamma \rangle\rangle^{(r)}(\zeta)$. We will apply Theorem 5.5 to check conditions (a)-(d) of Definition 5.2.

- (a) $a_n \in \mathbb{Z}[\zeta]$ as follows from Proposition 5.1.
- (b) Follows from Theorem 5.6: indeed the evaluation is a sum of integers multiplied by powers of a complex root of unity, where the sum of the absolute value of the integers is exponentially bounded.
- (c) Since $a_n \in \mathbb{Z}[\zeta]$ are algebraic integers, their common denominator is 1.
- (d) By theorems 5.4 and 5.5 the coefficients of the power series are holonomic, hence the series itself is holonomic as well.

This concludes the proof of Theorem 5.3. △

5.4 Examples

In this section we consider various simple examples to illustrate the theorems. For the sake of simplicity we suppress the function $A^{-Q(\gamma)}$ so we choose to work with $\langle \Gamma, \gamma \rangle$, rather than the more correct $\langle\langle \Gamma, \gamma \rangle\rangle$.

5.4.1 Evidence for Conjecture 5.1

Recall that Conjecture 5.1 relates the absolute value of the growth rates of the evaluation at the N -th root of unity to the classical evaluation at $q = 1$. All growth rates of a sequence of Nilsson type have equal absolute value. Denote by Λ_k the absolute value of the growth rates of the sequence of evaluations of $\langle\langle \Gamma, n\gamma \rangle\rangle$ at the k -th root of unity. Note that the distinction between $\langle\langle \Gamma, \gamma \rangle\rangle$ and $\langle \Gamma, \gamma \rangle$ is unimportant here since it is periodic in n .

The conjecture is that $\Lambda_N^N = \Lambda_1$. In the special case where Γ is a knot, the conjecture follows from the cyclotomic expansion of the colored Jones polynomial of a knot [GL2]. Making use of the notation $\{k\} = q^{k/2} - q^{-k/2}$ the cyclotomic expansion can be stated as follows.

$$\langle \Gamma, n \rangle(q) = \frac{(-1)^n}{\{1\}} \sum_{k=0}^n C_{\Gamma, k}(q) \{n+1-k\} \{n+1-k+1\} \dots \{n+1+k\}$$

If $q^N = 1$ we see that $\langle \Gamma, n \rangle(q)$ becomes $2N$ periodic in n . Therefore $\Lambda_N = 1$ for all N .

The theta graph evaluations provide a slightly more complicated example for which we will make use of the following lemma on multinomial coefficients.

Lemma 5.6. *Let $q = e^{\frac{2\pi i}{N}}$ and set $a_i = A_i N + \alpha_i$. We have*

$$\begin{aligned} \left[\begin{matrix} a_1 + \dots + a_n \\ a_1, a_2, \dots, a_n \end{matrix} \right] (q) &= q^{\frac{1}{2} \sum_{j < k} \alpha_j \alpha_k - a_j a_k} \binom{A_1 + \dots + A_n}{A_1, A_2, \dots, A_n} \left[\begin{matrix} \alpha_1 + \dots + \alpha_n \\ \alpha_1, \alpha_2, \dots, \alpha_n \end{matrix} \right] (q) \end{aligned} \quad (5.19)$$

This was proven for Gaussian (asymmetric) binomial coefficients in [De]. The extension to the multinomial case is straightforward and the power of q appears when one converts to symmetric multinomial coefficients. Note that the power of q is actually a sign since $\alpha_j \alpha_k - a_j a_k = -N(A_j A_k N + \alpha_j A_k + A_j \alpha_k)$.

Now consider the growth rates of the theta evaluations. Fix an admissible triple $a, b, c \in \mathbb{N}$, and set $A = \frac{-a+b+c}{2}$, $B = \frac{a-b+c}{2}$, $C = \frac{a+b-c}{2}$ then we have

$$\langle \Theta, an, bn, cn \rangle = \langle \bigcirc, n(A+B+C) \rangle \left[\begin{matrix} n(A+B+C) \\ nA, nB, nC \end{matrix} \right]$$

At $q = 1$ we find using *Stirling's formula* (see [O])

$$\Lambda_1 = \left\{ \frac{(A+B+C)^{A+B+C}}{A^A B^B C^C} \right\}$$

At the N -th root of unity we find

$$\langle \Theta, an, bn, cn \rangle (e^{\frac{2\pi i}{N}}) = P(n) \left(\begin{matrix} \lfloor \frac{nA}{N} \rfloor + \lfloor \frac{nB}{N} \rfloor + \lfloor \frac{nC}{N} \rfloor \\ \lfloor \frac{nA}{N} \rfloor, \lfloor \frac{nB}{N} \rfloor, \lfloor \frac{nC}{N} \rfloor \end{matrix} \right)$$

where $P(n)$ is a periodic function in n of period $2N$. Another application of Stirling shows that indeed $\Lambda_N^N = \Lambda_1$.

5.4.2 The q -difference equation of the regular 6j-symbol

We compute a second order recursion relation for the regular quantum 6j-symbol

$$a_n(q) = \langle \triangle, n \gamma \rangle (q), \quad \gamma = (2, 2, 2, 2, 2, 2).$$

using the q -WZ method, implemented in *Mathematica* by [PaRi] and used as in [GV]. The recursion has the form

$$\sum_{k=0}^2 c_k(q, q^n) a_{n-k}(q) = 0 \quad (5.20)$$

where

$$\begin{aligned} c_0(q, q^n) &= q^{2+12n} (q - q^n)^3 (-1 + q^n)^5 (q + q^n) (4q^{10} + 4q^{10n} + 6q^{9+n} + 4q^{8+2n} - q^{6+3n} + 5q^{7+3n} \\ &\quad - q^{8+3n} - 6q^{5+4n} - 2q^{6+4n} - 6q^{7+4n} - 4q^{4+5n} + 2q^{5+5n} - 4q^{6+5n} - 6q^{3+6n} - 2q^{4+6n} \\ &\quad - 6q^{5+6n} - q^{2+7n} + 5q^{3+7n} - q^{4+7n} + 4q^{2+8n} + 6q^{1+9n}) \end{aligned}$$

$$\begin{aligned}
c_1(q, q^n) = & -q^{-1+6n} (q - q^n)^3 (q - q^{2n}) (-4q^{14} - 4q^{15} + q^{18n} + 7q^{19n} + 10q^{20n} + 10q^{21n} + 7q^{22n} \\
& + q^{23n} - 10q^{13+n} - 8q^{14+n} - 10q^{15+n} - 10q^{12+2n} + 6q^{13+2n} + 6q^{14+2n} - 10q^{15+2n} \\
& + q^{10+3n} - 9q^{11+3n} + q^{12+3n} + 28q^{13+3n} + q^{14+3n} - 9q^{15+3n} + q^{16+3n} + 7q^{9+4n} \\
& + 4q^{10+4n} + 14q^{11+4n} + 13q^{12+4n} + 13q^{13+4n} + 14q^{14+4n} + 4q^{15+4n} + 7q^{16+4n} \\
& + 10q^{8+5n} + 2q^{9+5n} + 22q^{10+5n} + 36q^{11+5n} + 36q^{13+5n} + 22q^{14+5n} + 2q^{15+5n} \\
& + 10q^{16+5n} + 10q^{7+6n} - 3q^{8+6n} - 16q^{9+6n} + 4q^{10+6n} - 17q^{11+6n} - 17q^{12+6n} + 4q^{13+6n} \\
& - 16q^{14+6n} - 3q^{15+6n} + 10q^{16+6n} + 7q^{6+7n} - 3q^{7+7n} + q^{8+7n} + 6q^{9+7n} - 3q^{10+7n} \\
& + q^{11+7n} - 3q^{12+7n} + 6q^{13+7n} + q^{14+7n} - 3q^{15+7n} + 7q^{16+7n} + q^{5+8n} - 18q^{6+8n} \\
& - 31q^{7+8n} - 7q^{8+8n} - 47q^{9+8n} - 37q^{10+8n} - 37q^{11+8n} - 47q^{12+8n} - 7q^{13+8n} \\
& - 31q^{14+8n} - 18q^{15+8n} + q^{16+8n} - 8q^{5+9n} - 18q^{6+9n} + 4q^{7+9n} - 18q^{8+9n} - 12q^{9+9n} \\
& - 8q^{10+9n} - 12q^{11+9n} - 18q^{12+9n} + 4q^{13+9n} - 18q^{14+9n} - 8q^{15+9n} - 9q^{4+10n} \\
& - 8q^{5+10n} + 9q^{6+10n} - 7q^{7+10n} + 13q^{8+10n} + 13q^{9+10n} + 13q^{10+10n} + 13q^{11+10n} \\
& - 7q^{12+10n} + 9q^{13+10n} - 8q^{14+10n} - 9q^{15+10n} - 4q^{3+11n} - 2q^{4+11n} - q^{5+11n} \\
& - 13q^{6+11n} - 24q^{7+11n} + 2q^{8+11n} - 43q^{9+11n} + 2q^{10+11n} - 24q^{11+11n} - 13q^{12+11n} \\
& - q^{13+11n} - 2q^{14+11n} - 4q^{15+11n} + 11q^{3+12n} + 31q^{4+12n} + 21q^{5+12n} + 44q^{6+12n} \\
& + 53q^{7+12n} + 56q^{8+12n} + 56q^{9+12n} + 53q^{10+12n} + 44q^{11+12n} + 21q^{12+12n} + 31q^{13+12n} \\
& + 11q^{14+12n} - 4q^{2+13n} + 18q^{3+13n} - 12q^{4+13n} - 14q^{5+13n} - 26q^{6+13n} - 40q^{7+13n} \\
& - 36q^{8+13n} - 40q^{9+13n} - 26q^{10+13n} - 14q^{11+13n} - 12q^{12+13n} + 18q^{13+13n} - 4q^{14+13n} \\
& + 11q^{2+14n} + 31q^{3+14n} + 21q^{4+14n} + 44q^{5+14n} + 53q^{6+14n} + 56q^{7+14n} + 56q^{8+14n} \\
& + 53q^{9+14n} + 44q^{10+14n} + 21q^{11+14n} + 31q^{12+14n} + 11q^{13+14n} - 4q^{1+15n} - 2q^{2+15n} \\
& - q^{3+15n} - 13q^{4+15n} - 24q^{5+15n} + 2q^{6+15n} - 43q^{7+15n} + 2q^{8+15n} - 24q^{9+15n} \\
& - 13q^{10+15n} - q^{11+15n} - 2q^{12+15n} - 4q^{13+15n} - 9q^{1+16n} - 8q^{2+16n} + 9q^{3+16n} \\
& - 7q^{4+16n} + 13q^{5+16n} + 13q^{6+16n} + 13q^{7+16n} + 13q^{8+16n} - 7q^{9+16n} + 9q^{10+16n} \\
& - 8q^{11+16n} - 9q^{12+16n} - 8q^{1+17n} - 18q^{2+17n} + 4q^{3+17n} - 18q^{4+17n} - 12q^{5+17n} \\
& - 8q^{6+17n} - 12q^{7+17n} - 18q^{8+17n} + 4q^{9+17n} - 18q^{10+17n} - 8q^{11+17n} - 18q^{1+18n} \\
& - 31q^{2+18n} - 7q^{3+18n} - 47q^{4+18n} - 37q^{5+18n} - 37q^{6+18n} - 47q^{7+18n} - 7q^{8+18n} \\
& - 31q^{9+18n} - 18q^{10+18n} + q^{11+18n} - 3q^{1+19n} + q^{2+19n} + 6q^{3+19n} - 3q^{4+19n} + q^{5+19n} \\
& - 3q^{6+19n} + 6q^{7+19n} + q^{8+19n} - 3q^{9+19n} + 7q^{10+19n} - 3q^{1+20n} - 16q^{2+20n} + 4q^{3+20n} \\
& - 17q^{4+20n} - 17q^{5+20n} + 4q^{6+20n} - 16q^{7+20n} - 3q^{8+20n} + 10q^{9+20n} + 2q^{1+21n} \\
& + 22q^{2+21n} + 36q^{3+21n} + 36q^{5+21n} + 22q^{6+21n} + 2q^{7+21n} + 10q^{8+21n} + 4q^{1+22n} \\
& + 14q^{2+22n} + 13q^{3+22n} + 13q^{4+22n} + 14q^{5+22n} + 4q^{6+22n} + 7q^{7+22n} - 9q^{1+23n} \\
& + q^{2+23n} + 28q^{3+23n} + q^{4+23n} - 9q^{5+23n} + q^{6+23n} - 10q^{1+24n} + 6q^{2+24n} + 6q^{3+24n} \\
& - 10q^{4+24n} - 10q^{1+25n} - 8q^{2+25n} - 10q^{3+25n} - 4q^{1+26n} - 4q^{2+26n})
\end{aligned}$$

$$\begin{aligned}
c_2(q, q^n) = & \frac{1}{q^8} (1 + q^n) (q^2 - q^{3n})^4 (q^4 - q^{3n})^4 (q^2 + q^{2n} + q^{1+n})^4 (-4q + q^{3n} + 6q^{4n} + 4q^{5n} \\
& + 6q^{6n} + q^{7n} - 6q^{1+n} - 4q^{1+2n} - 5q^{1+3n} + q^{2+3n} + 2q^{1+4n} + 6q^{2+4n} - 2q^{1+5n} \\
& + 4q^{2+5n} + 2q^{1+6n} + 6q^{2+6n} - 5q^{1+7n} + q^{2+7n} - 4q^{1+8n} - 6q^{1+9n} - 4q^{1+10n})
\end{aligned}$$

The above recursion can be used to deduce a recursion relation for the sequence $a_n(\zeta)$ at every fixed root of unity ζ , following and illustrating the proof of Theorem 5.5. For example, to obtain the recursion of the sequence $a_n(1)$, use:

$$\begin{aligned}
c_0(q) &= -4((-1+n)^3 n^5 (106 - 230n + 115n^2))(q-1)^{10} + O((q-1)^{11}) \\
c_1(q) &= 4(-1+n)^3 (-1+2n) (-864 + 4470n + 2114n^2 - 51003n^3 \\
&\quad + 120089n^4 - 113505n^5 + 37835n^6) (q-1)^{10} + O((q-1)^{11}) \\
c_2(q) &= -324((8 - 18n + 9n^2)^4 (-9 + 115n^2))(q-1)^{10} + O((q-1)^{11})
\end{aligned}$$

An alternative method to obtain the recursion relation of the sequence $a_n(\zeta)$, using the WZ method, is described in the next section.

5.4.3 The regular 6j-symbol at roots of unity

The regular 6j-symbol corresponds to the labeling $\gamma = (2, 2, 2, 2, 2, 2)$ and set

$$a_n = \langle \triangle, n \gamma \rangle(1), \quad b_n = \langle \triangle, n \gamma \rangle(-1).$$

Equation (5.2) gives

$$a_n = \sum_{k=3n}^{4n} (-1)^k \frac{(k+1)!}{(k-3n)!^4 (4n-k)!^3}.$$

Using the WZ method (implemented in *Mathematica* by [PaRi] and using it as in [GV]) it follows that (a_n) satisfies the recursion relation

$$\begin{aligned} & -81(2+3n)^4(4+3n)^4(451+460n+115n^2)a[n] + \\ & (1+n)^3(3+2n)(319212+1427658n+2578232n^2+2423109n^3+1255139n^4+340515n^5+37835n^6)a[1+n] - \\ & (1+n)^3(2+n)^5(106+230n+115n^2)a[2+n] = 0 \end{aligned}$$

This linear recursion has two complex conjugate formal power series solutions $a_{\pm, n}$ where

$$\begin{aligned} a_{+, n} = & \frac{1}{n^{3/2}}(329 + 460i\sqrt{2})^n \left(1 + \frac{-304 - 31i\sqrt{2}}{576n} + \frac{25879 + 18352i\sqrt{2}}{331776n^2} \right. \\ & + \frac{71176912 + 6323071i\sqrt{2}}{573308928n^3} + \frac{5(-2742864803 - 10265264480i\sqrt{2})}{660451885056n^4} \\ & + \frac{-82823449457840 - 12750219708659i\sqrt{2}}{380420285792256n^5} \\ & \left. + \frac{-61273664686901989 + 213495822835779152i\sqrt{2}}{657366253849018368n^6} + O\left(\frac{1}{n^7}\right) \right) \end{aligned}$$

When $q = -1$, Equation (5.2) and Lemma 5.6 imply that $b_n = 0$ for odd n , and

$$b_{2n} = \sum_{k=3n}^{4n} (-1)^k \frac{k!}{(k-3n)!^4 (4n-k)!^3}.$$

It follows that the sequence (b_{2n}) satisfies the following recursion relation

$$\begin{aligned} & 81(1+3n)^4(2+3n)^4(3822+10779n+11352n^2+5290n^3+920n^4)a[n] - \\ & 4(1+n)^3(41796+522342n+2792052n^2+8292059n^3+15002105n^4+17158765n^5+12460766n^6+5571784n^7+1399895n^8+151340n^9) \\ & a[1+n] + (1+n)^3(2+n)^5(25+265n+1002n^2+1610n^3+920n^4)a[2+n] = 0 \end{aligned}$$

This linear recursion has two complex conjugate formal power series solutions $b_{\pm, 2n}$ where

$$\begin{aligned} b_{+, 2n} = & \frac{1}{n^{5/2}}(329 + 460i\sqrt{2})^n \left(1 + \frac{-472 - 19i\sqrt{2}}{576n} + \frac{105199 + 20632i\sqrt{2}}{331776n^2} \right. \\ & + \frac{22386472 - 9304565i\sqrt{2}}{573308928n^3} + \frac{-30711007135 - 48640734448i\sqrt{2}}{660451885056n^4} \\ & + \frac{-80744339543960 + 2822061829369i\sqrt{2}}{380420285792256n^5} \\ & \left. + \frac{17678244315725891 + 219394408835134568i\sqrt{2}}{657366253849018368n^6} + O\left(\frac{1}{n^7}\right) \right) \end{aligned}$$

Note that the observed growth rate is again in agreement with Conjecture 5.1.

5.5 Open problems

We already discussed Conjecture 5.1 in the introduction, which relates the absolute values of the growth rates at the N -th root to the classical evaluations in a very explicit way. Some evidence for this conjecture was given in Section 5.4. It is tempting to try to extend Conjecture 5.1 to include the actual set of growth rates and not only their absolute value. However, the case of the unknot already shows that the N -th power of the set of growth rates at the N -th root of unity might not coincide or even be included in the set of growth rates at $q = 1$. More precisely the set of growth rates for the unknot at $q = 1$ is $\{-1\}$, while the set of growth rates at $q = -1$ equals $\{1, -1\}$.

As a final open question consider a fixed cubic ribbon graph Γ with edge set $E(\Gamma)$, a complex root of unity ζ , and consider the *generating series*

$$S_{\Gamma, \zeta} = \sum_{\gamma} \langle\langle \Gamma, \gamma \rangle\rangle(\zeta) \prod_{e \in E(\Gamma)} z_e^{\gamma_e} \in \mathbb{Q}(\zeta)[[z_e, e \in E(\Gamma)]]$$

In [GV, Thm.5], we proved that when $\zeta = 1$, $S_{\Gamma, 1}$ is a rational function, i.e., belongs to the field $\mathbb{Q}(z_e, e \in E(\Gamma))$. It was explained in [GV, Thm.6] that the generating series $F_{\Gamma, \gamma, \zeta}$ (5.4) is a diagonal of $S_{\Gamma, \zeta}$, and consequently the rationality of $S_{\Gamma, \zeta}$ implies that $F_{\Gamma, \gamma, \zeta}$ is a G -function. The rationality of $S_{\Gamma, \zeta}$ follows from the so-called *chromatic evaluation* of classical spin networks. For details, see [GV] and also [We]. The chromatic evaluation seems to break down in the case of complex roots of unity.

Question 5.1. *Is it true that for all cubic ribbon graphs Γ and all complex roots of unity, $S_{\Gamma, \zeta}$ is a rational function, i.e., belongs to the field $\mathbb{Q}(\zeta)(z_e, e \in E(\Gamma))$?*

Chapter 6

A cabling formula for the colored Jones polynomial

6.1 Introduction

In this note we study how the unnormalized colored Jones polynomial or quantum sl_2 invariant of a link changes under the operation of cabling. We work with a banded link or ribbon link L so that every component is an embedded annulus. Given a diagram D of a banded link inside an annulus we can construct a satellite of L by embedding D into a component L_i of L . The (r, s) -cabling operation is the special case where we take D to be the closure of the (r, s) -torus braid $B_s^r = (\sigma_1 \cdots \sigma_{s-1})^r$, where $r \in \mathbb{Z}$, $s \in \mathbb{N}$. To turn B_s^r into a banded tangle we use the blackboard framing and add a positive curl to every overpassing arc, see figure 6.1 below. The banded link obtained by (r, s) -cabling the component L_i of a banded link L will be denoted by $L_{i;s}^r$, we will also call it the $(i; r, s)$ -cabling of L .

In order to state our cabling formula we need to introduce the following generalizations of the trinomial (not multinomial) coefficients defined in [And]. For a vector $\mathbf{N} = (n_0, \dots, n_{g-1})$ define $\binom{g}{w}_{\mathbf{N}}$ to be the coefficient of x^w in the expansion of the product $\prod_{k=0}^{g-1} (x^{\frac{N_k-1}{2}} + x^{\frac{N_k-1}{2}-1} + \dots + x^{-\frac{N_k-1}{2}})$.

Theorem 6.1. *Let $g = \gcd(r, s)$, $p = s/g$ and $\mathbf{N} = (N_0, \dots, N_{g-1})$. The unnormalized colored Jones polynomial of the zero framed $(i; r, s)$ -cabling of a banded link L with c components can be expressed as follows:*

$$J_{M_1, \dots, M_{i-1}, \mathbf{N}, \dots, M_c}(L_{i;s}^r)(q) = \prod_{j=1}^g q^{-\frac{rs}{g^2} \frac{N_j^2-1}{4}} \sum_{w=-\frac{|\mathbf{N}|-g}{2}}^{\frac{|\mathbf{N}|-g}{2}} \binom{g}{w}_{\mathbf{N}} q^{\frac{rw(wp+1)}{g}} J_{M_1, \dots, M_{i-1}, 2wp+1, \dots, M_c}(L)(q)$$

In the statement of the theorem we have used the notation $|\mathbf{N}| = N_0 + \dots + N_{g-1}$ and the convention that $J_{M_1, \dots, M_{i-1}, -j, \dots, M_c}(L)(q) = -J_{M_1, \dots, M_{i-1}, j, \dots, M_c}(L)(q)$. In the case where $g = 1$ and L is the unknot the above cabling formula agrees with Morton's formula for the (r, s) -torus knot [Mo], where his variables are

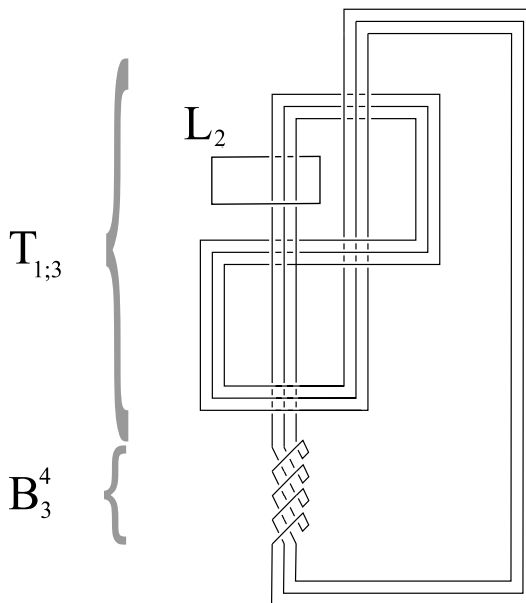


Figure 6.1: We have drawn the link $L_{1,3}^4$, the $(1; 3, 4)$ -cabling of $L = (L_1, L_2)$, where L_1 is the figure eight knot and L_2 is an unknot. We have indicated the torus braid B_3^4 and the opened tangle $T_{1,3}$ mentioned in section 2.

related to ours as $s^2 = q, m = r, p = s$. The case of a $(r, 2)$ -cabling is also known [Zh]. In all other cases our formula seems to be new.

Our main motivation for proving such a formula is to verify the volume conjecture [Ka2],[MM] in the cases where cabling is involved. The volume conjecture states that the normalized colored Jones polynomial $J'(L)$ of a link L determines the simplicial volume of the link complement as follows:

$$\lim_{N \rightarrow \infty} \frac{2\pi}{N} |J'_{N,N,\dots,N}(L)(e^{\frac{2\pi i}{N}})| = \text{Vol}(\mathbb{S}^3 - L)$$

As a corollary to our cabling formula we will prove the volume conjecture for all knots and links whose complement has zero simplicial volume in the following sense. We give a polynomial upper bound for the growth rate. The full volume conjecture would also include a lower bound. We can apply the cabling formula to this class of knots because it is shown in [Go] that all such links can be obtained from the unknot by repeated cabling and connected sum. Using the cabling formula we can therefore in principle write down the colored Jones polynomial of any such link.

Corollary 6.1. *For all links L of volume zero, $J_N(L)(e^{\frac{2\pi i}{N}}) = \mathcal{O}(N^c)$ as $N \rightarrow \infty$ for some c depending on L .*

So far the only zero volume and links for which the volume conjecture has been proven are the torus knots [KT] and the $(2, s)$ -torus links [Zh], [Hi2]. The cabling formula of Theorem 6.1 makes it possible to conduct a detailed study

of cabled knots and iterated cabling. In the context of the volume conjecture some natural questions would be the following:

Question 6.1. *Is the volume conjecture stable under cabling?*

Since cabling does not contribute to the simplicial volume this would mean that the existing exponential growth is unchanged under cabling.

Question 6.2. *What is the exact asymptotic expansion for a zero volume link?*

In [KT] and [DK] explicit asymptotic expansions are given in the case torus knots at the N -th root of unity. Away from the root of unity the asymptotics of torus knots has also been studied in the context of the generalized volume conjecture [MG]. It would be especially interesting to see whether the polynomial growth related to the roots of the Alexander polynomial predicted and studied in [Mh] persists.

Question 6.3. *How is the colored Jones polynomial of a zero volume link related to q -series identities?*

In the case of torus knots and and some special torus links K. Hikami has shown many interesting relations between colored Jones polynomials, modular forms and q -series [Hi1], [Hi2].

Question 6.4. *What is the behavior of the non-commutative A -polynomial of a knot under cabling?*

It is known [GaLe] that the colored Jones polynomial satisfies a linear recursion relation. This relation can be encoded in a two variable polynomial with q -coefficients called the non-commutative A -polynomial and it is conjectured [Ga0] to be related to the character variety of the knot group. The knot group behaves well under cabling and according to our cabling formula so does the colored Jones polynomial. It would be interesting to see how these two relate. As before the zero volume knots provide many cases where explicit computations can be made. So far these have only been done for torus knots [Hi1].

An investigation of these questions will be postponed to a subsequent publication.

Acknowledgment I would like to thank the organizers of the International Conference on Quantum topology 2007 in Hanoi for providing the atmosphere that got this paper started and Norbert A'Campo, Stavros Garoufalidis, Thang Le and Hitoshi Murakami for stimulating conversations.

6.2 Proof of the cabling formula

Let us fix a banded link L with c components L_1, \dots, L_c . Choosing a component L_i of L and opening it up we can write L as the closure of a banded $(1, 1)$ -tangle T_i . Define $T_{i,s}$ to be the banded (s, s) -tangle obtained from T_i by replacing the opened component L_i of T_i by s parallel bands. In terms of these tangles the $(i; r, s)$ -cabling of L is equal to the closure of the composition $T_{i,s} \circ B_s^r$, see also figure 6.1.

Note that the link $L_{i;s}^r$ has $c + g - 1$ components, where $g = \gcd(r, s)$, since the component L_i of L is replaced by the g -component torus link that is the closure of B_s^r . If we number the strands of the braid B_s^r starting at 0 then two strands are in the same component of the closure if and only if their numbers are congruent modulo g . Therefore each component of the closed braid consists of $p = s/g$ strands. Let us suppose that our link $L_{i;s}^r$ is colored by the integers $(M_1, \dots, M_{i-1}, \mathbf{N}, \dots, M_c)$, where the vector $\mathbf{N} = (N_0, \dots, N_{g-1})$ represents the new colors used to color the components of the torus link that replaces the component L_i .

We denote the the N -dimensional irreducible representation of quantum sl_2 by V_N . Using the above coloring, the torus braid corresponds to a morphism from $V = \bigotimes_{k=0}^{s-1} V_{N_k \bmod g}$ to itself. In terms of these morphisms we can now state that the unnormalized $(M_1, \dots, M_{i-1}, \mathbf{N}, \dots, M_c)$ -colored Jones polynomial of the $(i; r, s)$ -cabling of L (abbreviated by J) is the following quantum trace:

$$J = J_{M_1, \dots, M_{i-1}, \mathbf{N}, \dots, M_c}(L_{i;s}^r) = \text{Tr}_q(B_s^r \circ T_{i;s}, V) \quad (6.1)$$

The first step in calculating this trace is to expand it using the isotypical decomposition of the tensor product as quantum sl_2 representations:

$$V = \bigotimes_{k=0}^{s-1} V_{N_k \bmod g} \cong \bigoplus_{j=1}^{p|\mathbf{N}|-s+1} \text{Hom}(V_j, V) \otimes V_j \quad (6.2)$$

The range of the summation is calculated by the Clebsch-Gordan rule [Pr]. The isomorphism maps $(\alpha_j \otimes v)$ on the right to $\alpha_j(v)$ and $B_s^r \circ T_{i;s}$ acts on $\text{Hom}(V_j, V)$ only, while quantum sl_2 acts on the V_j only. We can therefore expand the quantum trace in (6.1) as follows:

$$J = \text{Tr}_q(B_s^r \circ T_{i;s}, V) = \sum_j \text{Tr}(B_s^r \circ T_{i;s}, \text{Hom}(V_j, V)) \text{Tr}_q(\text{Id}, V_j) \quad (6.3)$$

We know that $\text{Tr}_q(\text{Id}, V_j) = [j] = (q^{j/2} - q^{-j/2}) / (q^{1/2} - q^{-1/2})$. To calculate the other traces we study how $B_s^r \circ T_{i;s}$ acts on an element $\alpha \in \text{Hom}(V_j, V)$. The action is by composition so first we look at $T_{i;s} \circ \alpha$, the action of $T_{i;s}$. According to the graphical calculus [Tu] the colored tangle $T_{i;s}$ represents the same map as the $(1, 1)$ -tangle T_i colored with V . Furthermore we can depict α as a coupon connecting the top of a vertical strand colored V_j to the lower end of T_i (this end is colored V), see figure 6.2.

Now we can slide the coupon α up along the $(1, 1)$ -tangle T_i . We obtain α on top of T_i , where T_i is now colored with V_j . Since V_j is irreducible, the operator represented by T_i is multiplication by a scalar. By closing T_i one sees that this scalar is exactly $[j]^{-1} J_{M_1, \dots, M_{i-1}, j, \dots, M_c}(L)$. We conclude that $T_{i;s} \circ \alpha = [j]^{-1} J_{M_1, \dots, M_{i-1}, j, \dots, M_c}(L) \alpha$. The above argument shows that $B_s^r \circ T_{i;s} \circ \alpha = [j]^{-1} J_{M_1, \dots, M_{i-1}, j, \dots, M_c}(L) B_s^r \circ \alpha$. Therefore equation (6.3) becomes:

$$J = \sum_{j=1}^{p|\mathbf{N}|-s+1} \text{Tr}(B_s^r, \text{Hom}(V_j, V)) J_{M_1, \dots, M_{i-1}, j, \dots, M_c}(L) \quad (6.4)$$

Note that an equation such as (6.4) remains valid when one replaces B_s^r by any braid B . Such a satellite formula also appears in [MS].

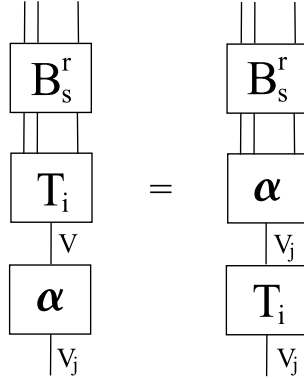


Figure 6.2: Sliding the coupon α up through the tangle $T_{i,s}$.

We now concentrate on calculating the trace $\text{Tr}(B_s^r, \text{Hom}(V_j, V))$. Note that $(B_s^r)^s = ((\sigma_1 \cdots \sigma_{s-1})^s)^r$ is a central element of the braid group. The element $C = (\sigma_1 \cdots \sigma_{s-1})^s$ can also be thought of as a curl in s parallel strands (hence the extra curls in the definition of B_s^r), so it acts on α as $C \circ \alpha = q^{\frac{j^2-1}{4}} \alpha$. If we set $D = q^{-\frac{r}{s} \frac{j^2-1}{4}} B_s^r$, then D^s acts as the identity on $\text{Hom}(V_j, V)$. An argument by Jones and Rosso [JR] shows that its trace does not depend on q . For the record we express the trace we were looking for in terms of D :

$$\text{Tr}(B_s^r, \text{Hom}(V_j, V)) = q^{\frac{r}{s} \frac{j^2-1}{4}} \text{Tr}(D, \text{Hom}(V_j, V)) \quad (6.5)$$

Since the trace of D does not depend on q we can calculate it at $q = 1$. In this case $B_s^r = D$ equals the permutation $(\sigma_1 \cdots \sigma_{s-1})^r$ and the representation V can be viewed as an $SL(2)$ representation. By collecting common factors in the tensor product we see that $V \cong \bigotimes_{k=0}^{g-1} V_{N_k}^{\otimes p}$, where $p = s/g$. Note that our permutation D acts on V by permuting the factors inside each tensor power. More precisely $D = c_0 \cdots c_{g-1}$ where the c_k are disjoint p -cycles and c_k permutes the factors of $V_{N_k}^{\otimes p}$. We can therefore interpret D as an element of the Cartesian product S_p^g .

One can view each of the tensor powers $V_{N_k}^{\otimes p}$ as a $S_p \times GL(V_{N_k})$ representation, where S_p acts by permuting the tensor factors and $GL(V_{N_k})$ acts diagonally. By Schur-Weyl duality [Pr] this space allows a simultaneous decomposition into irreducibles:

$$V_{N_k}^{\otimes p} \cong \bigoplus_{\lambda_k \vdash p} E_{\lambda_k} \otimes W_{\lambda_k}$$

Here E_{λ_k} is an irreducible S_p representation and W_{λ_k} is an irreducible $GL(V_{N_k})$ representation and the sum is over all partitions of length no more than N_k . Taking the tensor product over all such powers and rearranging the factors gives the following decomposition of V as an $S_p^g \times GL(V_{N_0}) \times \cdots \times GL(V_{N_{g-1}})$ representation.

$$V \cong \bigoplus_{\lambda_0 \cdots \lambda_{g-1} \vdash p} E_{\lambda_0} \otimes \cdots \otimes E_{\lambda_{g-1}} \otimes W_{\lambda_0} \otimes \cdots \otimes W_{\lambda_{g-1}}$$

The $GL(V_{N_0}) \times \cdots \times GL(V_{N_{g-1}})$ representation $W_{\lambda_0} \otimes \cdots \otimes W_{\lambda_{g-1}}$ is in a natural way also an $SL(2)$ -representation. We can therefore decompose it into irreducible $SL(2)$ -representation as follows:

$$W_{\lambda_0} \otimes \cdots \otimes W_{\lambda_{g-1}} \cong \bigoplus_j \text{Hom}(V_j, W_{\lambda_0} \otimes \cdots \otimes W_{\lambda_{g-1}}) \otimes V_j$$

Hence we find the following decomposition of V :

$$V \cong \bigoplus_j \left(\bigoplus_{\lambda_0 \dots \lambda_{g-1} \vdash p} E_{\lambda_0} \otimes \cdots \otimes E_{\lambda_{g-1}} \otimes \text{Hom}(V_j, W_{\lambda_0} \otimes \cdots \otimes W_{\lambda_{g-1}}) \right) \otimes V_j$$

Note that we only allow λ_k to have length $\leq N_k$. Comparing this decomposition with the isotypical decomposition (6.2) for $q = 1$ we see that:

$$\text{Hom}(V_j, V) \cong \bigoplus_{\lambda_0 \dots \lambda_{g-1} \vdash p} E_{\lambda_0} \otimes \cdots \otimes E_{\lambda_{g-1}} \otimes \text{Hom}(V_j, W_{\lambda_0} \otimes \cdots \otimes W_{\lambda_{g-1}}) \quad (6.6)$$

The action of D on this space is only on the E_{λ_k} . As above we write $D = c_0 \cdots c_{g-1}$ as a product of disjoint p -cycles and we note that the cycle c_k acts in E_{λ_k} . If we define $R_{j, \lambda_0, \dots, \lambda_{g-1}} = \dim(\text{Hom}(V_j, W_{\lambda_0} \otimes \cdots \otimes W_{\lambda_{g-1}}))$ and denote all c_k by c we have the following expression for the trace:

$$\text{Tr}(D, \text{Hom}(V_j, V)) = \sum_{\lambda_0, \dots, \lambda_{g-1} \vdash p} \chi_{\lambda_0}(c) \cdots \chi_{\lambda_{g-1}}(c) R_{j, \lambda_0, \dots, \lambda_{g-1}} \quad (6.7)$$

Here χ_λ is the character of the symmetric group S_p . To calculate these traces we note that the dimensions $R_{j, \lambda_0, \dots, \lambda_{g-1}}$ are encoded in the following product expansion of Schur functions:

$$\prod_{k=0}^{g-1} s_{\lambda_k}(t^{N_k-1}, t^{N_k-3}, \dots, t^{-N_k+1}) = \sum_{\mu \vdash p|\mathbf{N}|-s} R_{\mu_1-\mu_2+1, \lambda_0, \dots, \lambda_{g-1}} s_\mu(t, t^{-1}) \quad (6.8)$$

To see why this is true we consider the simple case where $g = 1$. Let (ρ_N, V_N) be the N dimensional irreducible $SL(2)$ representation, let $(\phi_\lambda, W_\lambda)$ be an irreducible $GL(V_N)$ representation indexed by λ and let (ψ_μ, V_μ) be an irreducible $SL(2)$ representation indexed by a two part partition μ . We will prove that we have the following equation, leaving the case for general g to the reader.

$$s_\lambda(t^{N-1}, t^{N-3}, \dots, t^{-N+1}) = \sum_{\mu} \dim(\text{Hom}(\psi_\mu, \phi_\lambda)) s_\mu(t, t^{-1})$$

Proof. (of the claim) We know that $s_\lambda(t_1, \dots, t_N) = \text{Tr} \phi_\lambda(\text{diag}(t_1, \dots, t_N))$. That is the Schur function is the character of the irreducible GLV representation on the diagonal elements. Note that $\text{diag}(t^{N-1}, t^{N-3}, \dots, t^{-N+1}) = \rho_N(\text{diag}(t, t^{-1}))$. Therefore we can write the left hand side of the equation

as $s_\lambda(t^{N-1}, t^{N-3}, \dots, t^{-N+1}) = \text{Tr}(\phi_\lambda \circ \rho_N)(\text{diag}(t, t^{-1}))$. Now decomposing the $\text{SL}(2)$ representation $\phi_\lambda \circ \rho_N$ into irreducibles we get:

$$\phi_\lambda \circ \rho_N = \bigoplus_{\mu} \text{Hom}(\psi_\mu, \phi_\lambda) \otimes \psi_\mu$$

In this decomposition we get

$$\text{Tr}(\phi_\lambda \circ \rho_N)(\text{diag}(t, t^{-1})) = \sum_{\mu} \dim(\text{Hom}(\psi_\mu, \phi_\lambda)) \text{Tr} \psi_\mu(\text{diag}(t, t^{-1}))$$

Since $\text{Tr} \psi_\mu(\text{diag}(t, t^{-1})) = s_\mu(t, t^{-1})$ the proof is finished. \triangleleft

The above condition on the direct sum in (6.6) that the length of λ_k is no more than N_k is now incorporated into the Schur functions, because an N -variable Schur function s_λ is nonzero only if λ has no more than N parts.

As a quick check that the above formula (6.8) includes all the dimensions R , note that $\lambda_k \vdash p$ and so the highest degree term of $s_\lambda(t^{N_k-1}, t^{N_k-3}, \dots, t^{-N_k+1})$ is t^{pN_k-p} , hence $\mu \vdash p|\mathbf{N}| - s$ because the highest degree term of $s_\mu(t, t^{-1})$ is t^{μ_1} . Note also that only length-two partitions μ contribute to the sum because the Schur functions s_μ have only two variables. In case $\mu = (\mu_1 \mu_2)$ we have $s_\mu(x, y) = \frac{x^{\mu_1+1}y^{\mu_2} - x^{\mu_2}y^{\mu_1+1}}{x-y}$ and $s_\mu(t, t^{-1}) = \frac{t^{\mu_1+1-\mu_2} - t^{-(\mu_1+1-\mu_2)}}{t-t^{-1}}$. The range of the summation in (6.8) therefore agrees exactly with the range of j in the decomposition of the tensor product (6.2). From now on we will parameterize this range by two part partitions $\mu \vdash p|\mathbf{N}| - s$ and set $V_\mu = V_j$, where $j = \mu_1 - \mu_2 + 1$.

Using the product of Schur functions in (6.8) as a generating function for the dimensions R we can compute $\text{Tr}(D, \text{Hom}(V_\mu, V))$ simultaneously for all μ . First we sum the right hand side and the left hand side of equation (6.8) with the characters as in the sum in (6.7):

$$\sum_{\mu \vdash |\mathbf{N}| - s} \left(\sum_{\lambda_0, \dots, \lambda_{g-1} \vdash p} \chi_{\lambda_0}(c) \cdots \chi_{\lambda_{g-1}}(c) R_{\mu, \lambda_0, \dots, \lambda_{g-1}} \right) s_\mu(t, t^{-1}) = \quad (6.9)$$

$$\begin{aligned} & \sum_{\lambda_0, \dots, \lambda_{g-1} \vdash p} \chi_{\lambda_0}(c) \cdots \chi_{\lambda_{g-1}}(c) \prod_{k=0}^{g-1} s_{\lambda_k}(t^{N_k-1}, t^{N_k-3}, \dots, t^{-N_k+1}) = \\ & \prod_{k=0}^{g-1} \sum_{\lambda_k \vdash p} \chi_{\lambda_k}(c) s_{\lambda_k}(t^{N_k-1}, t^{N_k-3}, \dots, t^{-N_k+1}) = \\ & \prod_{k=0}^{g-1} p_p(t^{N_k-1}, t^{N_k-3}, \dots, t^{-N_k+1}) \end{aligned} \quad (6.10)$$

In the last line we used the expansion of the power sum function p_p in terms of Schur functions [Mac] p.114. We can use the notion of plethysm [Mac] p.138 to write the power sums in terms of the complete symmetric functions h as follows:

$$p_p(t^{N_k-1}, t^{N_k-3}, \dots, t^{-N_k+1}) = (p_p \circ h_{N_k-1})(t, t^{-1}) = h_{N_k-1}(t^p, t^{-p})$$

As with partitions we define $h_{\mathbf{N}-1} = \prod_{k=0}^{g-1} h_{N_k-1}$ so that we can write the above product (6.10) as:

$$\prod_{k=0}^{g-1} p_p(t^{N_k-1}, t^{N_k-3}, \dots, t^{-N_k+1}) = h_{\mathbf{N}-1}(t^p, t^{-p}) \quad (6.11)$$

Comparing equations (6.9) and (6.11) we see that to compute the traces in (6.7) we need to express $h_{\mathbf{N}-1}(t^p, t^{-p})$ in terms of the $s_\mu(t, t^{-1})$. The coefficients in this expansion will be our traces.

First we consider the case where $p = 1$. Since we have $s = g$ there are $\lfloor (|\mathbf{N}| - g)/2 \rfloor + 1$ two part partitions $\mu \vdash |\mathbf{N}| - s$, that we will number by the half integers $w = (\mu_1 - \mu_2)/2$. Since $h_{\mathbf{N}-1}(t, t^{-1})$ is a product of geometric series we can use the notation defined in the introduction to write: $h_{\mathbf{N}-1}(t, t^{-1}) =$

$$\sum_{w=(|\mathbf{N}-g)/2-\lfloor (|\mathbf{N}-g)/2 \rfloor}^{(|\mathbf{N}-g)/2} \left(\binom{g}{w}_{\mathbf{N}} - \binom{g}{w+1}_{\mathbf{N}} \right) \frac{t^{2w+1} - t^{-2w-1}}{t - t^{-1}} \quad (6.12)$$

The above equation settles the case $p = 1$ since the Schur functions are exactly the geometric series in the two variable case. We will come back to the $p = 1$ case after we have found the coefficients for $p > 1$. We will then show that these cases can be unified into a single cabling formula for the colored Jones polynomial.

From now on let's assume that $p \geq 2$. We will carry out the expansion of $h_{\mathbf{N}-1}(t^p, t^{-p})$ into two variable Schur functions in a little more generality by setting $x_1 = t$ and $x_2 = t^{-1}$. As a first step consider the following fundamental identity [Mac] p.62 relating the complete symmetric functions to the Schur functions:

$$\sum_{\lambda} h_{\lambda}(x) m_{\lambda}(y) = \prod_{i,j} (1 - x_i y_j)^{-1} = \sum_{\lambda} s_{\lambda}(x) s_{\lambda}(y) \quad (6.13)$$

Here $m_{\lambda}(y)$ is the monomial symmetric function and $x = (x_1, x_2, \dots)$ and the sums range over all partitions λ . The first part of the identity (6.13) implies that $h_{\mathbf{N}-1}(x_1^p, x_2^p)$ is the coefficient of $\mathbf{y}^{p(\mathbf{N}-1)} = y_0^{p(N_0-1)} \dots y_{g-1}^{p(N_{g-1}-1)}$ in the expansion of the product $\prod_{k=0}^{g-1} (1 - x_1^p y_k^p)^{-1} (1 - x_2^p y_k^p)^{-1}$. Factoring we can also write this product as $\prod_{k=0}^{g-1} \prod_{u=0}^{p-1} (1 - x_1 \omega^u y_k)^{-1} (1 - x_2 \omega^u y_k)^{-1}$, where $\omega = \exp(2\pi i/p)$. Using the second half of the identity (6.13) we can expand the same product into two variable Schur functions:

$$\prod_{k=0}^{g-1} \prod_{u=0}^{p-1} (1 - x_1 \omega^u y_k)^{-1} (1 - x_2 \omega^u y_k)^{-1} = \sum_{\mu} s_{\mu}(y_0, \omega y_0, \dots, \omega^{p-1} y_{g-1}) s_{\mu}(x_1, x_2)$$

Taking the coefficient of $\mathbf{y}^{p(\mathbf{N}-1)}$ on the left gives $h_{\mathbf{N}-1}(x_1^p, x_2^p)$ back, while the coefficient of $\mathbf{y}^{p(\mathbf{N}-1)}$ on the right hand side is $\sum_{\mu} K_{\mu} s_{\mu}(x_1, x_2)$, where K_{μ} is the coefficient of $\mathbf{y}^{p(\mathbf{N}-1)}$ in $s_{\mu}(y_0, \omega y_0, \dots, \omega^{p-1} y_{g-1})$. It follows that the trace we wanted to calculate is equal to this coefficient: $\text{Tr}(D, \text{Hom}(V_{\mu}, V)) = K_{\mu}$.

We proceed with the calculation of K_{μ} . By [Mac] p.72 we can expand the Schur function $s_{\mu}(y_0, \omega y_0, \dots, \omega^{p-1} y_{g-1})$ in terms of skew Schur functions mak-

ing it possible to extract the powers of y_j .

$$s_\mu(y_0, \omega y_0, \dots, \omega^{p-1} y_{g-1}) = \sum \prod_{j=0}^{g-1} y_j^{|\nu^{(j)} - \nu^{(j-1)}|} s_{\nu^{(j)}/\nu^{(j-1)}}(1, \omega, \dots, \omega^{p-1})$$

The sum ranges over all sequences of partitions $0 = \nu^{(0)} \subset \nu^{(1)} \dots \subset \nu^{(g)} = \mu$. Only the sequences of partitions satisfying $|\nu^{(j)} - \nu^{(j-1)}| = p(N_j - 1)$ contribute to the coefficient of $\mathbf{y}^{p(\mathbf{N}-1)}$ in this sum. The contribution of such a sequence is $\prod_{j=0}^{g-1} s_{\nu^{(j)}/\nu^{(j-1)}}(1, \omega, \dots, \omega^{p-1})$. In the cases we are interested in μ has length 2 and it follows from [Mac] p.91 that this contribution is zero unless $\nu^{(j)}$ can be obtained from $\nu^{(j-1)}$ by attaching $N_j - 1$ border strips of length p . A set theoretical difference between two nested partitions is called a border strip of length p if it is connected, does not contain any 2×2 squares and has p elements. If this is the case for all j , then the contribution is $\sigma_p(\mu) = (-1)^{r_2}$, where $0 \leq r_2 < p$ is the residue of μ_2 modulo p .

The above argument shows that $K_\mu = \sigma_p(\mu)|K_\mu|$, and that $|K_\mu|$ is the number of sequences of partitions $0 = \nu^{(0)} \subset \nu^{(1)} \dots \subset \nu^{(g)} = \mu$ satisfying the condition that $\nu^{(j)}$ is obtained from $\nu^{(j-1)}$ by attaching $N_j - 1$ border strips of length p .

To count the number of such sequences we first look at all ways of constructing two part partitions by attaching length p -border strips, starting with the empty partition. One notices that the lower leftmost corner of a new border strip can be attached at exactly two places: either the end of the first row or the end of the second row. It follows that we can list all possibilities in a Pascal-like triangle, see figure 6.2.

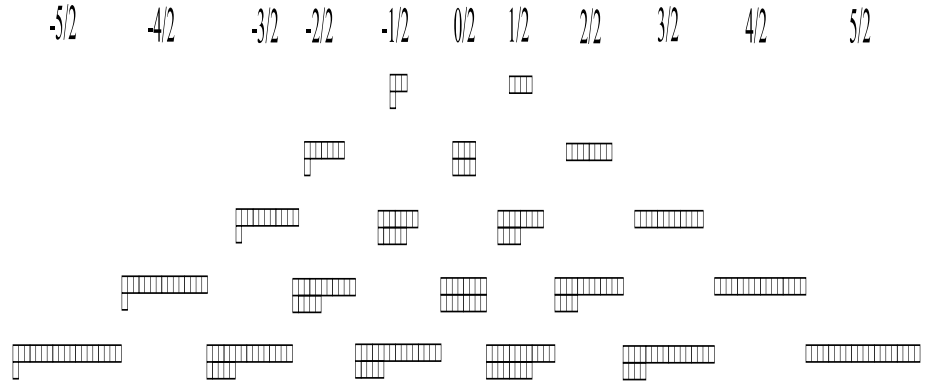


Figure 6.3: The Pascal-like triangle of all two part partitions that can be glued from 5 or less border strips of length $p = 4$.

The k -th row of our Pascal triangle contains $k + 1$ partitions that we index by the half integers $\frac{-k}{2}, \frac{-k}{2} + 1, \dots, \frac{k}{2}$. The triangle is ordered such that if μ has index $w(\mu) = w$ then $\mu_1 - \mu_2 + 1 = \text{sgn}(w)(2wp + 1)$ and $\text{sgn}(w) = \sigma_p(\mu)$, provided that we agree that $\text{sgn}(0) = 1$.

Interpreting $|K_\mu|$ in terms of the Pascal triangle we see that $|K_\mu|$ is equal to the number of ways to move from the (empty) top of the triangle to $\mu \vdash p|\mathbf{N}| - s$ in g steps of length $N_k - 1$, for $k = 0 \dots, g - 1$. A step of length A can go in $A + 1$

directions that are conveniently indexed by $\frac{-A}{2}, \frac{-A}{2} + 1, \dots, \frac{A}{2}$. The sum of these indices must be the index of μ , that is w . Therefore the number of ways is exactly the coefficient of x^w in the product $\prod_{k=0}^{g-1} (x^{-\frac{N_k-1}{2}} + x^{-\frac{N_k-1}{2}+1} + \dots + x^{\frac{N_k-1}{2}})$. Using the notation defined in the introduction we see that $|K_\mu| = \binom{g}{w}_{\mathbf{N}}$ and so $K_\mu = \text{sgn}(w) \binom{g}{w}_{\mathbf{N}}$.

We can now summarize the calculation of $J = J_{M_1, \dots, M_{i-1}, \mathbf{N}, \dots, M_c}(L_{i;s}^r)$ as follows. First we expressed it in equation (6.4) as a sum over the colors j of a trace times the colored Jones of the uncabled link. In (6.5) the dependence on q was extracted and finally the rest of the trace was shown to be given by the coefficients in equation (6.12) for $p = 1$ and by K_μ for $p \geq 2$. Along the way we changed the sum over colors into a sum over two part partitions μ , via $j = \mu_1 - \mu_2 + 1$. We just saw that we can enumerate the μ for which K_μ is nonzero by the half integers w . Combining all this we find for $p \geq 2$: $J_{M_1, \dots, M_{i-1}, \mathbf{N}, \dots, M_c}(L_{i;s}^r) =$

$$\sum_{w=-(|\mathbf{N}|-g)/2}^{(|\mathbf{N}|-g)/2} q^{\frac{rwp(wp+1)}{s}} \text{sgn}(w) \binom{g}{w}_{\mathbf{N}} J_{M_1, \dots, M_{i-1}, |2wp+1|, \dots, M_c}(L)$$

Remarkably this formula is also valid for $p = 1$. In this case the non-negative w run through all partitions and both w and $-(w+1)$ contribute to the same term $J_{M_1, \dots, M_{i-1}, |2w+1|, \dots, M_c}(L)$, thus producing the coefficients found in (6.12).

Finally the convention $J_{M_1, \dots, M_{i-1}, -k, \dots, M_c} = -J_{M_1, \dots, M_{i-1}, k, \dots, M_c}$ allows us to incorporate the sign into the colored Jones polynomial because $\text{sgn}(w) = \text{sgn}(2wp+1)$. Noting that $p = s/g$ the proof of Theorem 6.1 is complete.

6.3 Application to the volume conjecture

As an application of the cabling formula we just proved we will show that the volume conjecture holds true for all zero volume knots and links (Corollary 6.1) in the sense that we have an upperbound on the growth rate that is polynomial in N .

Theorem 6.2. *For all links L of volume zero, $J_N(L)(e^{\frac{2\pi i}{N}}) = \mathcal{O}(N^c)$ as $N \rightarrow \infty$ for some c depending on L .*

Proof. The zero volume links are related to cabling by the fact that all links of zero simplicial volume are obtained from the unknot by repeated cabling and connected sum [Go].

In the volume conjecture the usual normalization of the colored Jones polynomial for knots is to divide by the value of the unknot. However, if a link has s split components then the unnormalized Jones has at least an s fold zero at the N -th root of unity [V2]. We therefore choose to normalize it by dividing by $[N]^s$. For convenience we work with $A = q^{1/4}$ instead of q so that for the volume conjecture we need to evaluate at $A = e^{\pi i/2N}$.

The unnormalized colored Jones polynomial of a link with c components is a multi-sequence of Laurent polynomials in A of the form $P_{\mathbf{N}}(A) = \sum_j a_{j,\mathbf{N}} A^j$, where $\mathbf{N} = (N_1, \dots, N_c)$. We say that a multi-sequence is moderate if there exist $C, m > 0$ such that

$$\forall \mathbf{N} : \quad |\max \deg P_{\mathbf{N}}|, |\min \deg P_{\mathbf{N}}|, |a_{j,\mathbf{N}}| < C |\mathbf{N}|^m$$

It is clear that the set of moderate sequences is closed under products and differentiation with respect to A .

To prove the volume conjecture for all zero volume links we first show that their unnormalized colored Jones polynomials are moderate. Since such links are obtained from the unknot by repeated cabling and connected sum, we first need to show that $[N]$ is moderate (trivial). To deal with connected sum, note that $J_{\mathbf{N}}(K\#L) = \frac{J_{\mathbf{N}}(K)J_{\mathbf{N}}(L)}{[N_c]}$, where N_c is the color of the component on which we apply the connected sum. Here we already know that the product in the numerator is divisible by $[N_c]$ because both factors are. Hence we only need to check that if $[N]P$ is moderate, then so is P . This follows from the fact that $[N]$ is a finite geometric series. Finally we need to show that the set of moderate multi-sequences is closed under taking products and under an operation that generalizes cabling of links that we now define. Given two multi-sequences $P_{\mathbf{M}}(A)$ and $Q_{\mathbf{N},w}(A)$ define a new multi-sequence R by

$$R_{M_1, \dots, M_{i-1}, \mathbf{N}, \dots, M_c}(A) = \sum_{|w| \leq (|\mathbf{N}| - g)/2} Q_{\mathbf{N}, 2w}(A) P_{M_1, \dots, M_{i-1}, |2w|+1, \dots, M_c}(A)$$

The triangle inequality shows that that if P and Q are moderate then so is R . The cabling formula applied to the colored Jones polynomial J of any link is an example of the above defined operation where $P = J$ and $Q_{\mathbf{N},w}(A)$ is a multi-sequence that does not depend on the link and is readily read off from the cabling formula or rather the version at the end of the last section. It is not hard to see that this Q is indeed moderate.

Now that we know that the unnormalized colored Jones polynomial of a zero volume knot $J_{\mathbf{N}}(A)$ is moderate we conclude the proof of corollary 1 as follows. To evaluate the normalized Jones polynomial we will use 'l Hospital's rule after writing it as

$$J_{N, \dots, N}(A)/[N]^s = \tilde{J}_{N, \dots, N}(A)/(A^{2N} - A^{-2N})^s$$

where $\tilde{J} = (A^2 - A^{-2})^s J$ is again moderate. If we differentiate both numerator and denominator s times with respect to A and evaluate at $e^{\pi i/2N}$ we get $(\frac{e^{\pi i/2N}}{-4N}) \frac{d^s}{dA^s} \tilde{J}_{N, \dots, N}(e^{\pi i/2N})$. Since $\frac{d^s}{dA^s} \tilde{J}_{\mathbf{N}}$ is again moderate, it follows that:

$$\lim_{N \rightarrow \infty} \frac{2\pi}{N} \left| \frac{J_{N, \dots, N}}{[N]^k} (e^{\frac{\pi i}{2N}}) \right| = 0$$

△

Chapter 7

Samenvatting

Waarschuwing. In een oprechte poging om de materie van dit proefschrift op een toegankelijke manier over het voetlicht te brengen heb ik de waarheid hier en daar geweld aangedaan.

In deze samenvatting wil ik een informele indruk geven van vier thema's die ten grondslag liggen aan mijn proefschrift. Namelijk: kristallen, het roeren van melk in een kopje koffie, het rekenen met plaatjes, en de kwantumcomputer. Ik zal aangeven hoe deze vier allemaal op hun eigen manier passen binnen het hoofdonderwerp van het proefschrift: de wiskunde van knopen en vlechten.

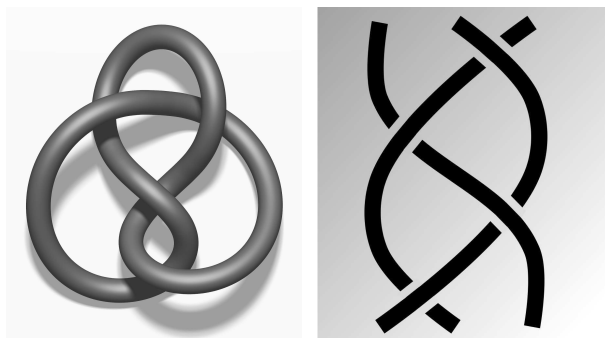


Figure 7.1: De achtknoop (links) en zijn bijbehorende vlecht (rechts).

Hieronder zal ik uitleggen hoe we de knoop uit het plaatje hierboven op vier verschillende manieren kunnen interpreteren: Als een kristal, als een stroming in een vloeistof, als een visuele berekening en als een bit in de computer van de toekomst. Maar hoe hangen deze interpretaties precies samen?

Een belangrijke stap in de richting van een antwoord op deze vraag is gezet door R. Kashaev. Vijftien jaar geleden formuleerde hij een heel specifiek vermoeden over de samenhang tussen de werelden achter de vier thema's van hierboven. Zijn vermoeden staat nu bekend als het *volume conjecture* en het verifieëren ervan is een van de grootste onopgeloste problemen in mijn specialisatie. Te meer omdat het waarschijnlijk het topje van een ijsberg aan nieuwe vondsten is.

Het doel van mijn proefschrift is om technieken te ontwikkelen om het volume conjecture te bewijzen en het in context te plaatsen. De wat technische titel

Asymptotics of quantum spin networks refereert aan de gevonden context, zoals hopelijk aan het einde van deze samenvatting wat duidelijker zal zijn. Hoewel in zekere zin succesvol, zijn mijn technieken verre van toereikend gebleken om een definitief antwoord te geven op de vraag of het volume conjecture waar is of niet. Mijn verwachting is dat het vermoeden voor de komende generatie wiskundigen een onbereikbaar maar inspirerend doel blijft.

7.1 Kristallen

Kristallen of veelvlakken zoals de afgeknotte octaeder in de figuur hierbeneden spelen een belangrijke rol in mijn onderzoek. Dit specifieke veelvlak speelt een sleutelrol in hoofdstuk 3 en daarom staat daarom in vermomming op de voorkant van dit proefschrift.

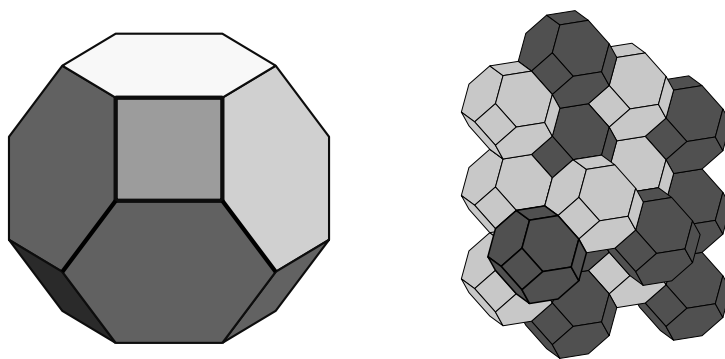


Figure 7.2: De afgeknotte octaeder (links) en een deel van het bijbehorende kristalrooster (rechts).

Om te begrijpen wat de rol van de veelvlakken is, doen we het volgende gedachtenexperiment. Stel je voor dat je in een vierkante kamer zit met in elke muur een deur. Het bijzondere van deze kamer is dat je, wanneer je door een van de deuren naar buiten loopt, vanzelf door de deur ertegenover de kamer weer binnenkomt. Er is dus geen ontsnapping mogelijk. Zelfs niet door het plafond, want als je er in slaagt een gat in het plafond te maken, en je klimt daar doorheen, dan kom je door de vloer weer naar boven. Stel je nu voor dat de muren doorzichtig zijn, wat zou je dan zien? Gegeven dat de lichtstralen net als jijzelf niet kunnen ontsnappen en steeds maar weer terugkomen door de wand tegenover waar ze doorheen gingen, zal het eruit zien als een spiegelpaleis. Behalve dat je jezelf alleen van achteren ziet.

In dit wat claustrofobische gedachtenexperiment hebben we een nieuw idee van ruimte geconstrueerd, een ruimte waaruit je niet kunt ontsnappen, maar die ook geen muren heeft. De ruimte is als het ware in zichzelf geknoopt. Zulke ruimten kunnen we gebruiken om knopen beter te begrijpen. Nemen we namelijk in plaats van de vierkante kamer een ander veelvlak waarvan we de vlakken aan elkaar praten, dan gebeurt er iets bijzonders. We hebben op deze manier de ruimte in de knoop gelegd en zo'n knoop in de ruimte is te zien als een gewone knoop.

Bij elke knoop hoort zo een veelvlak en veelvlakken zijn eenvoudiger om te bestuderen omdat ze een duidelijke vorm hebben. We kunnen nu bijvoorbeeld praten over de *inhoud van de knoop*, dat is namelijk de inhoud van het bijbehorende veelvlak. Dit getal is een heel goede graadmeter voor hoe ingewikkeld de knoop is. Het is het *volume* uit het volume conjecture. Voor de achtknoop hierboven (figuur 7.1) blijkt het bijbehorende veelvlak bijvoorbeeld twee driehoekige piramides op elkaar te zijn. Op mijn website kun je precies zien hoe je de vlakjes plakken moet en hoe de resulterende ruimte de achtknoop beschrijft.

Om beter te begrijpen hoe dit werkt kun je ook een vel papier nemen in plaats van je eigen kamer. Wat gebeurt er met het papier wanneer we de tegenoverliggende randen aan elkaar plakken? Als je het vel ombuigt en de tegenoverliggende randen aan elkaar plakt, krijg je een buis. Als je vervolgens de andere oorspronkelijk tegenover elkaar liggende randen ook aan elkaar plakt, krijg je met wat kreukelen en duwen een torus of *doughnut*. Net als in het bovenstaande experiment is het onmogelijk geworden om uit het papier te ontsnappen, het papier is in zichzelf geknoopt. Vaak is het verhelderend om in plaats van werkelijk te plakken het vel te herhalen. Van binnen gezien is het effect hetzelfde, denk aan het spiegelpaleis van hierboven. De aaneelkaar geplakte vellen vormen een regelmatig patroon van rechthoeken. Dit noemen we een kristalrooster (vergelijk figuur 7.2).

Een complicatie is dat de meeste knopen een kristalrooster hebben waarvan de hoeken niet netjes kunnen passen, waardoor het rooster gekromd is. Dit fenomeen is goed te zien aan het volgende experiment. Als je zeven evengrote munten neemt en ze netjes om de middelste heen op tafel legt, vormen ze een bloemetje. Dat bloemetje zou je kunnen herhalen en dan wordt het een netjes zeshoekig kristalrooster. Als je nu één bloemblad/munt weghaalt, moet je proberen er opnieuw een bloemetje van te vormen, zo dat de munten elkaar allemaal raken. Onmogelijk? Til de vijf munten wat op en ze vormen een mooi, maar krom bakje. Zou je dit herhalen dan vind je dat je met twaalf munten een kristalrooster op een bol krijgt (dodecaeder). Wat gebeurt er als je juist een munt had toegevoegd in plaats van weggehaald? Kun je nog steeds een bloemetje maken met 7 munten rond één in het midden? Het is niet heel makkelijk, maar het kan wel. Je krijgt dan een golvend oppervlak dat toch nog netjes met munten betegeld is. Het voortzetten van dit patroon is voor gevorderden maar geeft wel een glimp van de wereld van de roosters die bij de knopen horen.

7.2 Roeren

Hierboven hebben we kristallen aan knopen gerelateerd. Hierdoor wordt een flexibele knoop als het ware uitgehard tot een precieze meetkundige vorm. Een andere manier om knopen te beschrijven is door ze te zien als vlechten. Dat maakt verder weinig uit want bij elke vlecht kunnen we een knoop maken door de eindjes boven en onder aan elkaar te binden. Zo wordt bijvoorbeeld de vlecht in figuur 7.1 precies de achtknoop. Zoals we hieronder zullen zien, kunnen we een vlecht herkennen in de kolken die ontstaan tijdens het roeren in een kop chocolademelk (zie op het plaatje hieronder).

Stel je voor dat je twee vloeistoffen (bijvoorbeeld yoghurt en honing) in een

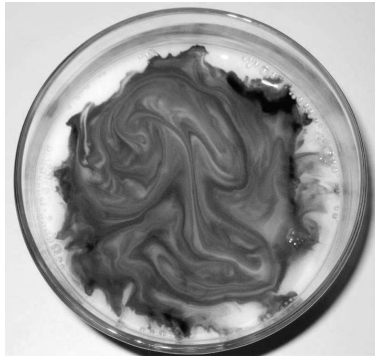


Figure 7.3: Chaos in een glas chocolademelk.

ondiep rond bakje wil mengen. Om het mengen te versnellen heb je een aantal roerstaafjes tot je beschikking. De vraag is nu: hoe kun je het beste roeren zodat het mixen zo efficiënt mogelijk gaat? Om verschillende strategieën met elkaar te vergelijken spreken we af om de bewegingen van de staafjes door de tijd heen te volgen. Zo ontstaat als vanzelf een vlecht waarvan ieder touwtje het pad van een van de staafjes beschrijft. In de figuur hierbeneden hebben we bijvoorbeeld twee roerstaafjes drie halve slagen linksom gegeven. Zo krijgen we een eenvoudige vlecht met drie kruisingen, een voor elke halve slag.

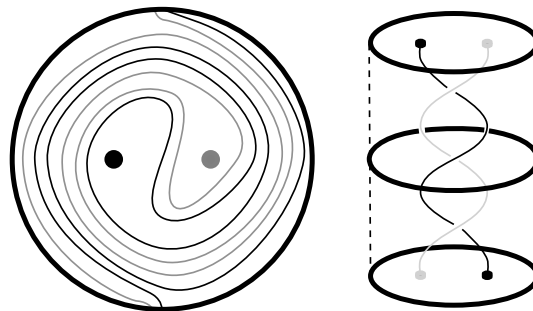


Figure 7.4: De stroomlijnen gemaakt na drie halve slagen van de twee roerstaafjes (links) de bijbehorende vlecht (rechts).

Het is zinvol om de vlecht bij een manier van roeren te betrekken want die vlecht beschrijft het kwalitatieve patroon in het roeren. Kleine verstoringen, bijvoorbeeld door het trillen van je hand, hebben geen effect op de globale vorm van de vlecht. Zolang de bijbehorende vlecht gelijk blijft is het effect op de vloeistof ook vrijwel gelijk. Welke vlechten zijn goede mixers? Dat blijkt hem te zitten in de inhoud van de bijbehorende knoop. Dat wil zeggen de inhoud van het veelvlak behorend bij de knoop zoals we gezien hebben in de vorige paragraaf. Hoe groter de inhoud, hoe beter de vloeistof gemixt wordt. Preciezer gezegd: de entropie van het roerproces is exact het inhoud van de vlecht.

Zo zien we dat het volume van een knoop op een onverwachte manier de complexiteit van de knoop aangeeft. Om goed te roeren moet een vlecht dus

een groot genoeg bijbehorend volume hebben. Een stroperige massa kun je bijvoorbeeld niet goed roeren met maar één staafje, omdat de bijbehorende vlecht een te laag volume heeft.

7.3 Tekenen

Rekenen en tekenen komen heel dicht bij elkaar wanneer we knopen bestuderen. Dit komt, omdat we met behulp van een plaatje aan iedere knoop een waarde kunnen toekennen. Deze waarde is het zogenaamde Jones-polynoom. Oorspronkelijk waren de tekeningen bedoeld als geheugensteun bij ingewikkelde berekeningen, maar gaandeweg zijn de rollen omgedraaid. De tekening is de berekening. Ons doel is om aan ieder plaatje van een knoop een getal toe te kennen, op zo'n manier dat twee plaatjes van dezelfde knoop altijd dezelfde waarde hebben. Op die manier kunnen we knopen van elkaar onderscheiden.

Om de waarde van een knoop uit te rekenen, passen we een bepaalde formule toe op iedere kruising. Deze formule is weergegeven in figuur 7.5 (boven). Met behulp van deze formule kunnen we een plaatje splitsen, zoals bijvoorbeeld in figuur 7.5 (beneden). Zo krijgen we eenvoudigere plaatjes waarvan we de waarde misschien al kennen. Zo niet dan passen we de formule opnieuw toe. Tot slot spreken we af dat elke gesloten lus die nergens aan vast zit, de waarde 0 krijgt. Een plaatje met zo'n lus erin is dus automatisch 0.

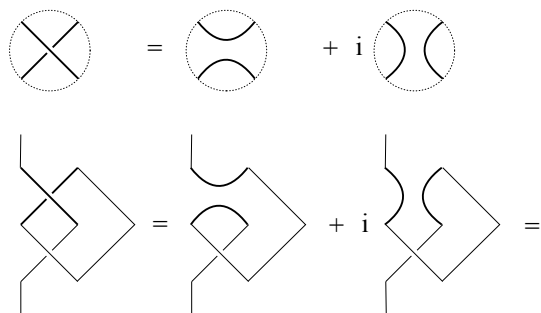


Figure 7.5: Boven: De formule om kruisingen te reduceren. Het getal i voldoet aan $i^2 = -1$. De gestippelde cirkel betekent dat het plaatje verder onveranderd blijft. Onder: Berekening van de waarde van de Hopf-link, stap 1.

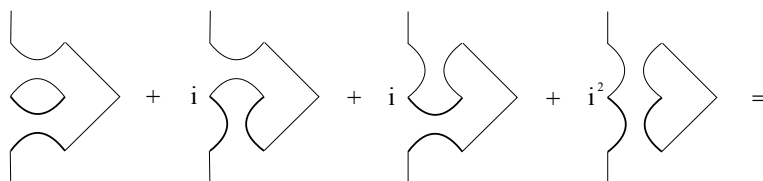


Figure 7.6: Stap 2. We splitsen in beide plaatjes de onderste kruising

Als voorbeeld berekenen we de waarde van de knoop linksonder in figuur 7.5. Deze knoop heet de Hopf-link en heeft precies twee kruisingen. Eerst passen

$$i \left[\text{diagram} \right] + i \left[\text{diagram} \right] = i \left| \right| + i \left| \right| = 2i \left| \right|$$

Figure 7.7: Stap 3. Het eerste en het laatste plaatje bevatten een losse lus en worden daarom verwijderd. Vervolgens worden de overgebleven touwtjes rechtgetrokken en opgeteld.

we de formule toe op de bovenste kruising (vet in figuur 7.5). Zo krijgen we twee nieuwe plaatjes met nog maar één kruising per stuk. Opnieuw toepassen van de formule geeft vier nieuwe plaatjes (zie figuur 7.6), maar twee hiervan bevatten een losse lus en krijgen dus waarde 0. Zo houden we uiteindelijk $2i$ maal de rechte lijn over (figuur 7.7). We zeggen dan dat de waarde van de oorspronkelijke knoop gelijk is aan $2i$.

Na even nadenken kom je er achter dat we op deze manier iedere knoop kunnen reduceren tot een getal keer de lijn. Dat getal is de waarde van de knoop op een macht van i na. Dit proces is een simpel geval van de berekening van het Jones-polynoom, dat een belangrijke rol speelt in dit proefschrift.

We sluiten af met een iets ingewikkelder voorbeeld voor de liefhebber, de overhandse knoop (zie figuur 7.8). De uitkomst van de berekening toont aan dat de overhandse knoop niet gelijk is aan de Hopf-link hierboven: $2i \neq -3$. Dat is de essentie van het Jones-polynoom: plaatjes van knopen zijn moeilijk met elkaar te vergelijken, getallen zijn makkelijk met elkaar te vergelijken.

$$\left[\text{overhand knot} \right] = \left[\text{simpler knot} \right] + i \left[\text{another knot} \right] = -3 \left| \right|$$

Figure 7.8: Bereken de waarde van de overhandse knoop (links).

7.4 Kwantumrekenen

De vorige sectie over rekenen met plaatjes van knopen leek misschien wat uit de lucht gegrepen. We zullen dergelijke berekeningen nu interpreteren in termen van de kwantumcomputer. Hoewel de kwantumcomputer nog niet echt praktisch toepasbaar is, ziet het ernaar uit dat dit de computer van de toekomst wordt. Gebaseerd op kwantummechanische principes kan de kwantumcomputer onvergelyklijk veel sneller rekenen dan een gewone computer ooit kan. Dat komt doordat de *qbits* waarin de informatie wordt verwerkt niet slechts 0 of 1

kunnen zijn, zoals bits in een gewone computer. De qbits van de kwantumcomputer kunnen *tegelijk* 0 en 1 zijn.

Voordat de grote beloften van de kwantumcomputer waargemaakt kunnen worden, zijn er nog een hoop praktische problemen om op te lossen. Een van de belangrijkste obstakels is dat qbits extreem instabiel zijn. Daardoor is de kans op fouten zo groot dat de kracht van de kwantumcomputer verloren gaat. Dit is waar de knopen en vlechten in het spel komen.

De stabiliteit van de kwantumcomputer kan enorm verbeteren door gebruik te maken van de vervlechttings-eigenschappen van anyonen. Anyonen zijn exotische deeltjes die alleen kunnen bestaan in een dun laagje gas rond het absolute nulpunt. Het bijzondere van anyonen is dat ze in hun kwantumtoestand onthouden of en hoe ze om elkaar heen gedraaid zijn. Het is alsof ze met onzichtbare touwtjes aan het plafond vast zitten: verwisselen ze van plaats, dan raken die touwtjes in de knoop. Alles wat de deeltjes doen wordt opgeslagen in de vlechten die zo gevormd worden. Dit beeld van virtuele vlechten doet sterk denken aan de vlechten die de paden van de roerstaafjes beschreven. Net zo als in die situatie speelt de vlecht achter de schermen een cruciale rol.

Het grote voordeel van de vlechten is als volgt. Net als met de roerstaafjes is de kwalitatieve vorm van de vlecht ongevoelig voor kleine verstoringen van de bewegende deeltjes. Als we al onze kwantumberekeningen doen in termen van de vlechten die de bewegende anyonen produceren, kunnen we dus veel betrouwbaardere berekeningen doen met de kwantumcomputer.

Zulke berekeningen in termen van vlechten zijn nauw verwant aan de grafische berekening van het Jones-polynoom die we in de vorige paragraaf deden. We kunnen deze berekeningen nu in termen van de deeltjes proberen te interpreteren. Het feit dat we een kruising uitdrukten in twee verschillende plaatjes is heel typisch voor de kwantumwereld. De kruising zelf stelt de interactie tussen twee anyonen voor. Kwantummechanisch kunnen we deze interactie beschrijven als de *combinatie* van twee uitkomsten: de linker is dat de deeltjes botsten en elkaar uitdoofden, de rechter is dat ze langs elkaar gingen zonder iets te merken. Allebei de uitkomsten zijn een beetje waar. Wat we eerder de waarde van de knoop noemden kan op een vergelijkbare manier geïnterpreteerd worden als de *kans* dat de specifieke interactie beschreven door de knoop zal plaatsvinden.

Voorlopig blijft de kwantumcomputer door technische obstakels nog toekomstmuziek, maar het is goed mogelijk dat de computers van de volgende generatie rekenen in termen van vlechten.

7.5 Asymptotiek van kwantum-spin-netwerken

Behalve dat alle bovengenoemde thema's met knopen te maken hadden is het nog niet duidelijk hoe en of ze echt iets met elkaar te maken hebben. Het sleutelwoord hier is *asymptotiek* ofwel *in de limiet*. Welke limiet? Een van de uitgangspunten van de kwantummechanica is dat twee deeltjes niet dicht bij elkaar kunnen komen dan een bepaalde afstand h . Vóór de kwantummechanica ging men er vanuit dat h nul was, dus dat deeltjes willekeurig dicht bij elkaar kunnen komen. Als we nu wiskundig gezien de limiet van h naar 0 nemen in de kwantummechanica, dan is de verwachting dat we de eenvoudigere ouderwetse beschrijving van de wereld terugzien.

Wat algemener kunnen we deze limiet bestuderen voor eenvoudige deeltjes-

modellen die we kwantum-spin-netwerken noemen (zie de titel van het proefschrift). Modellen van de kwantumcomputer en het Jones-polynoom zijn hier een speciaal voorbeeld van. Een belangrijke vraag over deze modellen is hoe ze zich gedragen in de bovengenoemde limiet. R. Kashaev gaf hierop een interessant antwoord in de vorm van zijn volume conjecture. We zouden dit kunnen parafraseren als de verwachting dat de vier thema's dan exact samenvallen: De veelvlakken, het roeren, de Jones-polynoom berekeningen en de kwantumvlechten beschrijven dan allemaal precies hetzelfde. In zekere zin wordt de kwantumvlecht in de limiet een echte vlecht.

We kunnen het volume conjecture preciezer formuleren door ons te concentreren op het inhoud van de knoop. Aan de ene kant refereert de inhoud van de knoop aan de inhoud van het veelvlak en de vorm van het kristalrooster. Aan de andere kant komt exact dit getal naarboven als de limiet van het Jones-polynoom van de knoop. In termen van vlechten kunnen we het zo zeggen: Als we de anyonen als roerstaafjes zien dan is de kans dat anyonen een specifieke vlecht maken is precies gelijk aan de entropie van de stroming die hoort bij die vlecht. Let op: dit geldt alleen in de limiet.

Hoewel het volume conjecture precies genoeg geformuleerd is om exact bewezen te kunnen worden, lijkt het gereedschap hiervoor nog te ontbreken. Mijn belangrijkste resultaten zijn de volgende.

1. Aan iedere knoop kunnen we een aantal ringen toevoegen zodat het volume conjecture waar is voor de nieuwe knoop.
2. Vervangen we de kwantum-spin-netwerken door de eenvoudigere klassieke spin-netwerken, dan bestaat de limiet. Voor het volume conjecture zelf is ook het bestaan van de limiet onbekend.
3. Een case study van de knopen met volume 0 om de beperkingen van de gebruikte technieken duidelijk te maken.

Bibliography

- [AB] S.A. Abramov and M. Bronshtein, *Solution of linear differential and difference systems with respect to some of the unknowns*, Zh. Vychisl. Mat. Mat. Fiz. **46** (2006) 229–241; translation in Comput. Math. Math. Phys. **46** (2006) 218–230.
- [And] J.E. Andersen, *The Witten invariant of finite order mapping tori I*, to appear in J. Reine Angew. Math.
- [An] Y. André, *Séries Gevrey de type arithmétique. I. Théorèmes de pureté et de dualité*, Ann. of Math. (2) **151** (2000) 705–740.
- [And] G. Andrews, *Euler’s “exemplum memorabile inductionis fallacis” and q -Trinomial coefficients*, J. Amer. Math. Soc., **3** (1990), 653–669.
- [Aw] G.E. Andrews, *The theory of partitions*, Cambridge University Press, Cambridge, 1998.
- [Bak] M. Baker, All links are sublinks of arithmetic links, *Pacific Journal of Mathematics*, **203**, 2, (2002), 257–263.
- [Ba] J. Barrett, *Geometrical measurements in three-dimensional quantum gravity*, Int.J.Mod.Phys. A18S2 (2003) 97–113.
- [BG] D. Bar-Natan and S. Garoufalidis, On the Melvin-Morton-Rozansky conjecture, Invent. Math. **125** (1996), 1, 103133.
- [BC] J.W. Barrett and L. Crane, *Relativistic spin networks and quantum gravity*, J. Math. Phys. **39** (1998) 3296–3302.
- [BB] S. Baseilhac, R. Benedetti, *QHI, 3-manifold scissors congruence classes and the volume conjecture*, Geom. Topol. Monogr. **4** (2002), 13–28.
- [BP] R. Benedetti, C. Petronio, *Lectures on hyperbolic geometry*, Springer 1992.
- [BL1] L. Biedenharn, J. Louck, *Angular momentum in quantum mechanics*, Encyclopedia of mathematics and its applications **8** 1981.
- [BL2] L. Biedenharn, J. Louck, *Racah-Wigner algebra in quantum theory*, Encyclopedia of mathematics and its applications **9** 1981.
- [BK] S. Bloch and D. Kreimer, *Mixed Hodge Structures and Renormalization in Physics*, preprint 2008 [arXiv:0804.4399](https://arxiv.org/abs/0804.4399).
- [Bl] L.M. Blumenthal, *Theory and applications of distance geometry*, Chelsea, 1970.
- [A’C] N. A’Campo, *Sur la monodromie des singularités isolées d’hypersurfaces complexes*, Invent. Math. **20** (1973) 147–169.
- [CFS] S. Carter, D.E. Flath, M. Saito, *The Classical and Quantum 6j-symbols*, Mathematical Notes 43, Princeton University Press, 1995.
- [Ch] J. Cho, *Yokota theory, the invariant trace fields of hyperbolic knots and the Borel regulator map*, preprint 2010, Arxiv 1005.3094.

- [Co1] F. Costantino, *Colored Jones invariants of links in $S^3 \#_k S^2 \times S^1$ and the volume conjecture*, J. Lond. Math. Soc. 2, 76, (2007), 1–15.
- [Co2] F. Costantino, *Integrality of Kauffman brackets of trivalent graphs*, preprint 2009 [ArXiv 0908.0542](#).
- [Co3] F. Costantino, *6j-symbols, hyperbolic structures and the Volume Conjecture*, Geometry & Topology 11 (2007), 1831-1853.
- [CM] F. Costantino, J. Murakami, *On $SL(2, C)$ quantum 6j-symbol and its relation to the hyperbolic volume*, preprint 2010, Arxiv 1005.4277.
- [CG1] O. Costin and S. Garoufalidis, *Resurgence of the Kontsevich-Zagier power series*, Annales de l' Institut Fourier, *in press*.
- [CG2] O. Costin and S. Garoufalidis, *Resurgence of 1-dimensional sums of quantum factorials*, preprint 2007.
- [De] J. Désarménien, *Un analogue des congruences de Kummer pour les q -nombres d'Euler*, European J. Combin. **3** (1982) 19–28.
- [Di] R. Diestel, *Graph theory* 3d edition, Springer, 2005.
- [DF] R. Dijkgraaf, H. Fuji, *The Volume Conjecture and Topological Strings*, Fortsch.Phys.57 (2009), 825–856.
- [DG] T. Dimofte, S. Gukov, *Quantum Field Theory and the Volume Conjecture* preprint 2010, Arxiv 1003.4808.
- [DGLZ] T. Dimofte, S. Gukov, J. Lenells, D. Zagier, *Exact Results for Perturbative Chern-Simons Theory with Complex Gauge Group* Comm. Num. Th. Phys., 3, 2 (2009), 363–443.
- [DK] J. Dubois, R. Kashaev, *On the asymptotic expansion of the colored Jones polynomial for torus knots*, preprint, Arxiv 0510.5607.
- [Ec1] J. Écalle, *Resurgent functions*, Vol. I-III Mathematical Publications of Orsay **81-05** 1981, **81-06** 1981, **85-05** 1985.
- [EPR] J. Engle, R. Pereira and C. Rovelli, *Flipped spinfoam vertex and loop gravity*, Nuclear Phys. B **798** (2008) 251–290.
- [FK] I.B. Frenkel and M.G. Khovanov, *Canonical bases in tensor products and graphical calculus for $U_q(\mathfrak{sl}_2)$* , Duke Math. J. **87** (1997) 409–480.
- [FS] P. Flajolet and R. Sedgewick, *Analytic combinatorics*, Cambridge University Press, 2009.
- [Fr] R. Frigerio, *Hyperbolic manifolds with geodesic boundary which are determined by their fundamental group*, Topology Appl. 145, (2004), 69–81.
- [Fr] R. Frigerio, *An infinite family of hyperbolic graph complements in S^3* , J. Knot Theory Ramifications 14, (2005), 479–496.
- [FP] D. Futer, J. Purcell, *Links with no exceptional surgeries*, Commentarii Mathematici Helvetici 8, 3, (2007), 629–664.
- [Ga0] S. Garoufalidis, *On the characteristic and deformation varieties of a knot, proceedings of the Casson fest*, Geometry and Topology Monographs, 7 (2004), 291–309.
- [Ga1] S. Garoufalidis, *q -terms, singularities and the extended Bloch group*, preprint 2007 [arXiv/0708.0018](#).
- [Ga2] S. Garoufalidis, *An ansatz for the asymptotics of hypergeometric multisums*, Adv. in Applied Mathematics **41** (2008) 423–451.
- [Ga3] S. Garoufalidis, *G -functions and multisum versus holonomic sequences*, Advances in Mathematics, **220** (2009) 1945–1955.

- [Ga6] S. Garoufalidis, *Resurgence of 1-dimensional hypergeometric multisums*, preprint 2007.
- [Ga5] S. Garoufalidis, *Applications of quantum invariants in low-dimensional topology*, *Topology* **37** (1998) 219–224.
- [GL1] S. Garoufalidis and Y. Lan, *Experimental evidence for the volume conjecture for the simplest hyperbolic non-2-bridge knot*, *Algebr. Geom. Topol.* **5** (2005) 379–403.
- [GL2] S. Garoufalidis, T. Le, *Asymptotics of the colored Jones function of a knot*, preprint 2005, ArXiv math/0508100.
- [GaLe] S. Garoufalidis, T. Le, *The colored Jones function is q -holonomic*, *Geometry and Topology*, **9** (2005) 1253–1293.
- [GM] S. Garoufalidis and M. Mariño, *Universality and asymptotics of graph counting problems in unoriented surfaces*, preprint 2008 arXiv:0812.1195.
- [GV] S. Garoufalidis and R. van der Veen, *Asymptotics of classical spin networks*, preprint 2009, arXiv:0902.3113.
- [GR] N. Geer, N. Reshetikhin, *On invariants of graphs related to quantum $\mathfrak{sl}(2)$ at roots of unity*, *Lett. Mat. Phys.* **88**, 1-3 (2009).
- [Go] C. Gordon, *Dehn surgery and satellite knots*, *Trans. Amer. Math. Soc.*, **275**, 2 (1983), 687–708.
- [GuM] S. Gukov, H. Murakami, *$SL(2, \mathbb{C})$ Chern-Simons theory and the asymptotic behavior of the colored Jones polynomial*, preprint 2005, ArXiv GT/0608324.
- [Gu] R. Gurau, *The Ponzano-Regge asymptotic of the $6j$ symbol: an elementary proof*, *Annales Henri Poincaré* **9** (2008) 1413–1424.
- [Ha] G.H. Hardy, *Divergent Series*, Oxford, at the Clarendon Press, 1949.
- [Hi1] K. Hikami, *Volume Conjecture and Asymptotic Expansion of q -series*, *Exp. Math.* **12**, 3 (2003) 319–337.
- [Hi2] K. Hikami, *Quantum invariant for torus link and modular forms*, *Commun. Math. Phys.*, **246** (2004), 403–426.
- [HL] V. Huynh, T. Le *On the colored Jones polynomial and the Kashaev invariant*, *J. Math. Sci.*, **146** (2007).
- [Joh] K. Johansson, *Homotopy equivalences of 3-manifolds with boundaries*, *Lecture Notes in Mathematics* **761**, Springer, (1979).
- [J] V. Jones, *Hecke algebra representation of braid groups and link polynomials*, *Annals Math.* **126** (1987) 335–388.
- [JR] V. Jones, M. Rosso, *On the invariants of torus knots derived from quantum groups*, *Journal of Knot Theory and its Ramifications*, **2**,1 (1993), 113–123.
- [Ju] R. Jungen, *Sur les séries de Taylor n'ayant que des singularités algébrico-logarithmiques sur leur cercle de convergence*, *Comment. Math. Helv.* **3** (1931) 266–306.
- [Jun] D. Jungreis, *Chains that realize the Gromov invariant of hyperbolic manifolds*, *Ergod. Th. & Dynam. Sys.* **17**, (1997), 643–648.
- [Ka1] R. Kashaev, *Quantum Dilogarithm as a $6j$ -Symbol*, *Modern Physics Letters A*, **9**, 40, (1994), 3757–3768.
- [Ka2] R. Kashaev, *The hyperbolic volume of knots from quantum dilogarithm*, *Lett. Math. Phys.* **39**, (1997), 269–275.
- [KT] R. Kashaev, O. Tirkkonen, *Proof of the volume conjecture for torus knots*, *J. Math. Sci.* **115** (2003) 2033–2036.

- [Kz] N.M. Katz, *A simple algorithm for cyclic vectors*, Amer. J. Math. **109** (1987) 65–70.
- [KL] L.H. Kauffman and S.L. Lins, *Temperley-Lieb recoupling theory and invariants of 3-manifolds*, Annals of Mathematics Studies **134** (1994) Princeton University Press.
- [KM] R Kirby, P Melvin, *The 3-manifold invariants of Witten and Reshetikhin-Turaev for $sl(2, C)$* , Invent. Math. 105 (1991) 473–545.
- [KK] M. Khovanov and G. Kuperberg, *Web bases for $sl(3)$ are not dual canonical*, Pacific J. Math. **188** (1999) 129–153.
- [KR] A.N. Kirillov and N.Yu. Reshetikhin, *Representations of the algebra $U_q(sl(2))$, q -orthogonal polynomials and invariants of links*, in Infinite-dimensional Lie algebras and groups, Adv. Ser. Math. Phys., **7** (1989) 285–339.
- [Ko1] S.L. Kokkendorff, *Geometry and combinatorics*, PhD thesis 2002.
- [KZ] M. Kontsevich and D. Zagier, *Periods*, in Mathematics unlimited—2001 and beyond, (2001) 771–808.
- [Ku] G. Kuperberg, *Spiders for rank 2 Lie algebras*, Comm. Math. Phys. **180** (1996) 109–151.
- [Li] W. Lickorish, *An Introduction to Knot Theory*, Springer, (1997).
- [LT] T.Le, A.Tran, *On the Volume Conjecture for Cables of Knots*, preprint ArXiv 0907.0172.
- [Mac] I. Macdonald, *Symmetric functions and Hall polynomials*, Clarendon Press, 1995.
- [Mas] G. Masbaum, *Skein-theoretical derivation of some formulas of Habiro*, Algebraic & Geometric Topology **3**, (2003), 537–556.
- [MV] G. Masbaum, P. Vogel, *3-valent graphs and the Kauffman bracket*, Pacific J. Math. **164**, 2, (1994), 361–381.
- [Ma] S. Matveev, *Algorithmic Topology and Classification of 3-Manifolds*, Springer, (2003).
- [Me] R. Meyerhoff, *Density of the Chern-Simons invariant for hyperbolic 3-manifolds*, Low dimensional topology and Kleinian groups, 217–239, Cambridge university press, Cambridge, 1986.
- [MS] H. Morton, P. Strickland, *Jones polynomial invariants for knots and satellites*, Math. Proc. Camb. Phil. Soc., **109** (1991), 83–103.
- [Mo] H. Morton, *The coloured Jones function and Alexander polynomial for torus knots*, Math. Proc. Camb. Phil. Soc., **117** (1995), 129–135.
- [Mou] J.P. Moussouris, *The chromatic evaluation of strand networks*, Advances in Twistor Theory, Research Notes in Mathematics, Huston, Ward eds. Pitman Pub. (1979) 308–312.
- [MuE] H. Murakami, *The colored Jones polynomials of the figure-eight knot and the volumes of three-manifolds obtained by Dehn surgeries*, Fund. Math. **184** (2004), 269–289.
- [MI] H. Murakami, *A quantum introduction to knot theory*, Primes and Knots: JAMI conference, Contemp. Math., 2006.
- [MG] H. Murakami, *An introduction to the volume conjecture and its generalizations*, preprint, Arxiv 0802.0039.
- [MIn] H. Murakami, *An introduction to the volume conjecture*, preprint 2010, Arxiv 1002.0126.
- [Mh] K. Hikami, H. Murakami, *Colored Jones polynomials with polynomial growth*, to appear in Comm. Contemp. Math, Arxiv 0711.2836.
- [MM] H. Murakami, J. Murakami, *The colored Jones Polynomials and the simplicial Volume of a Knot*, Acta Math. **186**, (2001), 85–104.

- [MMOTY] H. Murakami, J. Murakami, M. Okamoto, T. Takata, Y. Yokota, *Kashaev's conjecture and the Chern–Simons invariants of knots and links*, Experimental Math. **11**, 3, (2002), 427–435.
- [Ni] N. Nilsson, *Some growth and ramification properties of certain integrals on algebraic manifolds*, Ark. Mat. **5** (1965) 463–476.
- [No] N.E. Norlund, *Hypergeometric functions* Acta Math. **94** (1955) 289–349.
- [O] F. Olver, *Asymptotics and special functions*, Reprint. AKP Classics. A K Peters, Ltd., Wellesley, MA, 1997.
- [Ou] M. Ouyang, *A note on the Chern-Simons invariant of hyperbolic 3-manifolds*, Proc. A.M.S. **125**, 6 (1997) 1845–1851.
- [PW] H. Parks and D. Wills, *An elementary calculation of the dihedral angle of the regular n -simplex*, Amer. Math. Monthly **109** (2002) 756–758.
- [PaRi] P. Paule and A. Riese, Mathematica software: <http://www.risc.uni-linz.ac.at/>
- [PW1] R. Pemantle and M.C. Wilson, *Asymptotics of multivariate sequences. I. Smooth points of the singular variety*, J. Combin. Theory Ser. A **97** (2002) 129–161.
- [PW2] R. Pemantle and M.C. Wilson, *Asymptotics of multivariate sequences. II. Multiple points of the singular variety*, Combin. Probab. Comput. **13** (2004) 735–761.
- [Pe1] R. Penrose, *Angular Momentum: An approach to combinatorial space time*, in Quantum Theory and Beyond, edited by Ted Bastin, Cambridge University Press, (1971) 151–180.
- [Pe2] R. Penrose, *Applications of negative dimensional tensors*, in Combinatorial Mathematics and its Applications, (1971) 221–244.
- [Pz] A. Perez, *Spin foam models for quantum gravity*, Classical Quantum Gravity **20** (2003) R43–R104.
- [PWZ] M. Petkovšek, H.S. Wilf and D. Zeilberger, *A = B*, A.K. Peters, Ltd., Wellesley, MA 1996.
- [PR] G. Ponzano and T. Regge, *Semiclassical limit of Racah coefficients*, Spectroscopic and group theoretical methods in physics, North Holland (1968) 1–58.
- [Pr] C. Procesi, *Lie groups, an approach through invariants and representations*, Springer, 2007.
- [VPS] M. van der Put and M.F. Singer, *Galois theory of linear differential equations*, Springer-Verlag, Berlin, 2003.
- [Ra] G. Racah, *Theory of complex spectra I,II,III,IV*, Phys. Rev **61** (1942) 186–197, *ibid* **62** (1942) 438–462, *ibid* **63** (1943) 367–382, *ibid* **76** (1949) 1352–1365.
- [Rat] J. Ratcliffe, *Foundations of Hyperbolic Manifolds*, Springer, (1994).
- [Rb1] J. Roberts, *Classical 6j-symbols and the tetrahedron*, Geom. Topol. **3** (1999) 21–66.
- [Rb2] J. Roberts, *Asymptotics and 6j-symbols*, in Invariants of knots and 3-manifolds, Geom. Topol. Monogr. **4** (2002) 245–261.
- [Ro] C. Rovelli, *Quantum gravity*, With a foreword by James Bjorken. Cambridge Monographs on Mathematical Physics. Cambridge University Press, 2004.
- [RS] C. Rovelli and L. Smolin, *Discreteness of area and volume in quantum gravity*, Nuclear Phys. B **442** (1995) 593–622.
- [RT] N. Reshetikhin, V. Turaev, *Ribbon graphs and their invariants derived from quantum groups*, Comm. Math. Phys. **127**, 1 (1990), 1–26.

- [Si] C.L. Siegel, *Über einige Anwendungen diophantischer Approximationen*, Abh. Preuss. Akad. Wiss. **1** (1929) 1–70. Reprinted in *Gesammelte Abhandlungen*, vol. 1, no 16 (1966) 209–266.
- [St] R. Stanley, *Enumerative combinatorics*, Vol. 1, 2. second edition, Cambridge University Press, Cambridge, 1997.
- [SP] E. Suarez-Peiro, *A Schläfli differential formula for simplices in semi-Riemannian hyperquadrics, Gauss-Bonnet formulas for simplices in the de Sitter sphere and the dual volume of a hyperbolic simplex*, Pacific J. Math. **194** (2000) 229–255.
- [DTh] D. Thurston, *The algebra of knotted trivalent graphs and Turaev’s shadow world*, Geometry & Topology monographs, 4, (2002), 337–362.
- [Th] W. Thurston, *The Geometry and Topology of Three-Manifolds*, unpublished lecture notes, Princeton, (1980).
- [Th2] W. Thurston, *Three dimensional manifolds, Kleinian groups and hyperbolic geometry*, Bull. AMS, 6, 3 (1982), 357–381.
- [Tu] V.G. Turaev, *Quantum invariants of knots and 3-manifolds*, de Gruyter Studies in Mathematics **18** (1994).
- [TV] V.G. Turaev and O.Ya. Viro, *State sum invariants of 3-manifolds and quantum 6j-symbols*, Topology **31** (1992), 865–902.
- [V0] R. van der Veen, *The volume conjecture for Whitehead chains*, master thesis, 2006. [http://www.science.uva.nl/~sim\\$riveen/papers.html](http://www.science.uva.nl/~sim$riveen/papers.html)
- [V1] R. van der Veen, *Proof of the volume conjecture for Whitehead chains*, Acta Math. Vietnamica, 33, 3, (2008), 421–431.
- [V2] R. van der Veen, *The volume conjecture for augmented knotted trivalent graphs*, Algebraic and Geometric Topology 9 2 (2009), pp.691–723.
- [V3] R. van der Veen, *A cabling formula for the colored Jones polynomial*, preprint 2008, Arxiv 0807.2679.
- [VMK] D.A. Varshalovich, A.N. Moskalev, V.K. Khersonskii, *Quantum theory of angular momentum*, World Scientific 1988.
- [Wei] E. Weisstein *Erfc*, from MathWorld—A Wolfram Web Resource. <http://mathworld.wolfram.com/Erfc.html>
- [We] B.W. Westbury, *A generating function for spin network evaluations*, Banach Center Publ., **42** (1998) 447–456.
- [Wee] J. Weeks, M. Culler, N. Dunfield, *SnapPy software*, <http://www.computop.org>
- [Wi] E.P. Wigner, *On representations of certain finite groups*, Amer. J. Math. **63** (1941) 57–63.
- [Wit1] E. Witten *Quantum field theory and the Jones polynomial*, Comm. Math. Phys. 121, 3 (1989), 351–399.
- [Wit2] E. Witten *Analytic continuation of Chern-Simons theory*, preprint 2010, Arxiv 1001.2933.
- [WZ1] H. Wilf and D. Zeilberger, *An algorithmic proof theory for hypergeometric (ordinary and q) multisum/integral identities*, Inventiones Math. **108** (1992) 575–633.
- [WZ2] J. Wimp and D. Zeilberger, *Resurrecting the asymptotics of linear recurrences*, J. Math. Anal. Appl. **111** (1985) 162–176.
- [Yo] Y. Yokota, *Topological invariants of graphs in 3-space*, Topology **35** 1 (1996) 77–87.

- [YY] M. Yamazaki, Y. Yokota, *On the limit of the colored Jones polynomial of a non-simple link*, preprint, Tokyo Metropolitan University, 2009.
- [Zh] H. Zheng, *Proof of the volume conjecture for Whitehead doubles of a family of torus knots*, Chin. Ann. of Math. B, 28, 4 (2007), 375–388.
- [Z] D. Zeilberger, *A holonomic systems approach to special functions identities*, J. Comput. Appl. Math. **32** (1990) 321–368.